NASA CR-120885

GE-72SD4241

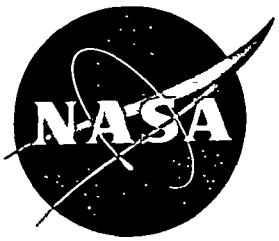

DEVELOPMENT OF A LIQUID METAL SLIP RING

by

S. M. Weinberger

GENERAL ELECTRIC COMPANY

SPACE SYSTEMS

Prepared for

NATIONAL AERONAUTICS & SPACE ADMINISTRATION

NASA Lewis Research Center

CONTRACT NAS 3-13730

Robert R. Lovell, Project Manager

NASA CR-120885

GE-72SD241

FINAL REPORT

DEVELOPMENT OF A LIQUID METAL SLIP RING

by

S. M. Weinberger

GENERAL ELECTRIC COMPANY
SPACE SYSTEMS
Valley Forge Space Center
P. O. Box 8555
Philadelphia, Pa. 19101

Prepared for

NATIONAL AERONAUTICS & SPACE ADMINISTRATION

November 1972

CONTRACT NAS 3-13730

NASA Lewis Research Center

Cleveland, Ohio

Robert R. Lovell, Project Manager
Spacecraft Technology Division

NOTICE

This report was prepared as an account of Government-sponsored work. Neither the United States, nor the National Aeronautics and Space Administration (NASA), nor any person acting on behalf of NASA:

A) Makes any warranty or representation, expressed or implied, with respect to the accuracy, completeness, or usefulness of the information contained in this report, or that the use of any information, apparatus, method, or process disclosed in this report may not infringe privately-owned rights; or

B) Assumes any liabilities with respect to the use of, or for damages resulting from the use of, any information, apparatus, method, or process disclosed in this report.

As used above, "person acting on behalf of NASA" includes any employee or contractor of NASA, or employee of such contractor, to the extent that such employee or contractor of NASA or employee of such contractor prepares, disseminates, or provides access to any information pursuant to his employment or contract with NASA, or his employment with such contractor.

Requests for copies of this report should be referred to:

National Aeronautics and Space Administration
Scientific and Technical Information Facility
P. O. Box 33
College Park, Md., 20740

FORWARD

The work described herein was done at the Space Systems Operation, General Electric Company, under NASA Contract NAS 3-13730 with Mr. Robert R. Lovell, Spacecraft Technology Division, NASA Lewis Research Center, as Project Manager.

TABLE OF CONTENTS

TABLE OF CONTENTS

APPENDIX B - TECHNICAL ANALYSES

APPENDIX C - VERIFICATION TEST PLAN

TABLE OF CONTENTS

LIST OF ILLUSTRATIONS

LIST OF ILLUSTRATIONS

LIST OF ILLUSTRATIONS

LIST OF TABLES

ABSTRACT

A liquid metal slip ring/solar orientation mechanism was designed and a model tested. This was a follow-up of previous efforts for the development of a gallium liquid metal slip ring in which the major problem was the formation and ejection of debris. Under this program, a number of slip ring design approaches were studied. The probe design concept was fully implemented with detail drawings and a model was successfully tested for dielectric strength, shock vibration, acceleration and operation. The conclusions of this program are that a gallium liquid metal slip ring/solar orientation mechanism is feasible and that the problem of debris formation and ejection has been successfully solved.

1.0 SUMMARY

A program was established to design a liquid metal slip ring/solar array orientation mechanism. This mechanism serves to continuously rotate a solar array with respect to the main body of a satellite and provide a means of transferring electrical power and signals across the rotating interface. The basic requirements for the LMSR/SAOM were for a slip ring having 116 rings capable of carrying currents ranging from 0.2 amps to 30 amps at voltages up to 15,000 volts. The orientation mechanism was to have torquer motors to provide rotary motion and a position sensor to indicate shaft location. The entire assembly was to be less than 10 inches diameter, 24 inches long and weigh less than 40 pounds. This effort was an extension of the work done on liquid metal slip rings under NASA contracts NAS 3-11537 and NAS 3-11538.

The overall program consisted of three major tasks: preliminary design, design verification and detail design. In the preliminary design task, a design study was made in which a number of design concepts for the liquid metal slip ring/solar orientation mechanism were evolved and investigated in detail by means of design and engineering studies. Based on these studies, recommendations were made and a design concept technically directed. The directed approach was the probe design concept.

A verification model of the probe concept was designed, fabricated and tested in order to verify the integrity of the approach. The verification model was designed to carry currents up to 30 amps per ring at voltages up to 15,000 volts in a six ring configuration The model was successfully tested for dielectric strength at 15,000 volts, launch and orbital vibration, acceleration and shock and operation. The cause of debris formation and ejection from gallium liquid metal slip rings appears to have been identified and the problem successfully solved.

A detailed design of the LMSR/SAOM was made using the probe concept configuration. Drawings were prepared in sufficient detail so that an engineering unit could be fabricated from them. The size and weight of the completed design were within the specified limits

2.0 INTRODUCTION

A program was undertaken to design a liquid metal slip ring/solar array orientation mechanism to transfer electric power and signals between a continuously rotating solar array and satellite body. The slip ring was to be capable of carrying currents varying from .2 amps to 30 amps dc per ring at voltages up to 15,000 volts between rings and to ground; the total number of rings required was 116. The nominal rotation rate of the slip ring was one revolution per day. The slip ring had to be operational both on the ground and in space and capable of withstanding handling and launch environments. In order to fully investigate the design, fabrication and performance parameters of the liquid metal slip ring/solar array orientation mechanism, a program with three major tasks was established. The tasks were:

Task 1 Preliminary Design Study

Task 2 Design Verification

Task 3 Detail Design

Task 1, Preliminary Design, consisted of a design study in which a number of design concepts were evolved. Engineering studies and design drawings were made on each concept to determine the best approach.

3.0 DESIGN VERIFICATION

3.1 Introduction

As a result of the preliminary design study (Task 1), the probe concept was technically directed as the design approach for which a detail design would be made. The probe concept as well as the overall requirements for the LMSR/SAOM presented new concents which had not been previously studied. Foremost of these were high voltage operation and the requirements for 116 rings. The previous contractual slip ring development effort was for high current, low voltage rings, these rings carried 100 amps at a maximum voltage of 3000 volts. The requirements for the LMSR/SAOM were for current in the range of 0.2 to 30 amps and a voltage of 15,000 volts, maximum. The 15,000 volt requirement was much more difficult to meet than the 3000 volt requirement because of more complex dielectric considerations. The requirements for 116 rings, as compared to 10 rings in the previous effort, also results in greater fabrication and assembly constraints.

A subject that required verification was the ability of the probe concept to produce a minimum of debris while rotating in a vacuum, and a determination of the efficacy of the probe geometry to retain debris during rotation in a vacuum and not produce ejected matter.

In addition to the new concepts and design requirements incorporated into the LMSR/SAOM, there were the requirements of shock, vibration and acceleration. There was not too much question concerning the ability to design the structural elements of the slip ring to with-

stand shock, vibration and acceleration. However, there was no test data demonstrating that the solid and liquid gallium can be retained under these conditions. Preliminary analytical work indicated that under the required shock, vibration and acceleration conditions, the solid gallium in the electrode cavity would not crack, chip or extrude. Similarly, the liquid gallium would be retained by the capillary forces and would not spill from the electrode cavity by sloshing, or by forces on the fluid.

A verification model of the slip ring was designed, fabricated and tested in order to ascertain the operational characteristics of the probe design. The verification model was designed to have the same physical geometry as the final design of the slip ring. The probes, electrode size and shape, insulation material type and thickness, gallium wetting and filling procedure and rotational speed were the same as on the slip ring. The structure was, however, made much more rigid than necessary so that the actual shock, vibration and acceleration characteristics of the probes, electrodes and gallium can be ascertained and kept independent of any structurally induced effects.

As part of the test program, four categories of tests were run:

(1) Dielectric

(2) Shock, vibration and acceleration, gallium solid

(3) Vibration and acceleration, gallium liquid

(4) Vacuum rotational tests

These tests were considered critical in establishing the basic integrity of the probe concept design.

The test sequence was as follows:

	Test Sequence
Dielectric Test	
Air	1
Vacuum	2
Acceleration, Vibration & Shock	
Vibration, gallium liquid	3
Acceleration, gallium liquid	4
Acceleration, gallium frozen	5
Vibration, gallium frozen	6
Shock, gallium frozen	7
Rotational Test	8
Post Test Evaluation	9

3.2 Verification Test Unit

3.2.1 Design and Fabrication

A verification test unit was designed and fabricated to verify the integrity of the probe concept. The test unit incorporated only those features of the probe design which were critical and which were to be evaluated: dielectric strength, vibration, acceleration and shock, and vacuum rotation. The structure of the test unit was deliberately made very heavy in order to preclude any structural resonance during vibration tests.

The test unit, shown in Figures 1 and 2, consisted of a 3" diameter shaft which was centrally located in a fixture suitable for shock and vibration testing. The fixture consisted of 1" thick aluminum alloy plates bolted together to form a box-like structure with partially open sides to permit visual observation of test disks. The top plate of the structure was removable by simple unbolting to permit installation of disks. The shaft was supported within the box by two thin, precision angular contact bearings at the bottom and one deep groove bearing at the top. The bottom bearings were pre-loaded to eliminate end play. The elimination of end play ensured that there was no vertical motion of shaft during vibration testing. See Figure 3. Disks containing liners, which contain the gallium were mounted midway along the shaft. The six disks were fabricated of

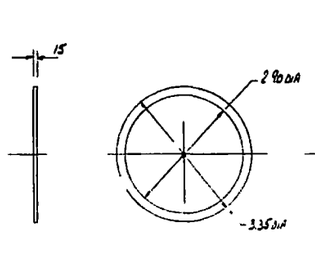

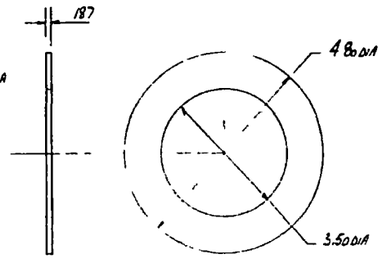

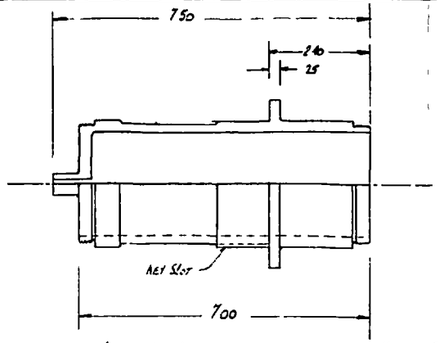

ALTERNATE METHOD OF MANUFACTURING ITEM 11, 13 & 15
FOR ALL OTHER DIMENSIONS SEE SEPARATE DETAILS

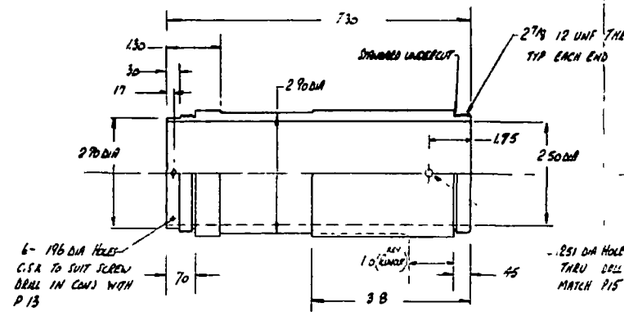

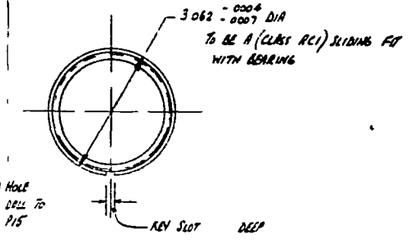

ITEM P 25
MAT'L AL ALLOY Nº REQD 2

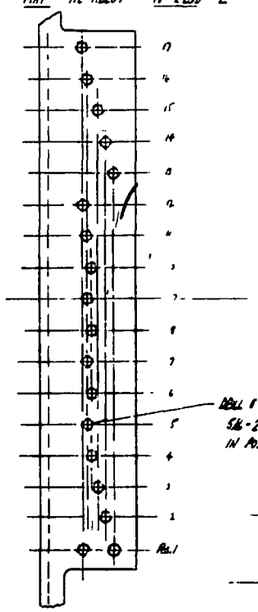

FLAT PATTERN OF P 21

ITEM P 29
MAT'L TEXTOLITE (GRADE 11541L)
1 REQD

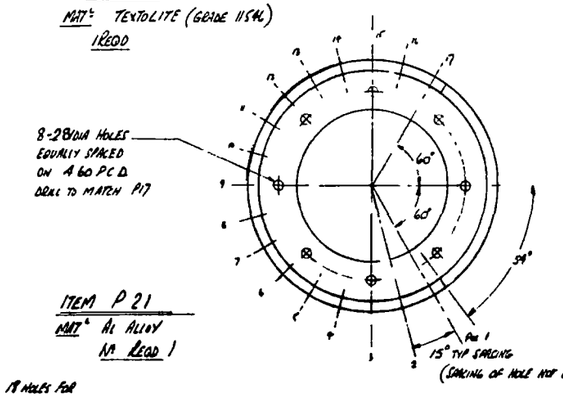

ITEM P 21
MAT'L AL ALLOY
Nº REQD 1

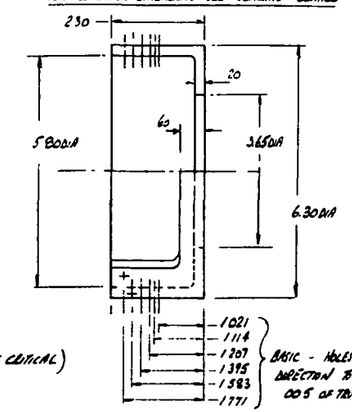

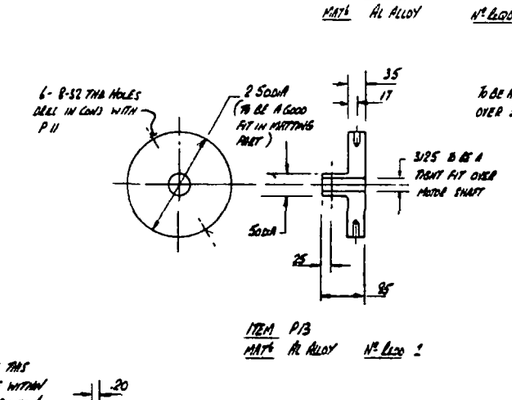

ITEM P 13
MAT'L AL ALLOY Nº REQD 1

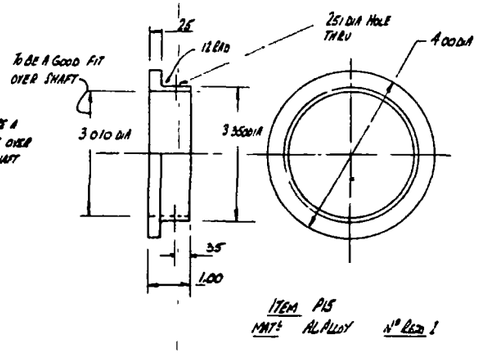

ITEM P15
MAT'L AL ALLOY Nº REQD 1

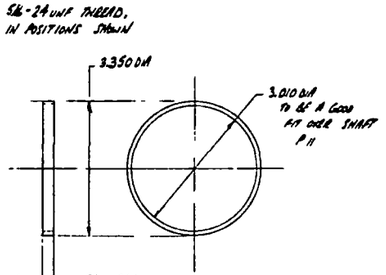

MACHINE WIDTH TO SUIT ON
ASSY FOR ANGULAR
CONTACT PAIR OF BEARINGS

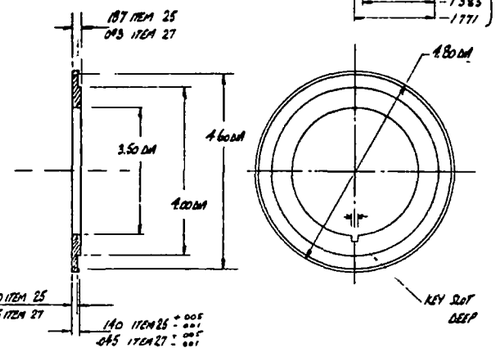

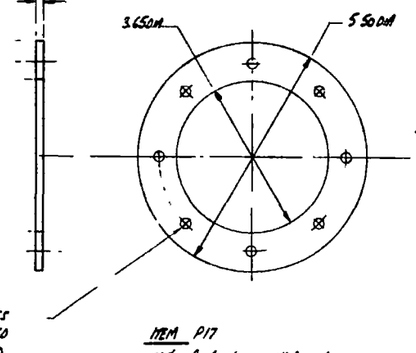

ITEM P17
MAT'L AL ALLOY Nº REQD 1

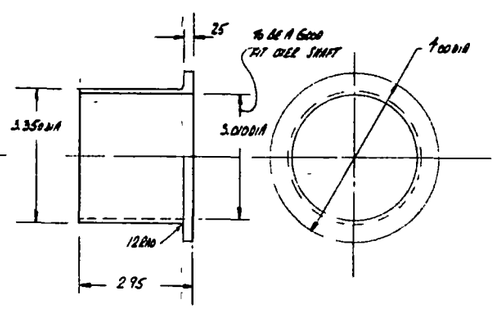

ITEM P19
MAT'L AL ALLOY Nº REQD 1

ITEM 23
MAT'L AL ALLOY Nº REQD 1

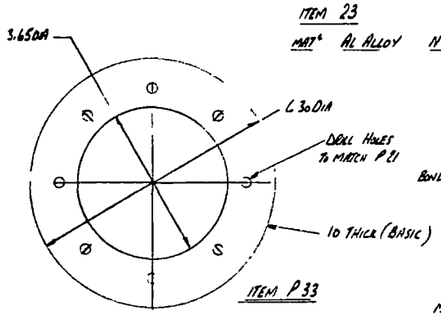

MAKE FROM .003 SHIM STOCK

ITEM P26 & P27
MAT'L TEXTOLITE - EPOXY 11546 G 10
Nº REQD 3 OFF ITEM 8
3 OFF ITEM 9

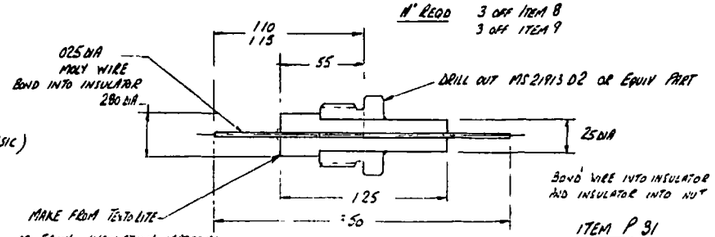

ITEM P 31
MAT'L AS NOTED Nº REQD

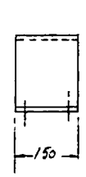

ITEM P23
MAT'L 3003 AL ALLOY Nº REQD 1

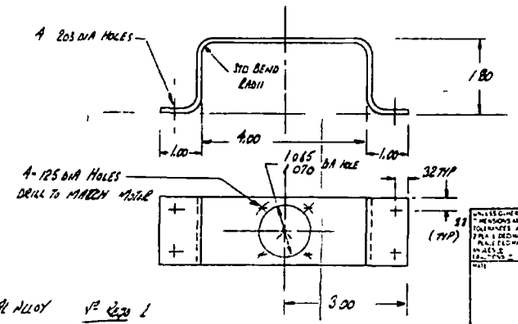

VERIFICATION MODEL

FIGURE 1

GENERAL ELECTRIC	ESD — VALLEY FORGE	
VERIFICATION TEST UNIT		
LIQUID METAL SLIP RING		
SK561197-904		

8

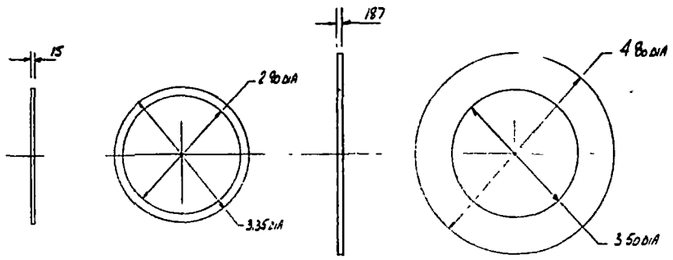

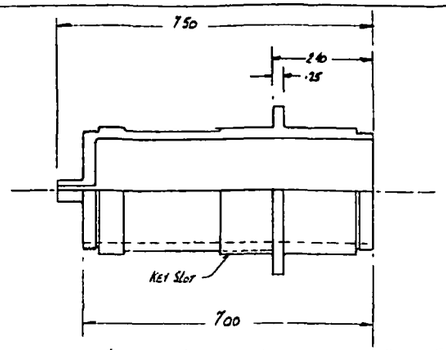

ALTERNATE METHOD OF MANUFACTURING ITEM 11, 13 & 15

FOR ALL OTHER DIMENSIONS SEE SEPARATE DETAILS

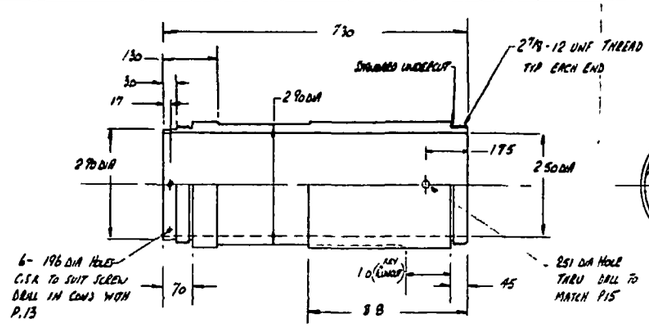

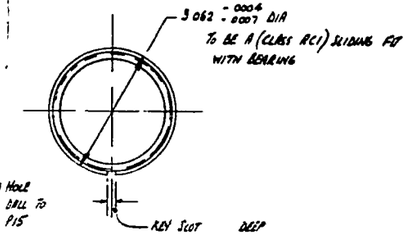

ITEM P 25

MAT'L AL ALLOY Nº REQD 2

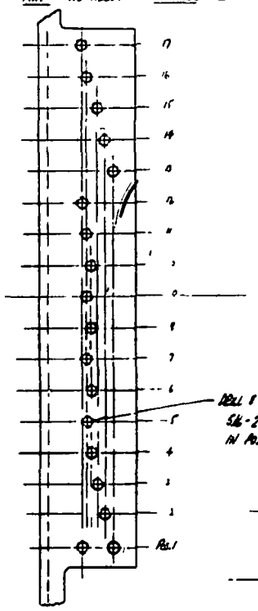

FLAT PATTERN OF P 21

ITEM P 29

MAT'L TEXTOLITE (GRADE 11541)

1 REQD

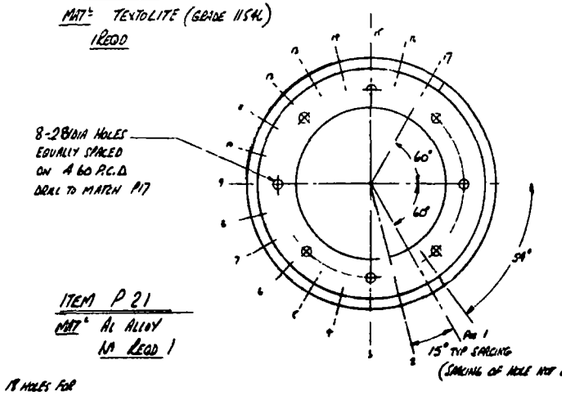

ITEM P 21

MAT'L AL ALLOY

NA REQD 1

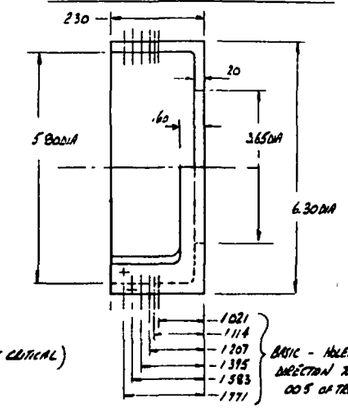

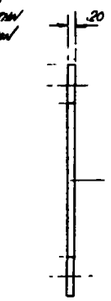

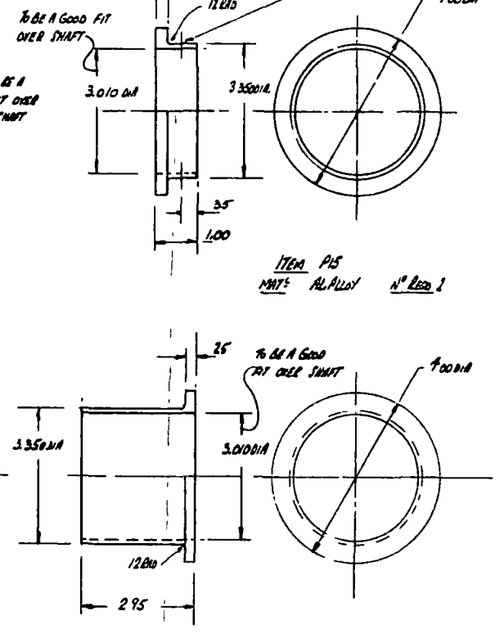

ITEM P 11

MAT'L AL ALLOY Nº REQD 1

ITEM P 13

MAT'L AL ALLOY Nº REQD 2

ITEM P 15

MAT'L AL ALLOY Nº REQD 1

MACHINE WIDTH TO SUIT ON ASSY FOR ANGULAR CONTACT PAIR OF BEARINGS

ITEM 23

MAT'L AL ALLOY Nº REQD 1

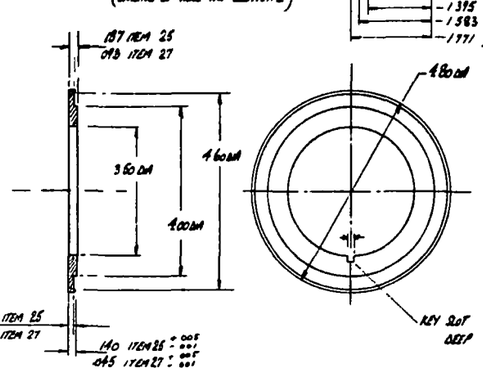

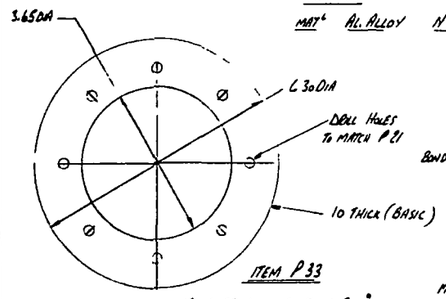

ITEM P 33

MAKE FROM .003 SHIM STOCK

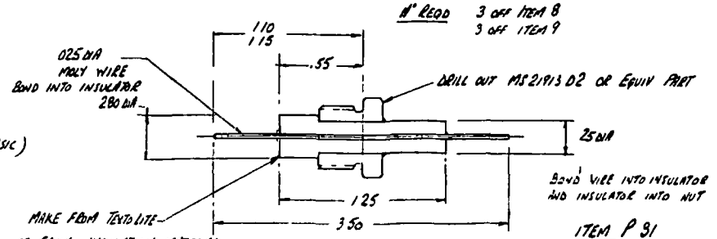

ITEM P 26 & P 27

MAT'L TEXTOLITE - EPOXY 11546 G 10

Nº REQD 3 off ITEM 8
3 off ITEM 9

ITEM P 31

MAT'L AS NOTED Nº REQD

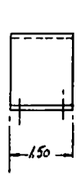

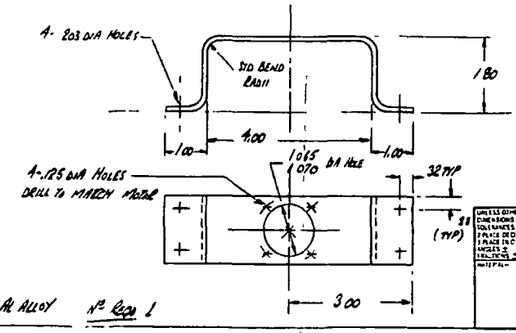

ITEM P 23

MAT'L 0.50 AL ALLOY Nº REQD 1

ITEM P 17

MAT'L AL ALLOY Nº REQD 1

ITEM P 19

MAT'L AL ALLOY Nº REQD 1

VERIFICATION MODEL

FIGURE 2

GENERAL ELECTRIC — SSD — VALLEY FORGE

VERIFICATION TEST UNIT

LIQUID METAL SLIP RING

SK56197-904

9

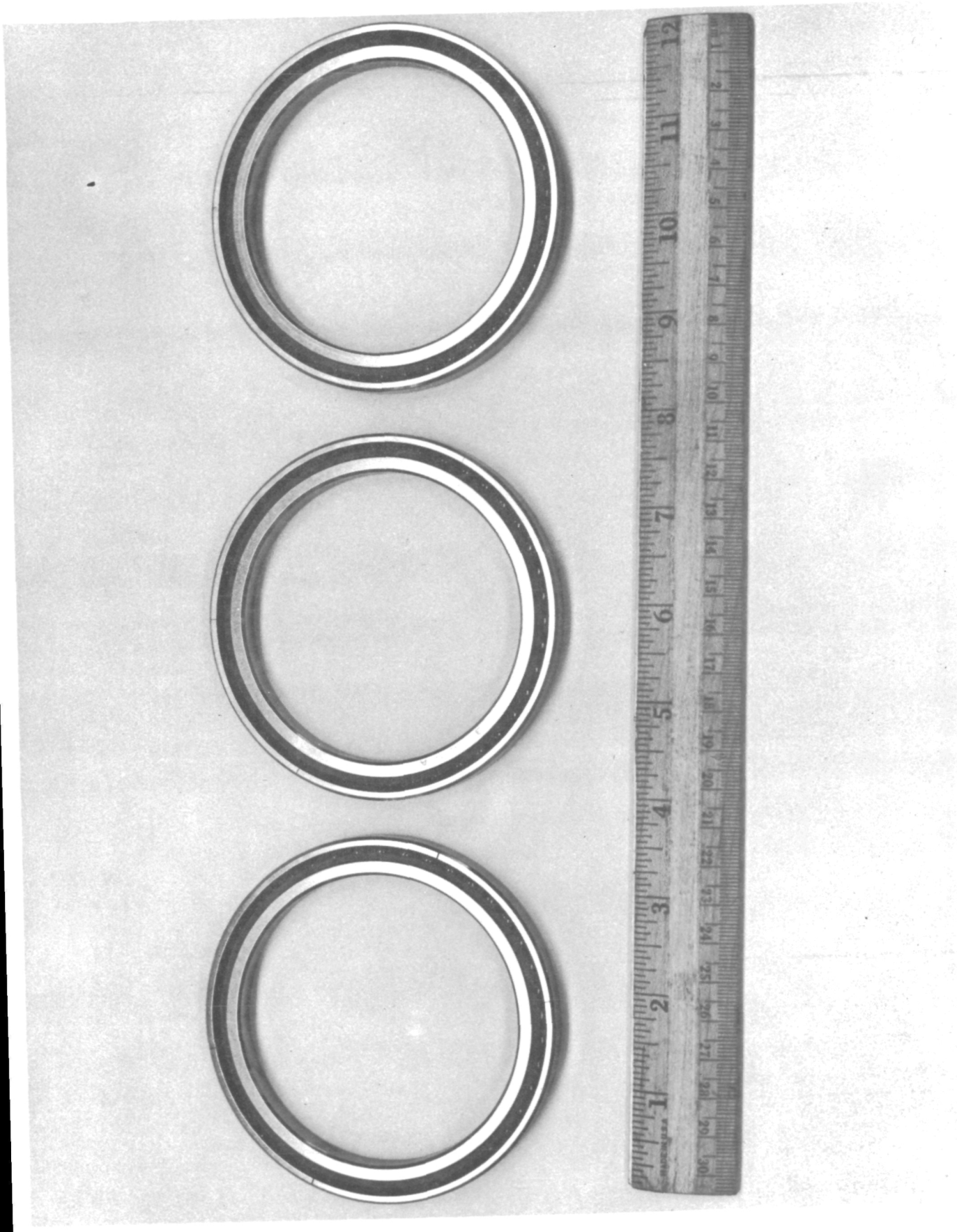

Fig. 3. Verification Model Bearings

epoxy glass, manufactured under the name Textolite, in two thicknesses -- three disks 3/16" thick for 15,000 volt dielectric testing, and three disks 3/32" thick for 3000 volt dielectric testing. The disks were machined such that there was a .020" lip at the outer periphery. This lip served two functions: first, as a labyrinth for contamination retention; and second, to retain the liquid gallium should there be an inadvertent lateral shock applied to the fixture. The disks were held in position on the shaft by means of clamping.

A U-shaped liner, .003 inch thick, was used in the cavity formed by the Textolite disks. Molybdenum was initially selected as the liner material because of its excellent chemical and metallurgical compatibility with gallium; however, 303-series stainless was actually used in the slip ring because of problems in procuring a molybdenum liner. Metallurgical and test data had indicated that 300-series stainless was a satisfactory electrode material for use with gallium. The liner served to retain the gallium by being wetted at the bottom and by having the oxide at the top. The use of the liner also eliminated problems of potential gallium leakage between disks. Figures 4 and 5 show disks, liners and probes. Handling and filling techniques and oxide removal procedures were established for loading the rings with gallium.

As shown in Figures 6, 7 and 8 an external shell was mounted on the fixture base and was concentrically located around the shaft. Part of the shell was cut away to further aid in visual inspection of probes and gallium during testing.

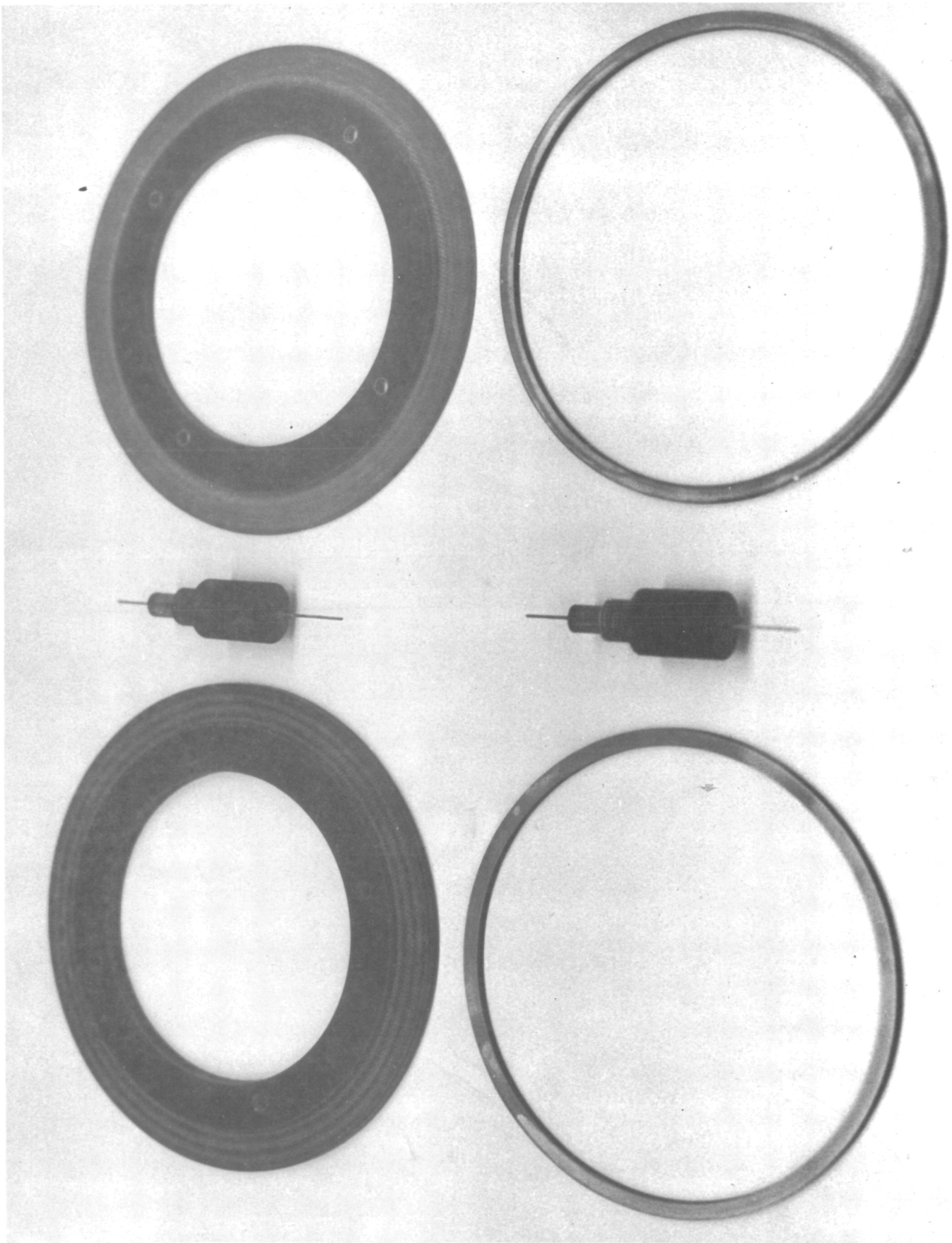

Fig. 4. Verification Model Disks, Liners and Probes

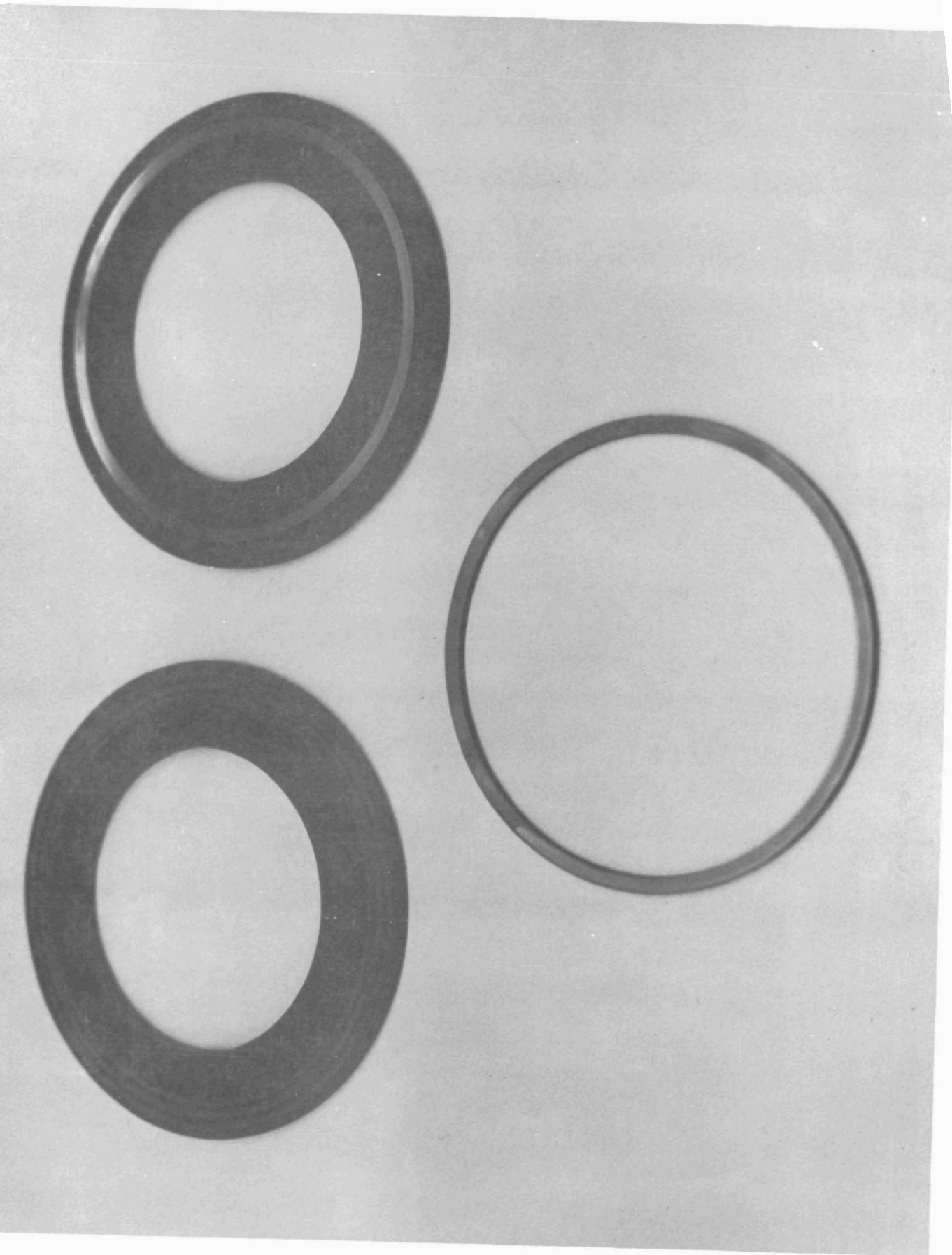

Fig. 5. Verification Model Disks and Liners

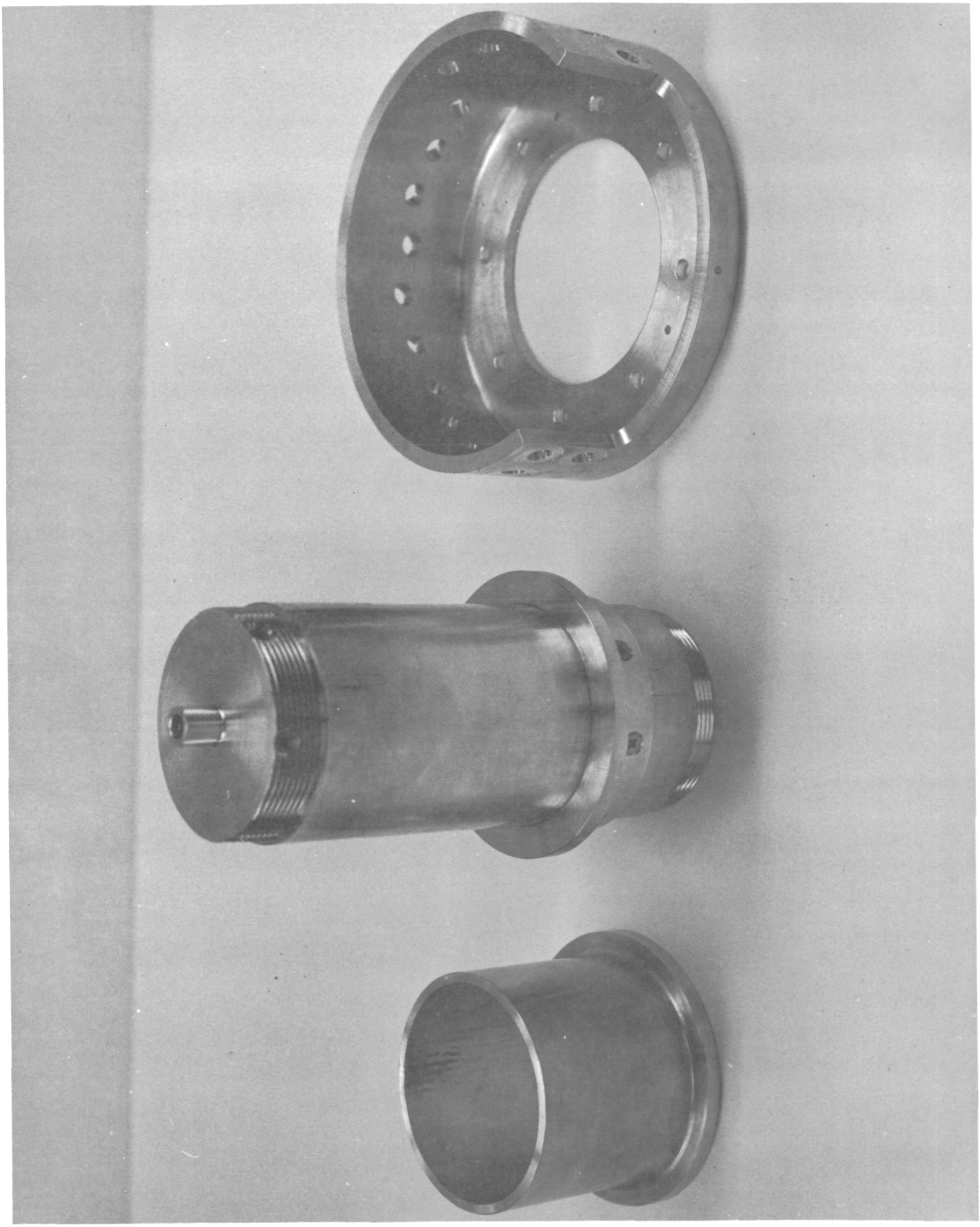

Fig. 6. Shaft and Shell

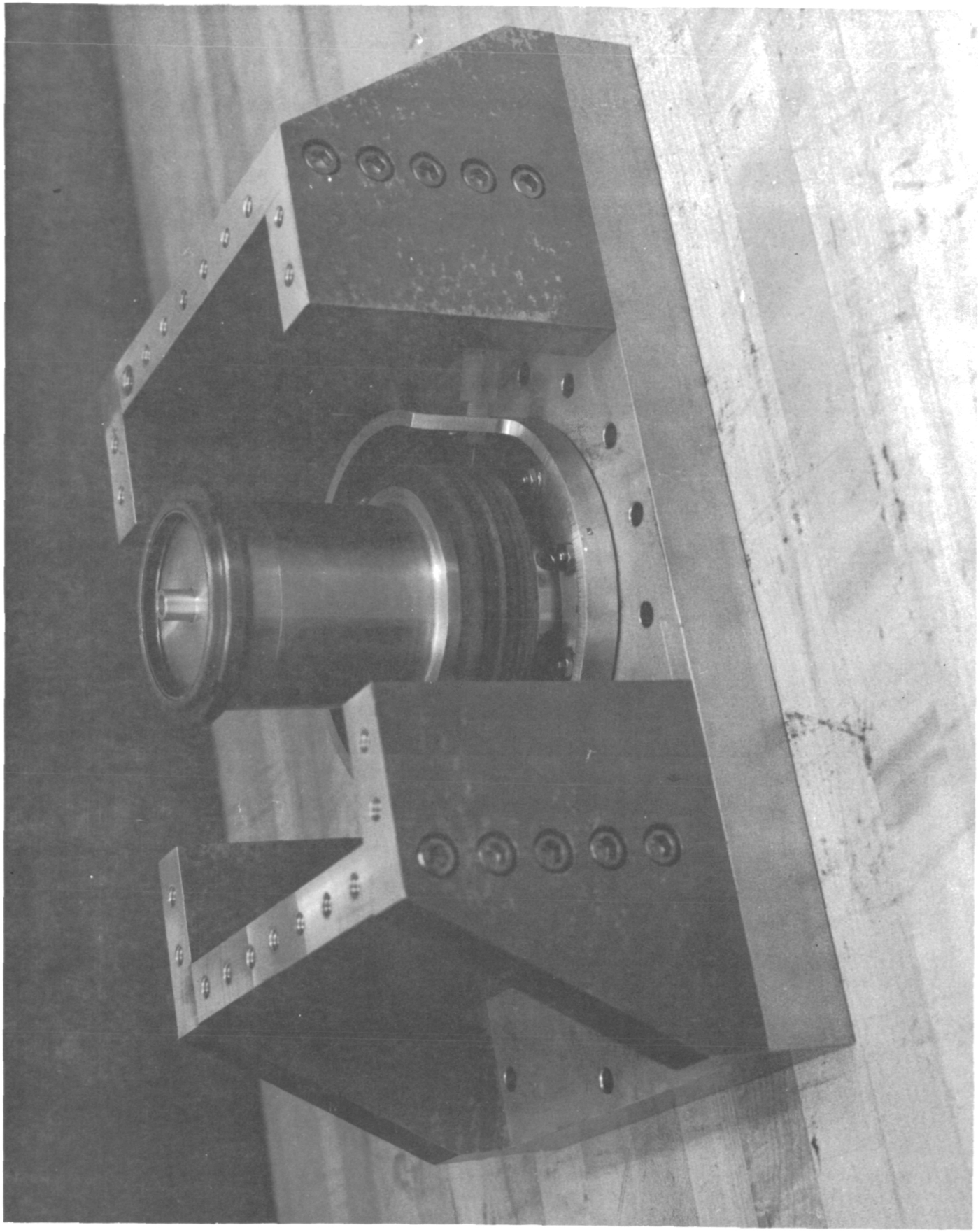

Fig. 7. Partially Assembled Verification Model

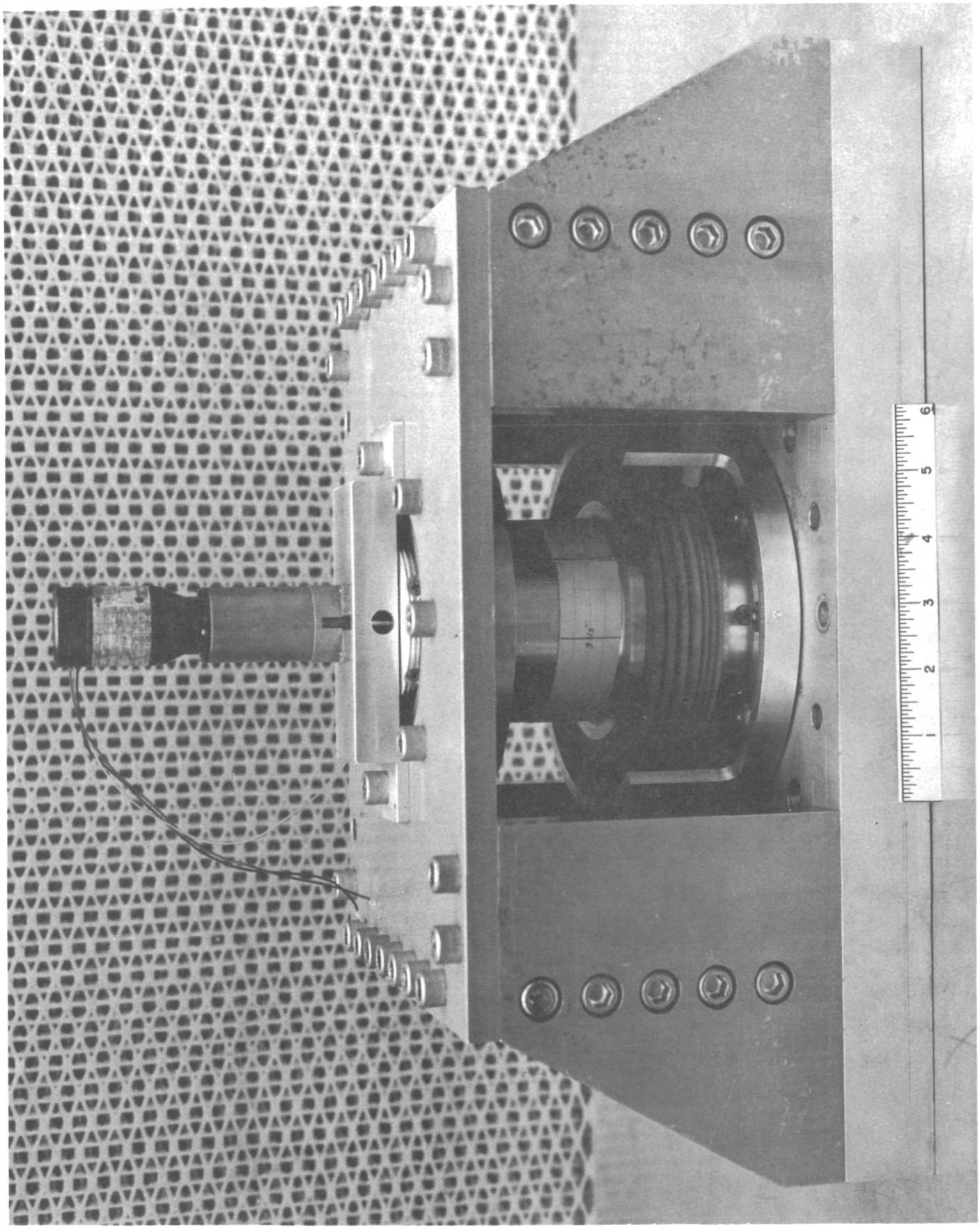

Fig. 8. Verification Model

This shell was drilled and tapped to permit installation of the probes. The probes were spaced radially around the shell to simulate their actual locations in the slip ring. The angular spacing varied from 30° to 180° for different rings. The number of probes per ring were between two and four, depending on their angular spacing. Three rings had two probes, one ring had three probes, and two rings had four probes.

The drive motor was mounted on top of the fixture. It was mounted on a bracket which was removable during the vibration and shock tests. The motor drive was a 60 Hz, 115 volt hysteresis synchronous motor. The rotational speed was reduced to 1 revolution per day through a planetary gear integrally mounted with the motor. The bearing and gear were lubricated by the motor vendor TRW/Globe, with a proprietary lubrication system which was suitable for vacuum operation.

Vibration tests were performed on a C-150 MB shaker. The fixture hole pattern permitted direct mounting to shaker head.

Task 2, Design Verification, was an effort in which a model of the design concept selected, as a result of the Task 1 work, was built and tested to verify the basic integrity of the design concept with respect to dielectric strength, vibration, acceleration, shock, vacuum rotation and debris formation.

Task 3, Detail Design, consisted of making detail design drawings of the selected design concept.

3.2.2 Wetting & Filling Procedures

WETTING & FILLING PROCEDURE FOR 300-SERIES STAINLESS STEEL LINER RINGS

1. Clean rings ultrasonically with acetone for 10 minutes.
2. Sandblast inner ring surfaces with slurry of 10 micron mesh size quartz grit in water. Use approximately 30 psi air pressure.
3. Rinse sandblasted rings immediately in deionized water.
4. Transfer rings to container containing methanol, keep rings submerged until ready for use.
5. Melt and maintain gallium at 175° - 200°F.
6. Dry and heat ring to 100°to 120°F.
7. Place a lint-free cotton cloth securely on a holder and wet cloth with gallium. Insert cloth into the ring groove and rub all inner surfaces until good wetting is obtained.
8. Transfer ring to freezer until ready for fitting.
9. Close ring groove opening with neoprene gasket allowing desired depth at bottom of ring for gallium. Leave small opening in gasket.
10. Warm ring to approximately 150°F.
11. Load a syringe with melted gallium taken from center of gallium pool. Inject gallium into the ring groove through opening in neoprene gasket. Tap lightly to force out any trapped air.
12. Freeze ring and remove neoprene gasket.
13. Machine gallium from sides of ring cutting slightly into stainless. Machine top surface of gallium. Keep gallium frozen during machining with dry ice in ring support fixture.

GALLIUM WETTING PROCEDURE FOR MOLYBDENUM PROBE WIRE

1. Clean molybdenum wire with "X-acto" knife by scraping off epoxy resulting from the probe casting process.
2. Mount probe in lathe and abrade molybdenum wire with fine India stone to remove any remaining epoxy and any scale or oxide build-up.
3. Clean ultrasonically for 10 minutes with Genesolv "D" as a solvent.
4. Place tip of molybdenum wire in 1/2" diameter pool of liquid gallium and abrade end of wire under the gallium with "X-acto" knife. Rotate wire while abrading. Maintain gallium liquid with infra-red lamp.
5. Verify wetting by removing wire from gallium and examining microscopically for complete gallium coverage. Wipe end of probe gently with "kim wipe". Redip in gallium and re-examine for coverage.
6. If wetting is not complete, repeat abrading procedure.
7. When wetting is satisfactory, remove excess gallium by shaking.
8. Place probe in polyethelene bag, freeze and store frozen.

This procedure was followed and appeared to provide satisfactory wetting of the probe wire, and can be utilized in future work with molybdenum wire probes.

ALTERNATE GALLIUM WETTING PROCEDURES FOR MOLYBDENUM WIRE

The following procedures were recommended by a vendor to remove the oxide from molybdenum. Although these procedures were abandoned in preference to abrading the wire under a pool of gallium, they are of interest and perhaps could be implemented after some initial experimentation.

1. Electrolytic polish technique

   Place equal volumes of water and NaOH in a beaker. Place molybdenum in beaker and connect to positive terminal of 6 volt battery. Place stainless steel electrode in beaker and connect to negative terminal of battery.

   Results:

   This procedure was followed but resulted in attack upon molybdenum wire. As an alternative to water and NaOH, 10% H_2SO_4 and methyl alcohol was suggested. However, this was not tried.

2. Chemical cleaning

   (a) Make a solution of

   10 parts NaOH

   30 parts potassium ferricyanide

   100 parts water

   Dip molybdenum into solution for several minutes, wash with cold water, 10% HCl and cold water again.

   This procedure was not tried.

(b) Place equal volumes of water and NaOH in a beaker and insert molybdenum wire in solution for several minutes. Wash thoroughly with water. This procedure produced no noticeable reaction with surface oxide.

(c) Make a solution of

50% HF

30% HNO_3

20% water

Dip molybdenum wire into solution for several minutes. Then wash thoroughly with water. This procedure resulted in attack upon the molybdenum wire.

Although these procedures were recommended by a vendor of molybdenum, none appeared to work satisfactorily. The reason for this is not known but may be due to the fact that the procedures were developed for other forms of molybdenum, such as sheets or strips and would require some modification for thin wires.

3.3 Tests

3.3.1 Dielectric Tests

Dielectric tests were run on the verification model to verify the dielectric characteristics of the insulation as well as the electrode and probe spacings in both air and vacuum. The initial dielectric testing was performed in air under room conditions of temperature, pressure and humidity. There was no gallium in the electrode rings in order to simplify handling and to preclude the possibility of gallium inadvertently melting and spilling. Electrical contact was made between the probe wires and rings by bending the probe wires slightly. Electrical contact between the probe wires and electrodes was checked by measuring continuity using an ohmmeter.

The test voltages were obtained with a DC dielectric test set capable of output voltages from 0 to 30 kv. The test set is equipped with a circuit breaker that will trip if there is a breakdown. A micro-ammeter as well as provision for four milliamps were placed in the circuit in order to be able to monitor current continuously so that any incipient breakdown could be detected. The meters had the following ranges: 0 - 50 micro-amps, 0 - 1 milliamps, 0 - 10 milliamps, 0 - 50 milliamps and 0 - 100 milliamps. See Fig. 9.

Fig. 9. Air Dielectric Test of Verification Model

The dielectric test voltage was applied two ways: probe to probe and probe to ground. The verification model was designed with insulations and spacings to withstand two different voltage levels, 15,000 volts and 3000 volts. The magnitude of the test voltage was 15,000 and 4000 volts depending upon the design levels. In addition, in order to determine the ultimate dielectric capability of insulation system, the voltage on the 15,000 volt rings was raised until there was indication of incipient breakdown as determined by a spitting or hissing sound.

The dielectric voltage was applied using a controlled rise time in order to preclude a breakdown due to the imposition of a step-function of voltage. Similarly, the decay time at test voltage was a minimum of 3 seconds.

A summary of the air dielectric tests and test results is given below:

Air Dielectric Test

Conditions:	Room temperature and pressure
	No gallium in rings
	Probes bent slightly to make contact with liner
Test Equipment:	DC Test Set 0 - 30 kv
	DC milliammeter 0 - 100 ma

Voltage Application: Probe to probe

Probe to ground

Rise time

High voltage rings - 15 seconds

Very high voltage rings-- 30 seconds

Hold time - 3 minutes, at test voltage, minimum

Decay time - 3 seconds

Test Procedure: Voltage was applied, probe to probe or probe to ground and increased slowly (15 to 30 seconds) until test voltage was reached. The test voltage was held for three minutes, minimum. For some rings, the voltage was then increased further until there was evidence of incipient breakdown. The voltage was reduced to zero in approximately 3 seconds.

Test Results:

Probes Very High Voltage Rings	Test Voltage	Breakdown Voltage
1 - 2	15,000	17,000
2 - 3	15,000	18,000
3 - 4	15,000	18,000
1 - ground	15,000	18,000
2 - ground	15,000	17,500
3 - ground	15,000	17,000

The physical location on the slip ring of the voltage breakdown could not be determined because of limited visibility and access dictated by consideration of safety.

High Voltage Rings	Test Voltage
4 - 5	4,000
5 - 6	4,000
4 - ground	6,000
5 - ground	6,000
6 - ground	6,000

Upon completion of the dielectric tests in air, the verification model was disassembled and cleaned. The rings were wet and filled with gallium and the probes were wet with gallium. The model was then reassembled, mechanically checked out and dielectric tests run, first in air as a check on the previously run dielectric tests and then in vacuum. The air and vacuum dielectric tests in this series of tests were run in similar manner as the previous dielectric tests.

The dielectric test methods and results for air and vacuum tests are summarized as follows:

Air & Vacuum Dielectric Tests

Conditions:	Gallium in rings, melted Atmospheric pressure & vacuum Room temperature Model mounted in vacuum chamber
Test Equipment:	DC Test Set 0-30 KV DC milliammeter 0-100 ma

Voltage Application:

Probe to probe
Probe to ground
Rise time
  High voltage rings - 15 seconds
  Very high voltage rings - 30 seconds
Hold Time - 3 minutes, at test voltage, mimimum
Decay Time - 3 seconds

Test Procedure:

Voltage was applied, probe to probe or probe to ground and increased slowly (15 to 30 seconds) until test voltage was reached. The test voltage was held for three minutes, minimum. For some rings, the voltage was then increased further until there was evidence of incipient breakdown. The voltage was reduced to zero in approximately 3 seconds.

Results:

- Conditions - Air, normal pressure & temperature

Very High Voltage

Rings	Test Voltage	Breakdown Voltage
1-2	15,000	Not run
2-3	15,000	17,000
3-4	15,000	16,000
1-ground	15,000	Not run
2-ground	15,000	18,000
3-ground	15,000	17,000

High Voltage

Rings	Test Voltage	Breakdown Voltage
4-5	6,000	Not run
5-6	6,000	Not run
4-ground	6,000	17,000
5-ground	6,000	Not run
6-ground	6,000	Not run

- Conditions - Vacuum 10^{-6} torr

Very High Voltage

Rings	Test Voltage	Breakdown Voltage
2-3	15,000	Not run
3-4	Not run	13,200
2-ground	15,000	Not run
3-ground	Not run	13,200

High Voltage Rings	Test Voltage	Breakdown Voltage
4-5	6,000	Not run
5-6	6,000	Not run
4-ground	6,000	13,200
5-ground	6,000	Not run
6-ground	6,000	Not run

It will be noted that there was a slight degradation in breakdown of dielectric characteristics in vacuum as compared with air. The reason for this is not known, especially since it occurred on one set of rings and not on the other. Since the model was mounted in the vacuum chamber, there was restricted visual access and it was not possible to see where the breakdown was taking place.

Although the requisite test voltages were run on all rings, breakdown voltage tests were not run on all rings. Breakdown tests were not run in order to preclude permanent damage to the insulation which might occur due to the arcing which accompanies the breakdown.

3.3.2 Acceleration, Vibration & Shock Tests

Acceleration, vibration and shock tests were performed on the verification model in order to verify the integrity of the mechanical design under conditions simulating the pre-launch, launch and operating environments to which the slip ring will be subjected. To date, no dynamic tests had been run on any slip ring configuration to determine what the characteristics of the frozen gallium and liquid gallium were. There was some concern that under acceleration, vibration or shock tests, solid gallium in the electrode cavities could crack, chip or possibly extrude. With the gallium liquid, the concern related to a gallium spillage due to sloshing of the gallium in the electrode cavity due to applied acceleration or resonance effects.

3.3.2.1 Vibration and Acceleration Tests - Gallium Liquid

Vibration and acceleration tests were run on the verification model with the gallium liquid with motion in the two horizontal axes, lateral and transverse. Two horizontal axes were run primarily because the probes were not symmetrically placed around the periphery of the electrode rings and it was desirable to determine whether this unsymmetrical probe arrangement would cause a difference in gallium motion. Because of the set-up of the test equipment, it was not possible to run low frequency vibration in the vertical axis. Acceleration was run only in the horizontal axis since with this ring configuration and its dimensions the capillary forces are not sufficient to retain the gallium in a 1-g field when the verification model is mounted on its side.

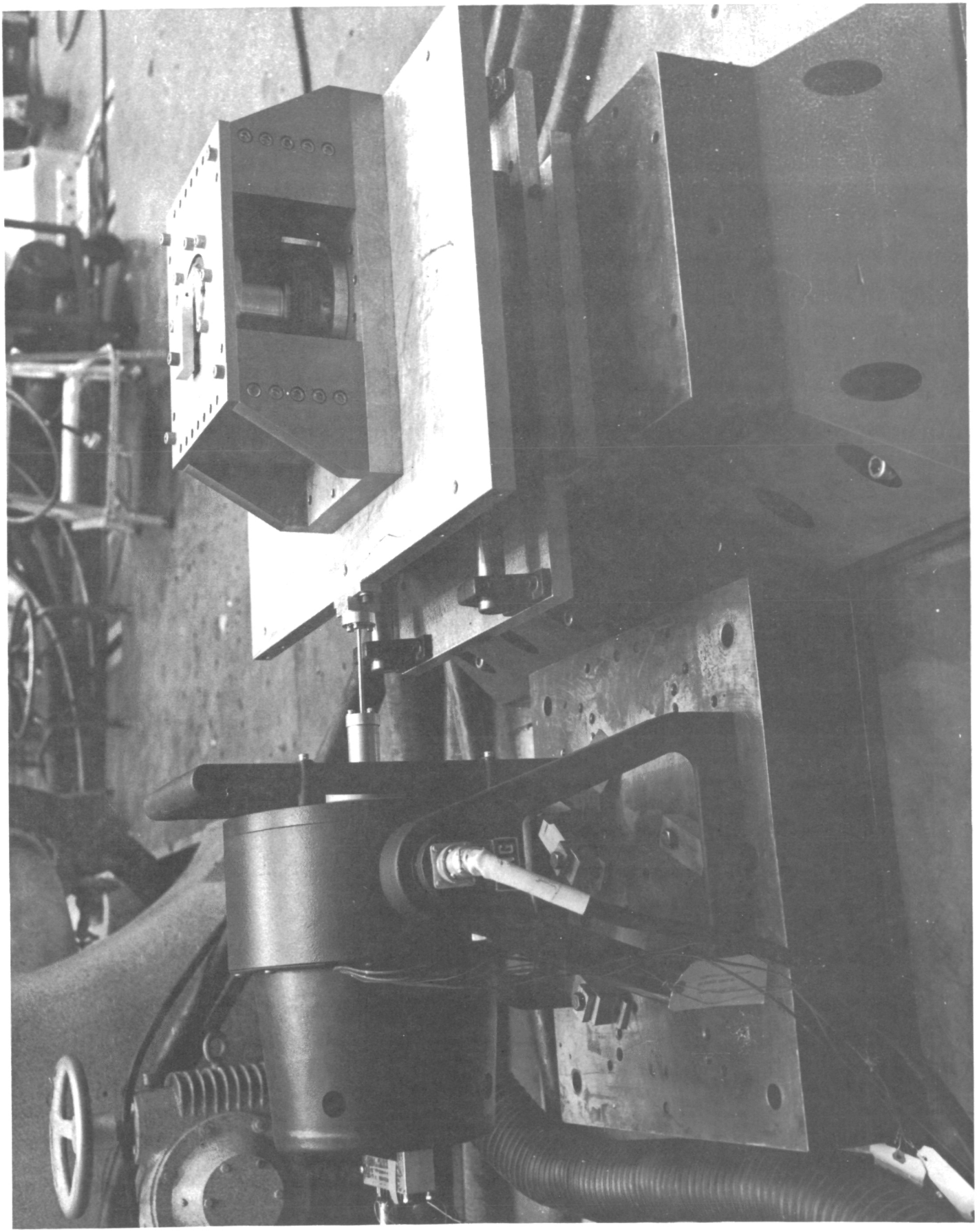

Fig. 10. Vibration Test, Gallium Liquid

The results of the tests are summarized as follows:

Vibration Test, .008 Hz to 4 Hz

Conditions: Gallium liquid

Rings horizontal (axis of rotation along local gravity vector)

Test Equipment: Ling Shaker

Bafco & CGS Controls
(See Fig. 10)

Test Procedure: Input - Sine wave

Frequency Range - .008 Hz to 4.0 Hz

Vibration Level

.008 Hz to .064 Hz, 3" p-p

.128 Hz to 4 Hz, 10^{-3} g

Time at each frequency

10 cycles or 10 minutes, whichever is longer

Two horizontal axes, lateral & transverse

Gallium visually observed during test

Results:

Frequency (Hz)	Amplitude (Inches - Double Amplitude)	Acceleration	Remarks	
			Lateral Axis	Transverse Axis
.008	3.0	10^{-5}	No movement of gallium	
.016	3.0	4×10^{-5}	Slight ripple in Ring 3, perhaps due to table uneveness	
.032	3.0	1.5×10^{-4}	Slight ripple in Ring 3, perhaps due to table uneveness	

Results:

Frequency (Hz)	Amplitude (Inches - Double Amplitude)	Acceleration	Remarks	
			Lateral Axis	Transverse Axis
.75	.034	10^{-3}	No movement of gallium	
1.0	.019			
1.25	.012			
1.50	.0085			
1.75	.0062			
2.00	.0048			
2.25	.0038			
2.50	.0030			
2.75	.0025			
3.00	.0021			
3.25	.0018			
3.50	.0016			
3.75	.0014			
4.00	.0012			

There was no evidence of sloshing or instability in the test regime. The unit passed vibration test requirements.

Vibration Test, 20 Hz to 2000 Hz

Conditions:

Gallium liquid

Rings horizontal (axis of rotation along local gravity vector)

Room temperature and pressure

Vibration Test, 20 Hz to 2000 Hz (Continued)

Test Equipment:	MB C 150 vibration system
Test Procedure:	Input, Sine wave
	Frequency range, 20 - 2000 Hz
	Rate of scan - 1 octave per minute
	Acceleration level - 0.1 g
	Horizontal axis and vertical axis
Results:	When vibrated along horizontal axis, there was a slight ripple in ring number 5 only, between 20 and 40 Hz. Rippling amplitude decreased as frequency increased. No evidence of rippling above 40 Hz.
	When vibrated along vertical axis, there was no evidence of rippling at any frequency.
	The unit passed .1 g vibration requirement.

Acceleration

Conditions:	Gallium liquid
	Axis of rotation vertical
	Room Temperature and Pressure
Test Equipment:	Rucker RCT-2 Centrifuge See Figs. 11 and 12

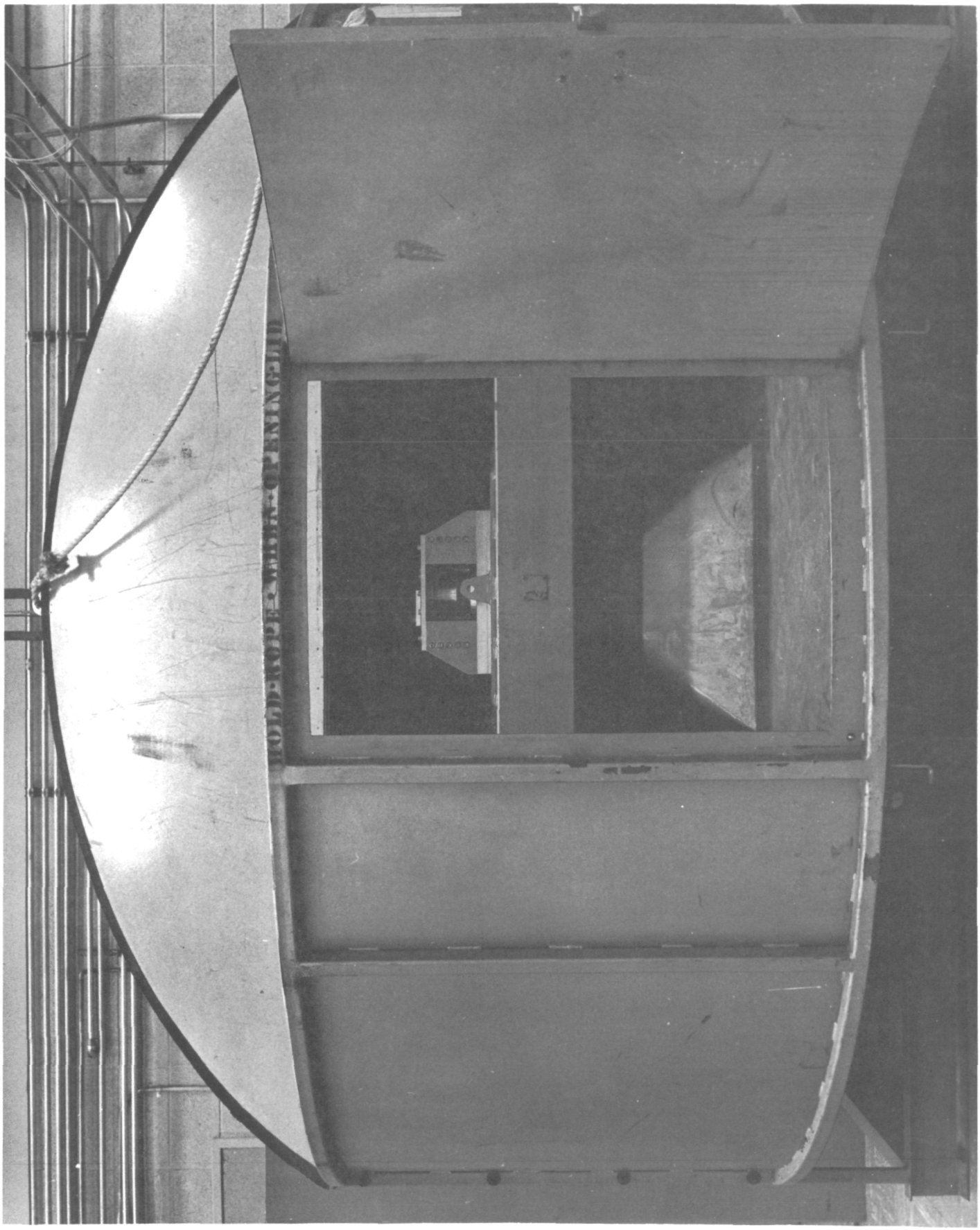

Fig. 11. Acceleration Test

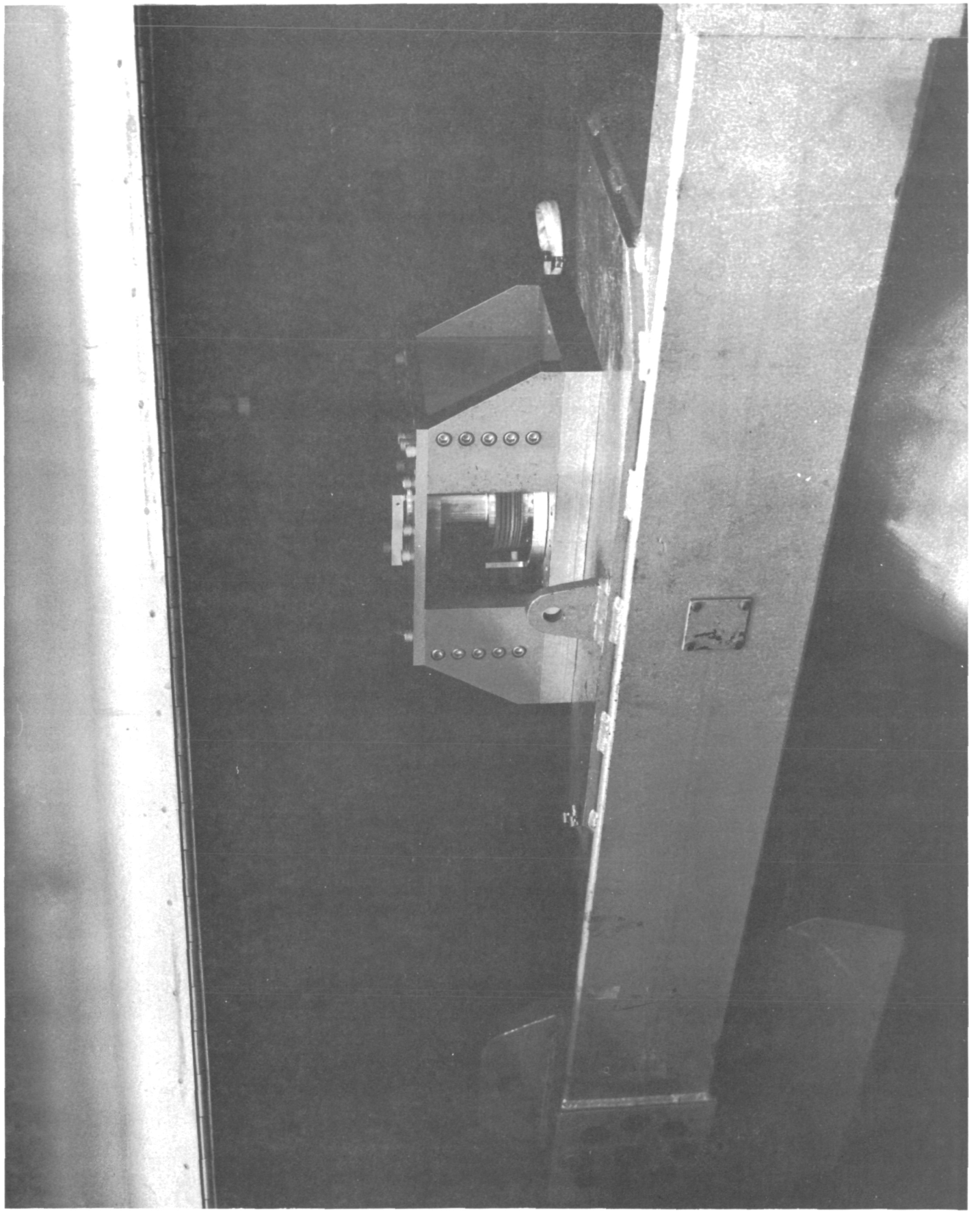

Fig. 12. Acceleration Test

Test Procedure:	Slip ring mounted in centrifuge, 8 1/4" from center of rotation to center of slip ring shaft.
	Speed of centrifuge increased slowly to 2.5 rpm (1.4×10^{-3}g). Held at 2.5 rpm for 15 minutes.
	Speed increased to 3.0 rpm (2.0×10^{-3}). Held at 3.0 rpm for 5 minutes.
Results:	No evidence of gallium instability or spillage.
	The unit passed 10^{-3} g acceleration requirement.

3.3.2.2 Vibration, Acceleration and Shock - Gallium Solid

Vibration, acceleration and shock tests were performed on the verification model with the gallium solid. The vibration and acceleration tests were performed along one horizontal and one vertical axis. Because of symmetry in the horizontal axis, it was not considered important to test along the orthogonal horizontal axis. The shock test was performed along three axes, two horizontal and one vertical. In order to be assured that the gallium remained solid for the duration of the testing, the verification model was cooled by soaking for two hours in a container of dry ice.

Vibration Test

Conditions: Gallium solid
Rings horizontal
Room temperature & pressure

Test Equipment: MB C150 Vibration System
See Figs. 13 and 14

Test Procedure:

Sinusoidal

Frequency Range (Hz)	Level g, (O-P)	Sweep Rate Octaves/Minute
5 - 10	0.9 in D. A.	2.0
10 - 50	±4 g	2.0
50 - 200	±3	2.0

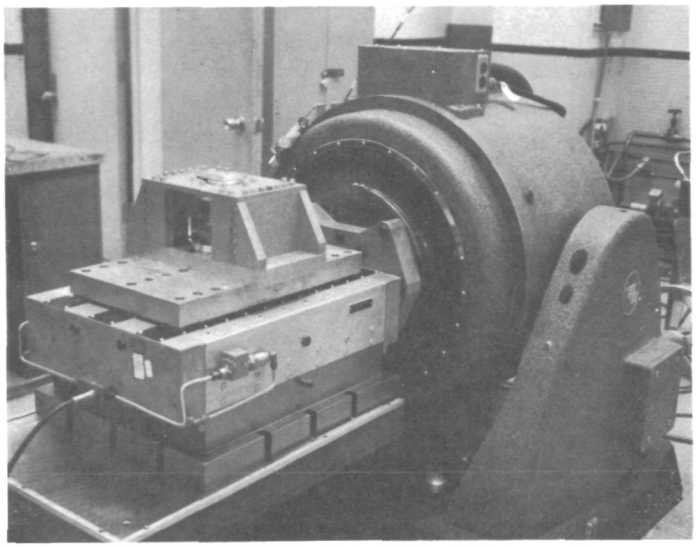

Fig. 13. Vibration Test, Gallium Solid, Horizontal Axis

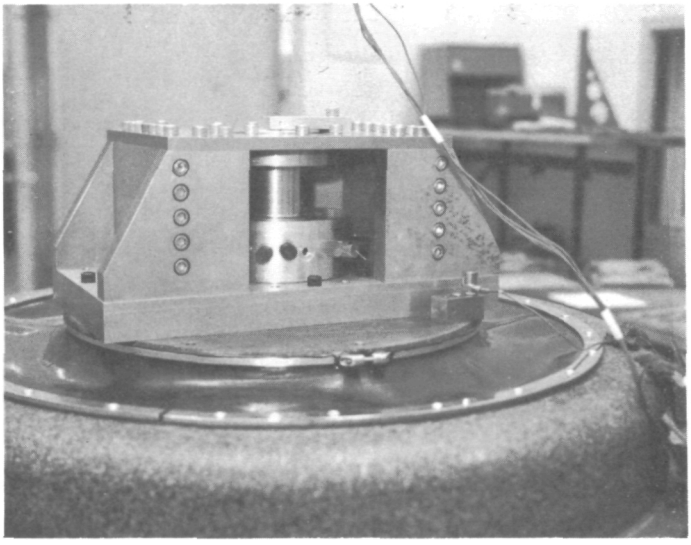

Fig. 14. Vibration Test, Gallium Solid, Vertical Axis

Random

Frequency Range (Hz)	PSD Level g^2/Hz	Acceleration (g-rms)	Duration
20 - 250	0.001 to 0.16 increasing from 20 Hz at a rate of 6 dB/octave	17.0	4 minutes each axis
250 - 2000	.16 roll off above 2000 Hz greater than 40 dB/octave		

Results: Axes - Horizontal & Vertical

No evidence of gallium cracking, chipping, flowing, etc. Probes, disks, hardware and structure show no evidence of degradation.

The unit passed vibration requirement.

Acceleration

Conditions: Gallium solid

Rings horizontal

Room temperature and pressure

Test Equipment: Rucker RCT-2 Centrifuge
See Figs. 11 & 12

Test Procedure: Slip ring mounted in centrifuge, 36 inches from center of rotation to center of slip ring shaft.

Speed of centrifuge increased slowly to give 5g acceleration and held for 1 minute. Centrifuge stopped slowly and slip ring examined. Repeated for 10g level for

1 minute. Repeated 15g level, held for 5 minutes. Test with slip ring axis vertical and horizontal.

Results: No evidence of gallium cracking, chipping, flowing, etc. Probes, disks, hardware and structure show no evidence of degradation.

The unit passed 15g acceleration requirement.

Shock Test

Conditions: Gallium solid
All axes
Room temperature and pressure

Test Equipment: CEC 6" HYGE Shock Tester

Test Procedure: 22g, 1/2 sine wave
11 millisecond duration

Results: No evidence of gallium cracking, chipping, flowing, etc. Probes, disks, hardware and structure show no evidence of degradation.

The unit passed shock requirement.

3.3.3 Vacuum Rotation Tests

Rotational tests were run in vacuum in order to determine whether contamination was formed continuously and whether there would be any balling up and ejection of the contamination. The rotational rate was 1 revolution per day. No current was applied to the rings nor was any voltage applied between rings during the rotational tests.

The rotational tests were run after the completion of all other tests. Purposely, no effort was made to clean up any contamination which may have formed on the surface of the gallium (a) during the vibration and acceleration tests which were run with the gallium liquid or (b) during successive gallium melting and freezing cycles which were necessary to permit handling the model.

The verification model was instrumented with thermocouples on the motor and structure. In order to prevent possible gallium freeze-up during the test, the model was mounted on a water heated platen. Even though the drive motor was supposed to operate in a vacuum environment, a water jacket, through which cooling water flowed, was placed around the drive motor in order to maintain a low temperature during test and to prevent a possible failure in the motor due to overheating. See Figs. 15 and 16.

With the model in the diffusion pump vacuum chamber and the gallium frozen, the chamber was pumped down. After a vacuum of 10^{-4} torr was achieved, the gallium was melted by passing hot water through the heating platen.

The water was allowed to flow for twelve hours at which time it was determined that the gallium was melted based on the structure temperature being 100°F and stabilized for two hours and a movement of the gallium in all rings was observed when the chamber was jarred slightly. The drive motor was then energized and rotation observed.

Although the diffusion pump vacuum chamber used for the verification model is capable of maintaining a vacuum of 10^{-6} torr, there was an outgassing of the model which resulted in a working vacuum of 10^{-4} torr. The outgassing was identified as resulting from the probe assembly by placing similar probe assemblies into another vacuum chamber and noting that a vacuum below 10^{-4} could not be reached. An investigation was undertaken to determine the exact cause of the probe outgassing. The results were as follows:

The probe assembly consists of a molybdenum wire cast into a plastic holder and oven cured. The materials, casting and curing procedure were as follows:

Probe Wire:	.025" diameter, molybdenum
Holder:	Epon 815, TETA curing agent, Shell Chemical Co.
	LP 3 - (Flexibilizer) polysulfide polymer,
	Thiokol Chemical Co.

Cast and evacuated at 10 - 20 mm Hg prior to curing.

Over cured at 150°F

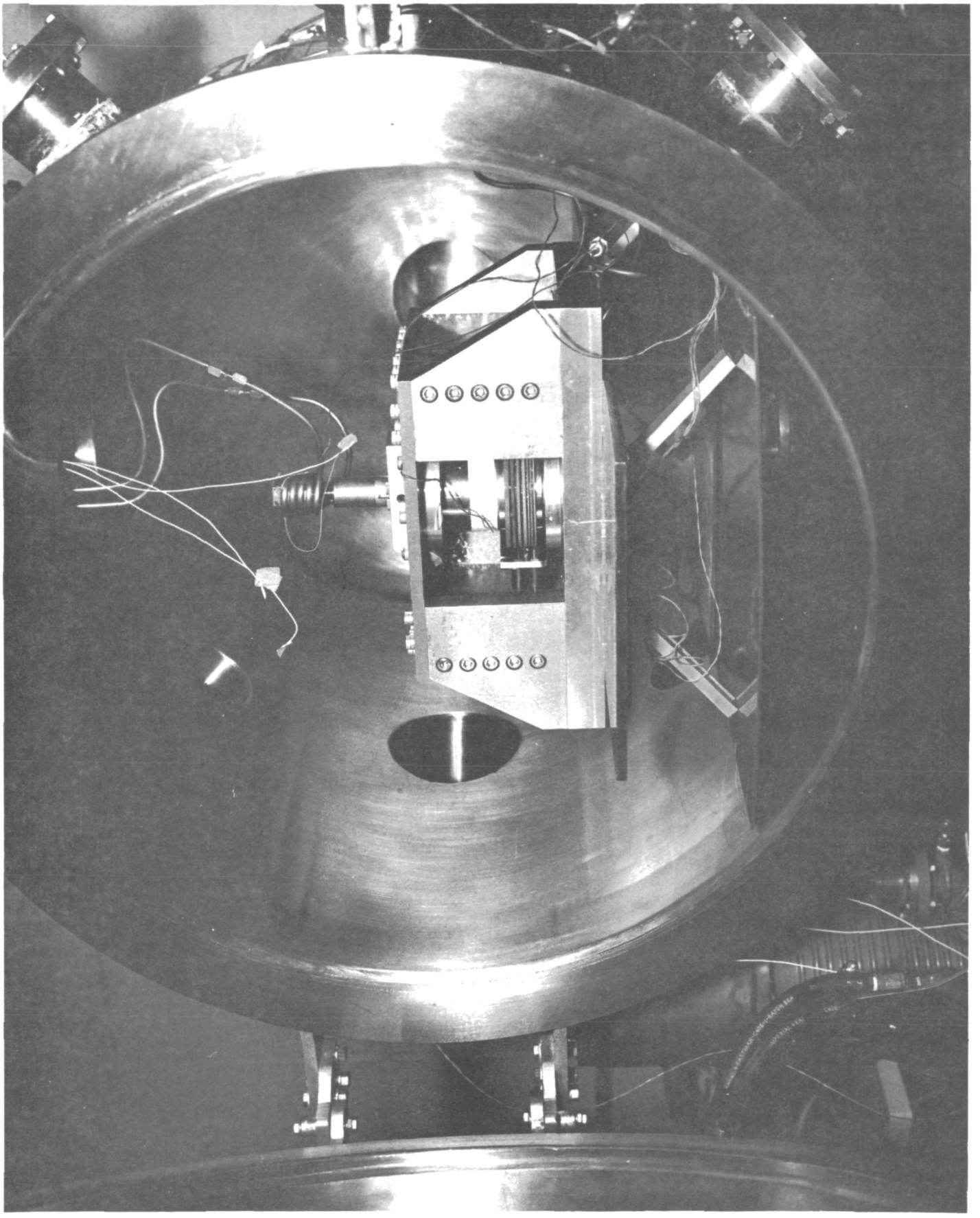

Fig. 15. Verification Model in Vacuum Chamber

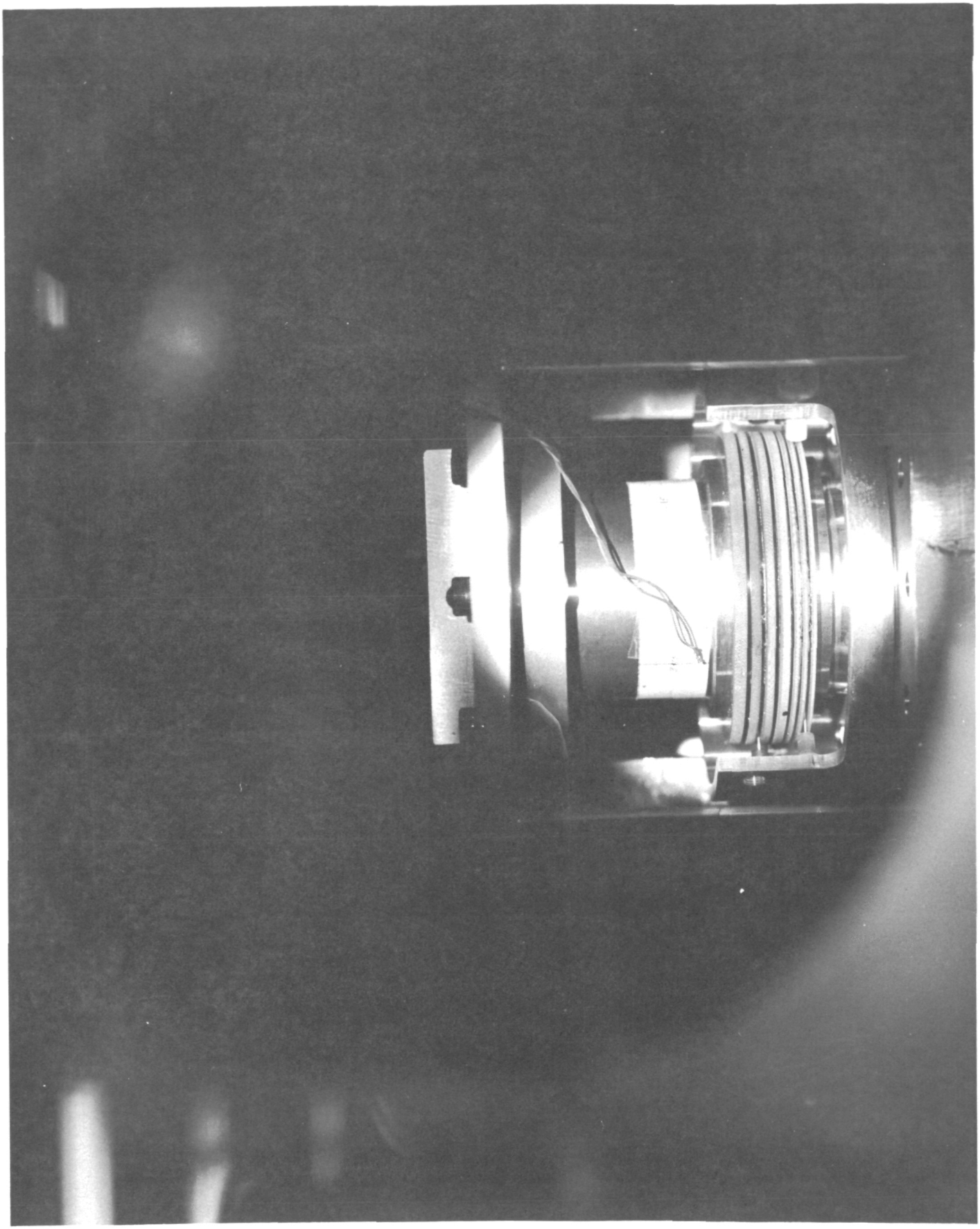

Fig. 16. Verification Model Viewed Through Chamber Port

Epon 815 is a satisfactory material for vacuum applications. However, in order to reduce the brittleness and to permit the machining of the holder, a flexibilizer, LP 3, was added to the Epon 815. It is believed that the addition of the LP 3 is the primary cause of the outgassing of the probe assembly, since LP 3 tends to outgas. The outgassing problem can be remedied by a change of materials, for example, to Versamid 140, Epon 828 and TETA.

After 4 weeks of rotation at 1 revolution per day in a vacuum of 10^{-4} torr, there did not appear to be any contamination ejection, excessive build-up on the probe wires, or balling up in the liners. It appeared that almost all of the contamination build-up took place during the first several revolutions of the probe through the gallium. This was in accordance with the postulated operational characteristics of the probe concept: as the probe moves through the gallium for the first time, it cuts a path through the contamination. Some contamination may be deposited on the leading edge of the probe but the bulk of the contamination is either pushed aside or remains undisturbed by the passage of the probe. There is a clean gallium in the wake of the probe and since the model is in a vacuum, there will be no reformation of the oxide layer beyond a monolayer, or so, in thickness. Then, as the probe moves through the gallium a second time, there is little further contamination that is deposited on the probe edge. In slip rings utilizing cylindrical electrode configurations, the continuous parallel surfaces will tend to roll the contamination deposited between electrodes into balls as the surfaces rotate relative to each other. These balls then can be ejected due to the electrode geometry and hydrodynamic forces. In the probe concept, there are not continous surfaces to ball up the contamination.

After five weeks of rotation at one revolution per day in vacuum, the verification model was removed from vacuum test and examined. As reported above, after four weeks of rotation in vacuum, the model was operating satisfactorily. When the vacuum chamber was opened and the model was examined, the following observations were made: See Figs. 17 & 18.

1. The gallium in the slip ring had frozen and caused the probe wires to be bent. This freeze-up apparently occurred between the fourth and fifth weeks of testing since there was no prior indication of gallium freezing.

   There is no clear explanation of what caused the gallium to freeze in the slip ring. A possible explanation is that there was excessive cooling of the drive motor since cooling coils had been placed around the drive motor to prevent possible overheating during the vacuum tests. A thermocouple placed on the drive motor indicated that its temperature had reached 69°F. It is possible that during the period that the motor temperature was 69°F, the gallium temperature became low enough to cause it to freeze. The gallium was liquid through at least four of the five weeks of test, since the vacuum chamber was jarred periodically and a gallium motion was observed. At no time was there any indication of gallium freeze-up.

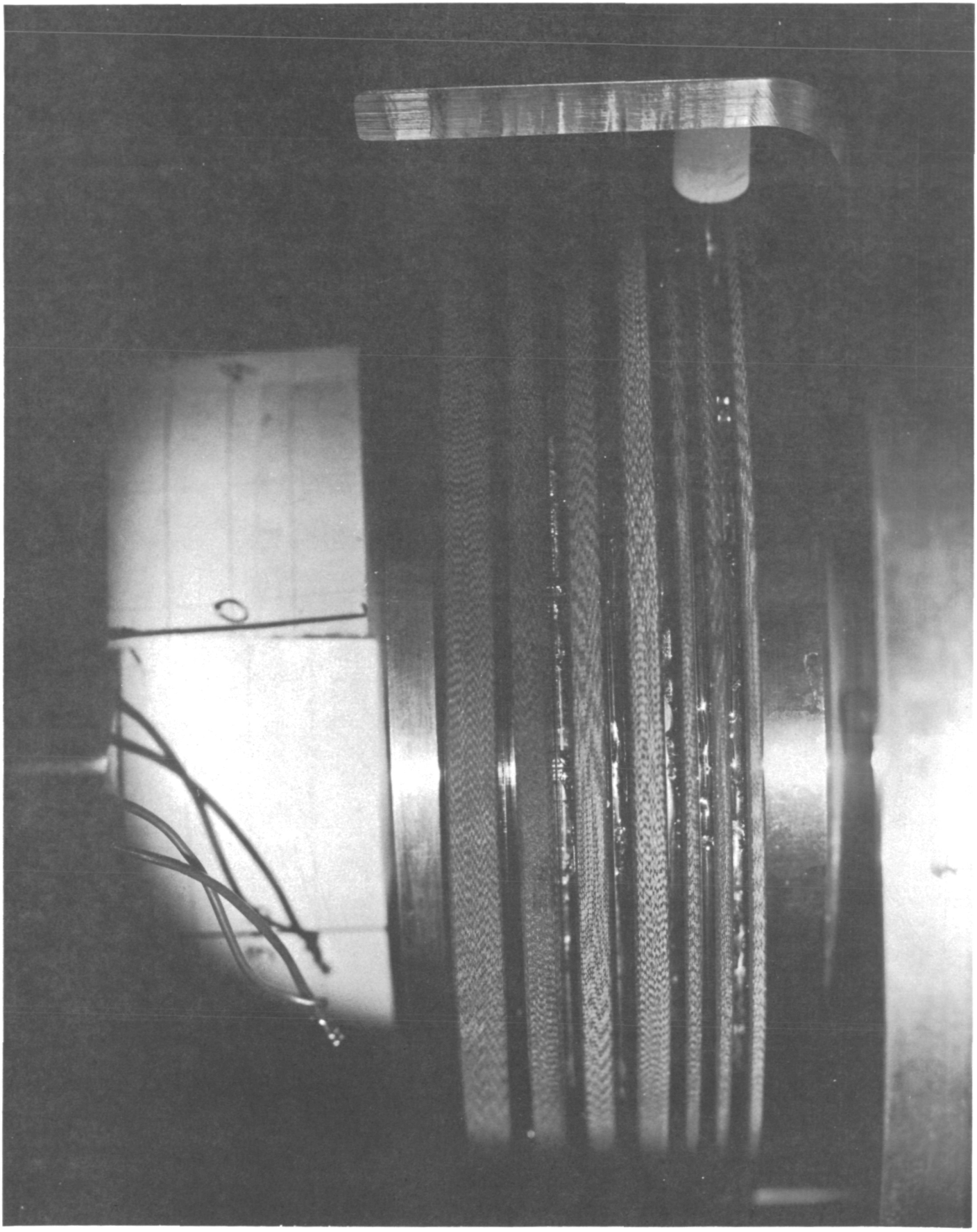

Fig. 17. Gallium in Verification Model After Vacuum Tests

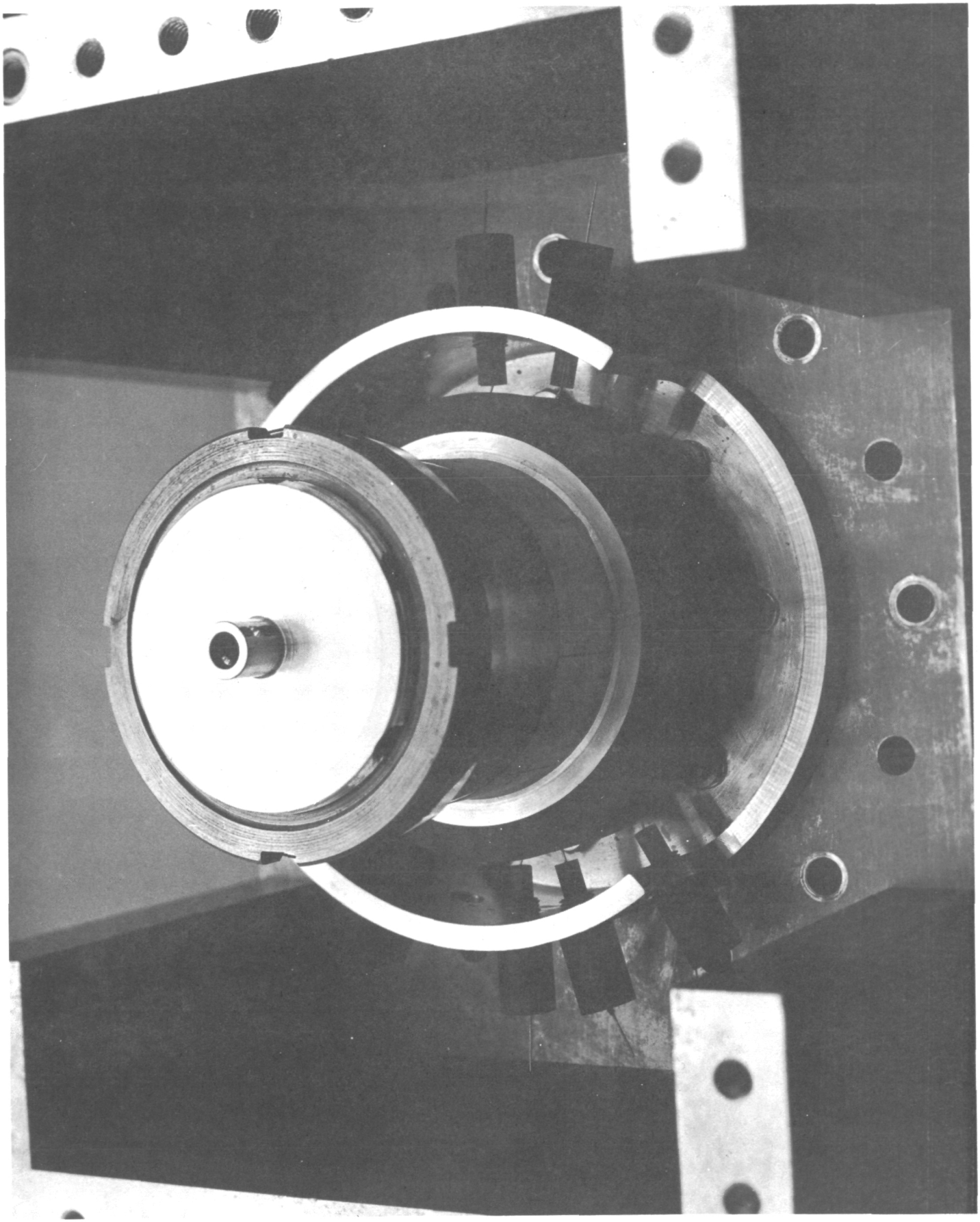

Fig. 18. Verification Model Partially Disassembled After Vacuum Test

2. Portions of the stainless steel liners appeared to be dewet. See Fig. 19. In subsequent work on the liners, the liners were heated in an oven, in air, to approximately 130°F to remove the gallium. It was observed that the liners appeared to be rewet with gallium. The gallium could not be removed from the liner walls by shaking or swabing. It was necessary to use vapor honing to clean the gallium completely out of the liner. It was therefore not clear as to what gave the appearance of being dewet; perhaps the cause was incomplete wetting, initially.
3. Oil was present on the surface of the cooling tube used for the drive motor cooling.

   This oil was analyzed by an infrared absorption test using an infrared spectrophotometer. This showed that the oil originated in the roughing and diffusion pumps. The cause of this oil contamination is unknown except perhaps there was back-streaming in the vacuum chamber due to temporary pump malfunction or a power interruption to the pump motor.
4. There was no debris build-up on the probes, surface of the gallium, or meaningful amounts of debris ejected from the slip rings. This is a crucial and positive result obtained from the tests even though there was a gallium freeze-up. The verification model was placed under vacuum test after being subjected to vibration and acceleration tests with gallium liquid and after many gallium melting and freezing cycles which were necessiated for handling purposes. No effort was made to clean any debris on the surface of the gallium prior to the vacuum tests. In spite of the slight

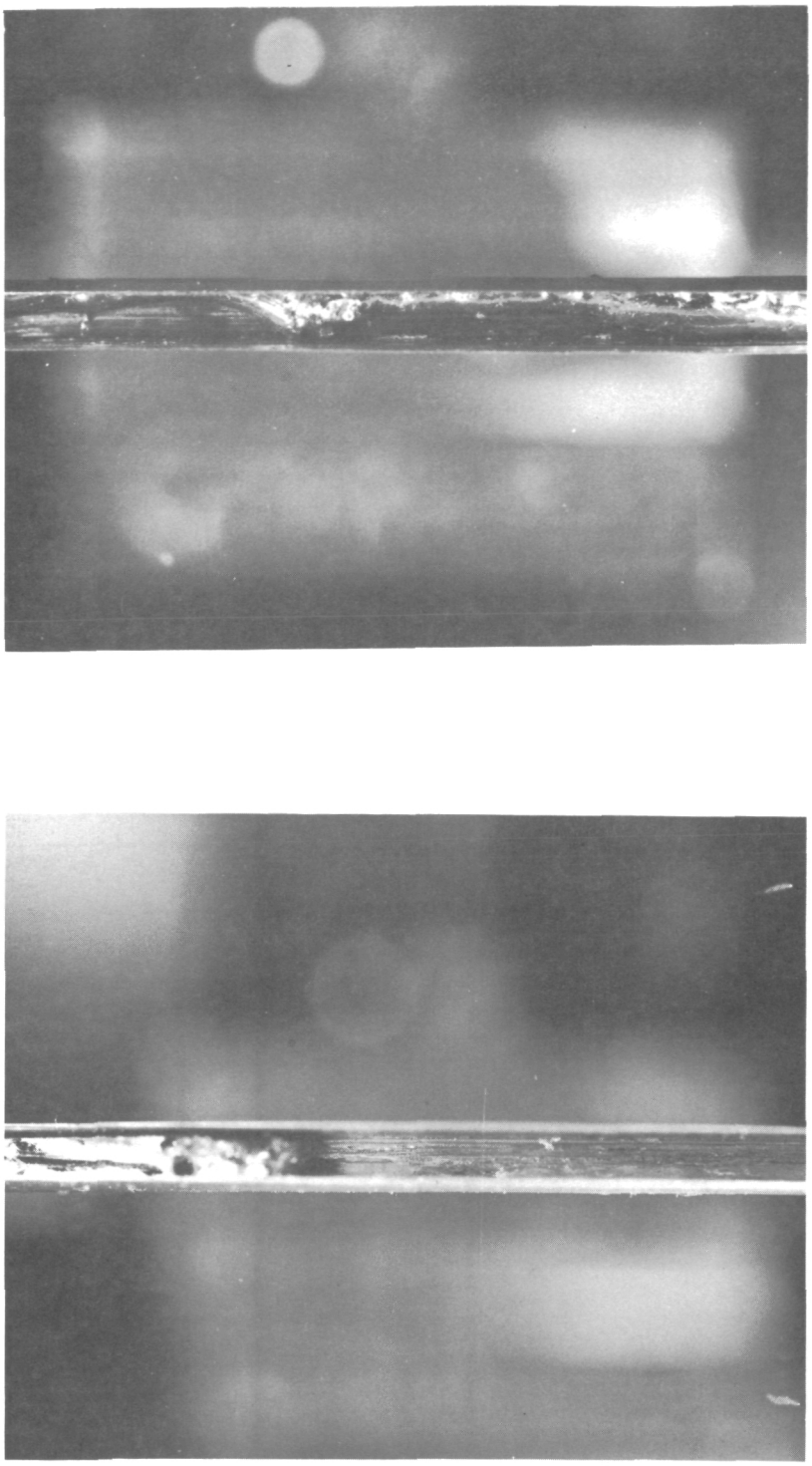

Fig. 19. Partially Dewet Rings

amount of debris that was formed, there was no serious accumulation, balling, or ejection of the debris. The probe concept still appeared to be a valid slip ring approach.

3.3.4 Refurbishment and Retest

Because of the promising results obtained during the first four weeks of vacuum testing of the verification model: slight formation and no ejection of contamination, it was decided to refurbish and rerun vacuum tests on the verification model.

3.3.4.1 Refurbishment

The refurbishment was to consist of the following:

1. Nickel plating of liners
2. New probes
3. New probe wire material
4. Gallium wetting and filling under nitrogen

The liners had been fabricated of 303 stainless steel. Two aspects of the use of stainless steel were observed. First, some difficulty was encountered in fully wetting the liners, mainly because of their cavity geometry and there were indications that even though the surface appeared to be completely wetted, the wetting occured only in localized areas in close proximity to each other. Second, a pronounced dewetting of portions of the liners was noted after the completion of the vacuum tests. Therefore, in order to improve the wetting characteristics of the liners, it was decided to nickel plate them.

Three basic nickel plating processes were considered:

1. Electrolytic
2. Vapor deposition
3. Electroless

The electrolytic method required the design and fabrication of an anode and necessary fixturing to assure the proper deposition in the cavity of the liner. The electrolytic process had a potential problem, inherently, in that there would be a build up of nickel around the sharp edges of the liner.

The vapor deposition technique has two inherent problems. The first is that the narrow width of the liner, approximately .050" compared with its depth, approximately .150", makes glow and hence deposition quite difficult at the bottom of the liner. Furthermore, the inherent coating thickness of vapaor depositions were considered too small for this application.

The electroless nickel process appeared to be the best process to use: it permits uniform deposition in recessed areas, there is no plating build up at sharp edges, and it results in a hard, bright adherent deposition. One potential problem area was identified with the electroless technique. This stemmed from the fact that the liners had previously been wet with gallium. The successful utilization of electroless plating entailed the complete removal of gallium from the liners.

The following is the procedure used to electroless nickel plate the liners. Prior to plating the liners, coupons of 303 stainless steel were electroless nickel plated and then wet with gallium in order to check out the plating procedure. The plating procedure for the liners consisted of three steps:

1. Preparation
2. Activation
3. Plating

Preparation of Liners

The liners were heated to 100°F in an oven in order to melt the gallium. Bulk gallium was spilled out with any small remaining amounts removed by gentle tapping of the liners. The last visible amounts of gallium were removed by vapor blasting of the liner surfaces. The liner was then wiped with a cotton swab moistened with acetone and rinsed with tap water. The surfaces were pumice scrubbed with a Tampico brush until the surfaces were water-break free. After scrubbing, the liners were thoroughly rinsed with water. The liners were then immersed first in concentrated nitric acid at room temperature for 2 minutes, rinsed with water, and then immersed in a potassium hydroxide solution for 1 minute and rinsed with water.

Activation

The liner was activated in a Wood's nickel strike bath. The strike bath consisted of the following:

45 ml	concentrated hydrocholoric acid
45 gm	nickel chloride hexahydrate
810 gm	distilled water

The liner was placed in the bath between nickel anodes and connected to the cathode of a dc power supply. The strike was for 3 minutes at 5 amps. After removal from the strike bath it was rinsed thoroughly with water and placed into the electroless nickel solution.

Plating

The electroless nickel plating solution consisted of Enplate NI-410. This is a proprietary solution manufactured by Enthone, Inc., New Haven, Conn. It produces a deposition which is nominally 93% nickel and 7% phosphorus. The phosphorus which is present in the nickel plate has not been found, generally, to signifigantly alter the physical characteristics of the deposit when compared with a deposit of pure nickel. This plate is commonly used as an alternative for pure nickel in difficult to plate parts. The solution was heated to a temperature of 190 to 195°F. The liner was placed in the solution for 2-1/2 hours and agitated slowly to prevent streaking of deposit or pitting by gas bubbles evolved as a result of the deposition of the nickel. The nickel plating thickness was measured at .001", as required.

As was noted previously, probe holders had been fabricated with Epon 815 and TETA with LP3 added as a flexibilizer. These probe holders outgassed sufficiently to prevent the pressure from going below 10^{-4} torr in the diffusion pump chamber. In order to eliminate this outgassing problem new probe holders were fabricated. These were case of Versamid 140, Epon 828 and TETA. The probe wire material was changed from stainless steel to pure nickel in order to permit easier wetting. These wires were 0.025" in diameter and were cast integrally with the epoxy.

In order to verify their outgassing characteristics the probes were placed in an ion pump chamber and pumped down to 10^{-6} torr. This procedure was done twice, once after casting and second, after being machined. In both cases, the probes showed no tendency to outgas.

The gallium wetting and filling procedure of the liners was started after the completion of the electroless nickel plating. A Labconco glove box was connected to the "house" nitrogen supply and nitrogen was passed through at the rate of 40 cfh for two days. The "house" nitrogen comes from the boil-off of the liquid nitrogen which is used in conjunction with vacuum chambers; the purity of this is monitored continuously and is quite good, approximately 3 ppm oxygen and less than 0.1 ppm water vapor. This nitrogen was circulated through the glove box in order to have a minimum oxygen and water vapor content present when the liners were wet and filled with gallium.

One of the coupons of stainless steel which had been previously nickel plated was placed in the glove box and wetted with gallium by abrasion with a cotton swab in order to check out the procedure. The water vapor content of the glove box was measured at 11 ppm prior to the start of the wetting. It appeared to be somewhat more difficult to wet the coupons in the nitrogen environment of the glove box than in air; however, they were wet satisfactorily, in the glove box.

The liners were then placed in the glove box for wetting and filling. After considerable effort using such approaches as cotton swabs, cloth over shaped wooden sticks and pipe cleaners, it was not possible to wet the liners. A number of different liners were tried, all with no success. A coupon however was satisfactorily wet. It was then decided to attempt to wet a liner on a laminar flow bench. This was done successfully by rubbing with a pipe cleaner. Consequently, all liners were wet in air on the laminar flow bench.

After being wet, the liners were filled with gallium in the glove box. This was accomplished by mounting the liner in a fixture, placing an o-ring slightly wider than the liner width around the periphery of the liner and then filling with gallium injected from a hypodermic needle. After the liners were filled they were placed in the glove box feed-through and frozen by introducing cold nitrogen into the feed-through. The liners were then bagged and stored in a refrigerator.

The nickel probe wires were then wet. An attempt was first made to wet them by rubbing with a cotton swab in the glove box under nitrogen but this was unsuccessful. Wetting was then attempted in air on the laminar flow bench. This, too, proved to be unsuccessful perhaps due to a very tenacious oxide which was formed during the wire drawing process. Wetting was finally achieved by first dipping the nickel wire into concentrated hydrochloric acid for five seconds, rinsing under running tap water, drying with a "kim-wipe" and then rubbing under gallium with a cotton swab.

Prior to their assembly, the liners were machined to remove excess gallium and gallium and nickel from the outer edges exposing the base stainless steel material. This was done so that the surface would be non-wetting and the gallium in the bottom of the liner would be retained by capillary forces. The machining was done on a special fixture which held the liner and was hollow so that it could be packed with dry ice to assure that the gallium would not melt while being machined.

The slip ring was assembled on a laminar flow bench. The gallium was kept frozen during all phases of assembly except when the probes were assembled. Melting the gallium was accomplished by heating the slip ring with infrared lamps. After the probes were assembled the gallium was refrozen by cooling the entire model with cold nitrogen gas.

3.3.4.2 Retest

After the completion of the assembly of the verification model it was placed in the ion pump chamber where it was instrumented with thermocouples and voltage and current leads to monitor intra-ring resistance. The thermocouples were placed on the probes, motor, structure and heating platen and were connected to a multipoint potentiometer recorder which provided a continuous record of temperatures. See Figures 20, 21 and 22.

After checkout of the slip ring and instrumentation, the chamber was pumped down. Care was exercised to maintain the gallium solid until outgassing had stopped and a vacuum of 10^{-6} torr was reached. The gallium was then melted by circulating hot water through the heating platen on which the model was mounted. After it was verified by the thermocouple readings on the probes that the gallium was melted, the motor was energized and rotation started. See Figures 23 and 24.

Data on residual gases remaining inside the test chamber after pump down and during operation of the slip ring assembly were obtained using a General Electric Model 22PT120 partial pressure analyzer tube. This was flanged directed to the test chamber with the ion source exposed inside the vacuum chamber. The device uses magnetic focusing

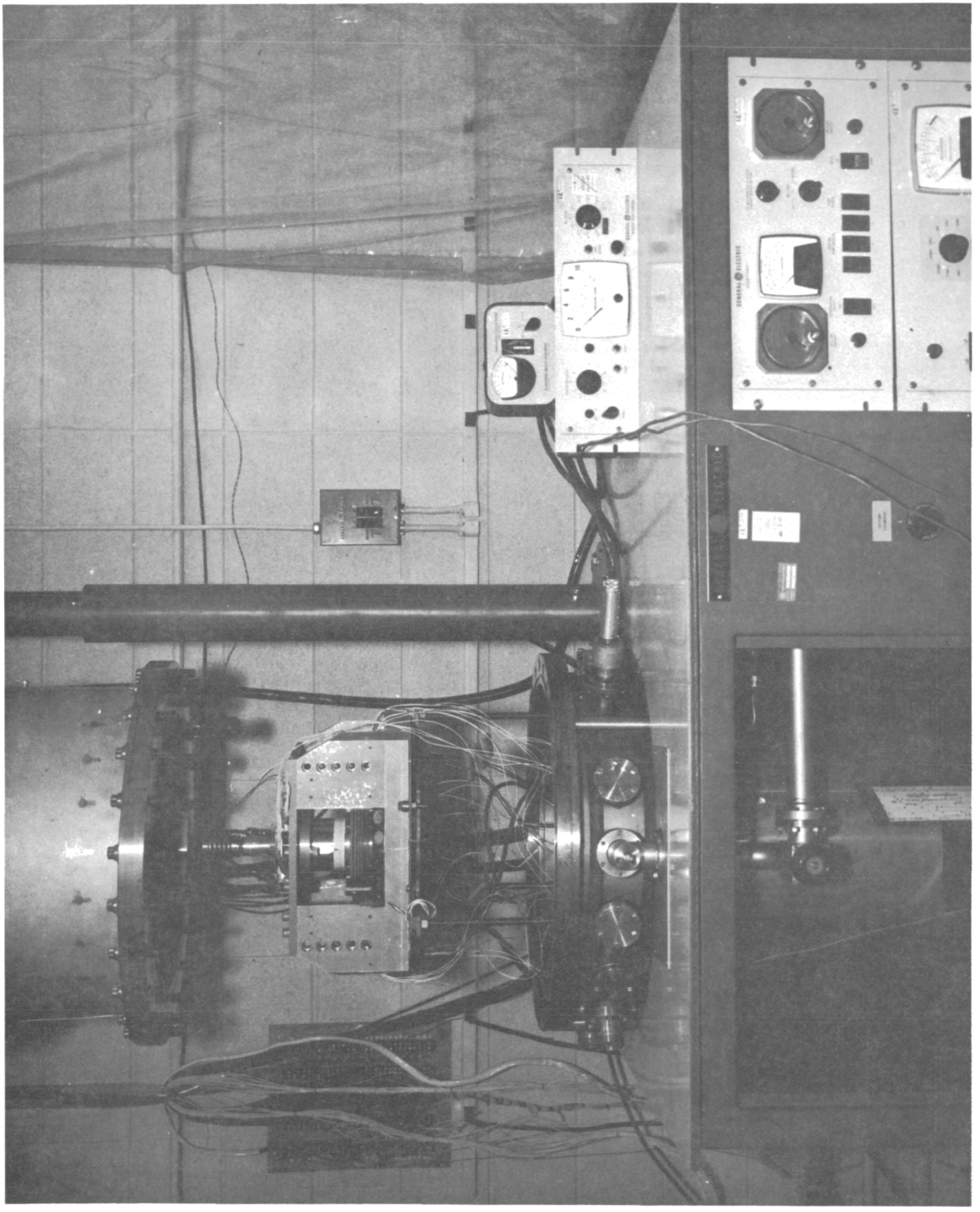

Fig. 20. Verification Model in Vacuum Chamber

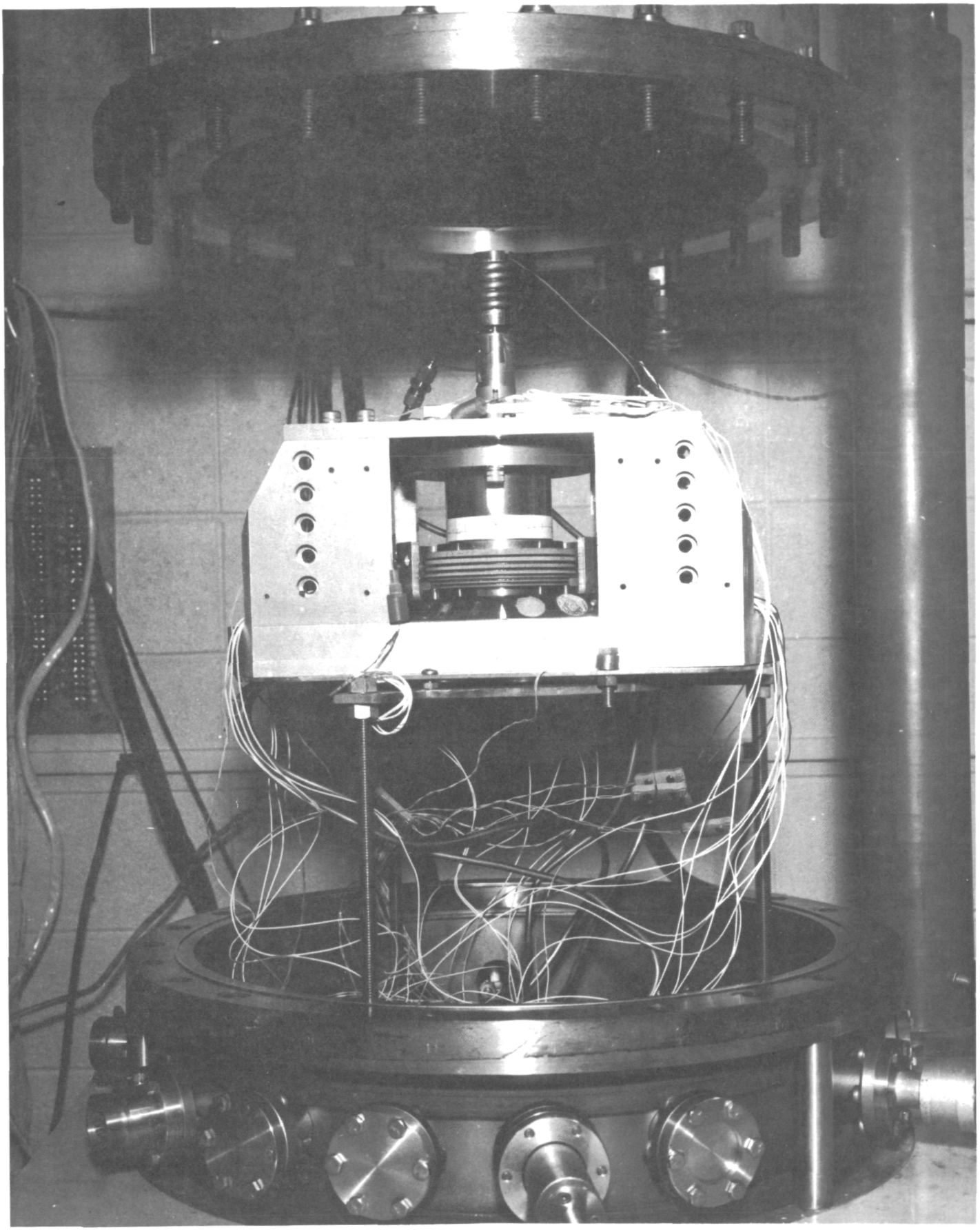

Fig. 21. Verification Model in Vacuum Chamber

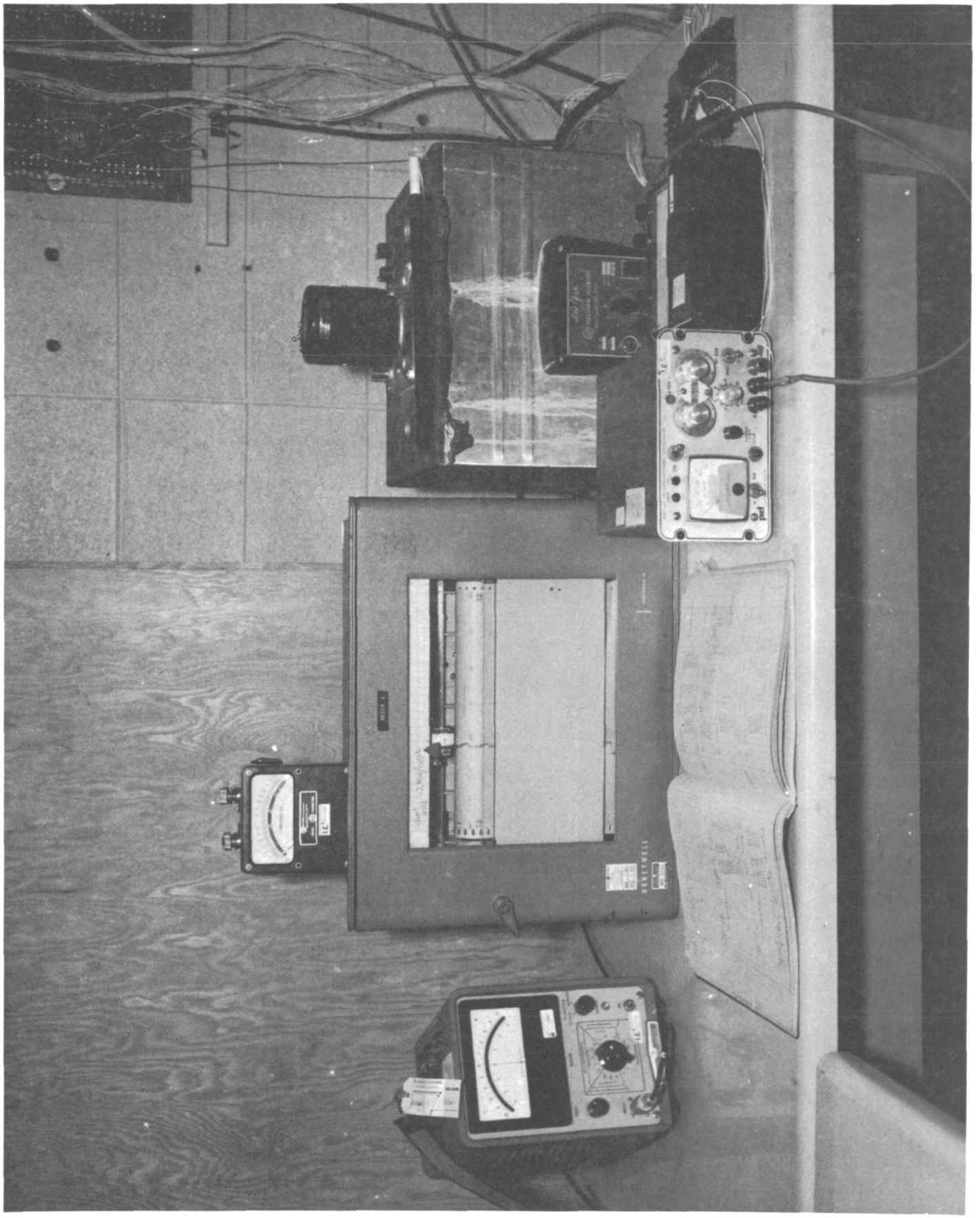

Fig. 22. Test Equipment

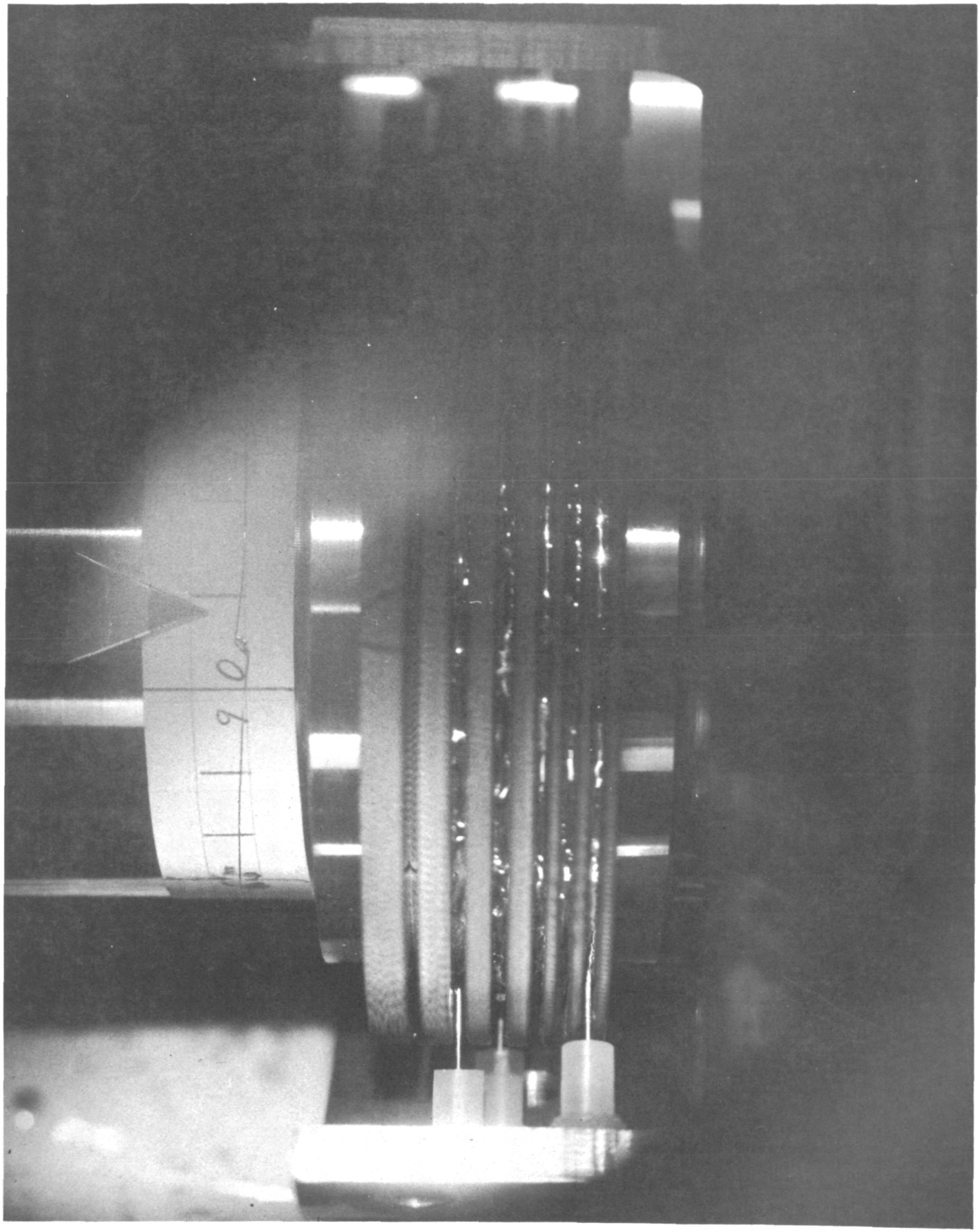

Fig. 23. Rings and Probes at Start of Vacuum Test

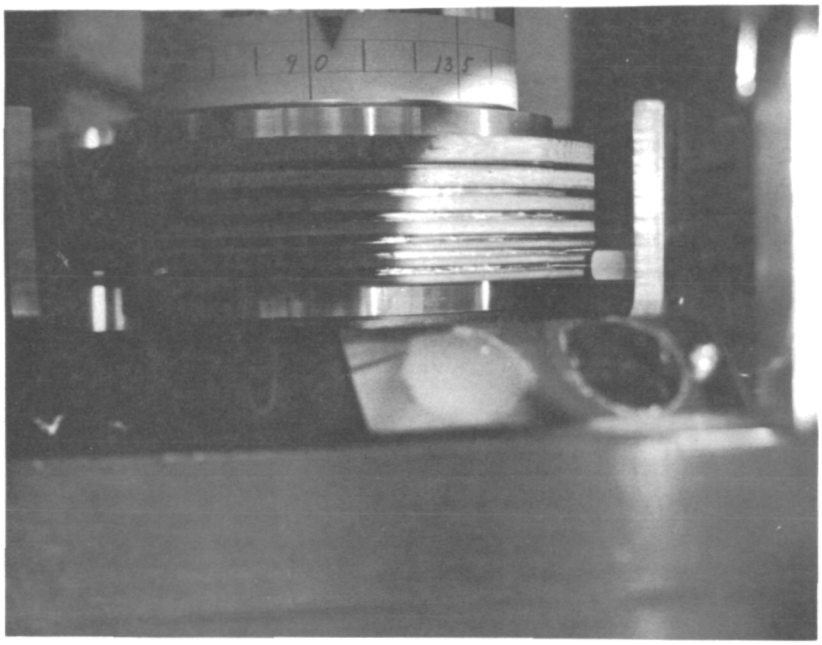

Fig. 24. Rings and Probes at Start of Vacuum Test

to resolve masses 10-100 with a 5 kilogauss magnet. The ions are accelerated electrostatically with a periodically swept voltage to present an ion current signal detected by an electron multiplier and recorded on a strip chart recorder. Initially the background spectrum showed major peaks at mass numbers of 14, 18, 28 and 40. The peak at 40 is argon which appears in the spectrum since this gas is used to leak check the system and as a consequence is continually being re-evolved by the system ion pump. The peaks at 14 and 28 indicate the presence of N_2, but some of the mass 28 peak is also due to CO. The peak at mass 18 indicates water vapor which appears to contribute on the order of 20% of the total background. This is typical of an unbaked vacuum system. There was a peak at 32 indicating the presence of O_2. Partial pressure was of the order of 1% of the total (approx. 10^{-9} torr).

When the motor was turned on to operate the slip ring assembly, the peaks due to water vapor increased, probably due to thermal outgassing of motor components; clusters of peaks became more prominent in mass ranges that indicated the presence of hydrocarbon residues and residues as heavy as C_6 were observed. The signal strengths indicated partial pressures for these materials of the order of 10^{-10} torr.

During the vacuum tests, pressure, temperatures and ring resistance were monitored continuously. Typical readings are as follows.

	READINGS		
	Initial	After 14 days	After 30 days
Pressure	1×10^{-6} torr	7×10^{-7} torr	1×10^{-6} torr
Probe Temperature			
Probe #3	109°F	111°F	113°F
Probe #4	104°F	109°F	110°F
Probe #5	109°F	111°F	113°F
Probe #6	109°F	110°F	113°F
Platen	135°F	135°F	145°F
	147°F	145°F	141°F
Structure	135°F	135°F	133°F
Motor	136°F	136°F	133°F
Ring Resistance (Ohms)			
Ring #2	45.0×10^{-3}	44.0×10^{-3}	43.8×10^{-3}
Ring #3	45.5×10^{-3}	44.3×10^{-3}	44.0×10^{-3}
Ring #4	42.5×10^{-3}	41.0×10^{-3}	41.5×10^{-3}
Ring #5	46.0×10^{-3}	44.2×10^{-3}	44.0×10^{-3}
Ring #6	44.0×10^{-3}	44.0×10^{-3}	44.0×10^{-3}

The resistance of the rings as measured between probes using the Kelvin double-bridge method was found to be approximately 45×10^{-3} ohms. This is somewhat higher than expected since values in the micro-ohm regime were anticipated. An investigation showed that the voltage and current connections to the probes were made at the same point rather than having the current connections outboard of the voltage connections. When the connections are made to the same point in this fashion, the resistance of the joint is included.

After one complete revolution, the gallium in the rings was observed and there appeared to be a path at the surface where the probes had cut through the contamination. This path was not smooth but appeared to be jagged. There was no excessive build up of contamination in the rings or on the probe. See Figures 25 and 26.

It should be noted that Figures 25 and 26, as well as those following, appear to show a large contamination build up and a poor gallium surface; however, these photographs tend to be misleading. This is the result of a number of factors including the great difference in reflectivity of gallium and that of the contamination, the pick-up of highlights off the gallium, the curvature of the rings, and the fact that the photographs were taken outside the chamber through a viewing port. The actual quantity of contamination build-up and surface condition was better than might be inferred from the photographs.

Coupons of nickel plated stainless steel wetted with gallium had been placed in the vacuum chamber. It was noted that after several days at vacuum, portions of the gallium changed from silvery to a white powdery appearance. After approximately ten days in vacuum, the rate of change of appearance had slowed down appreciably and did not change appreciably after that time. It is conjectured that the overall change in appearance is due to a dehydration of the gallium oxide which was present on the surface of the gallium.

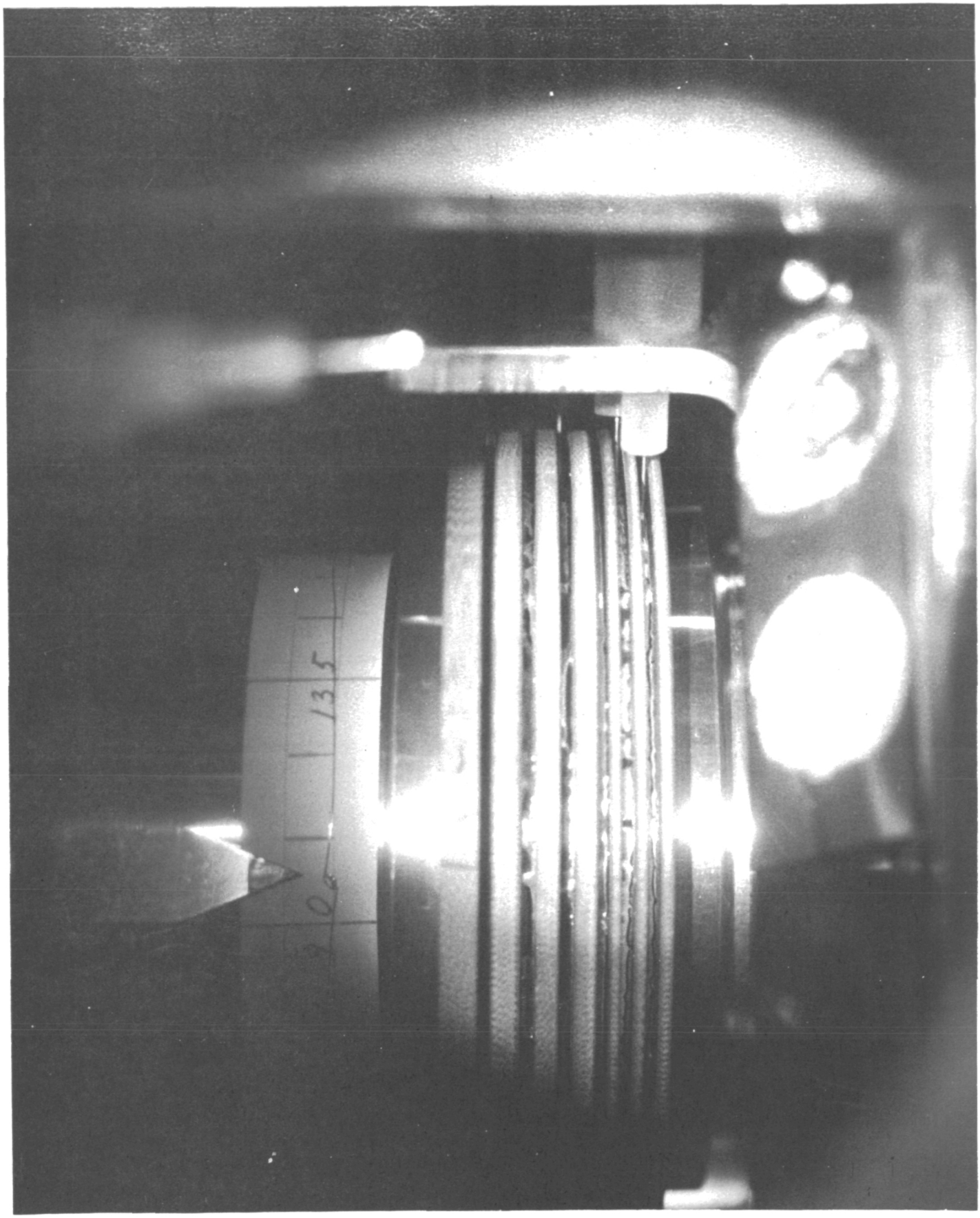

Fig. 25. Rings and Probes After One Revolution

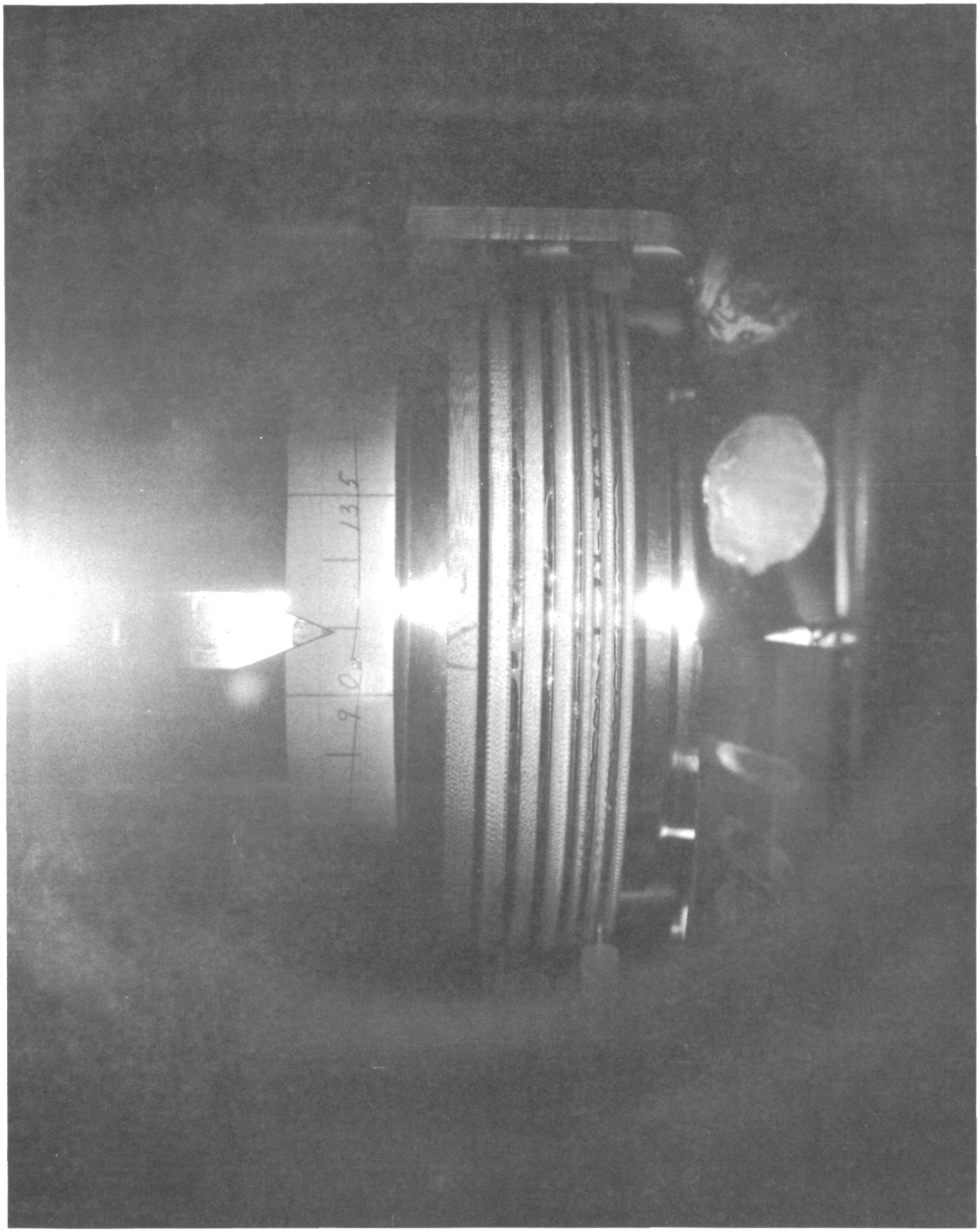

Fig. 26. Rings and Probes After One Revolution

3.3.4.3 Test Results

The verification model was operated in vacuum for 35 days at which time the test was completed, as planned. At the completion of the vacuum tests and prior to the removal of the model from the vacuum chamber, extensive observations were made of the probe and liners to determine if there was any evidence of excessive contamination build-up on the probes or in the liners, or of contamination or gallium having been ejected from the liners. These observations showed that there was no ejected contamination or gallium, and that there was no excessive buildup of contamination either on the probes or in the liners. There was substantially no change in appearance of the probes, liners or gallium surface at the end of the vacuum test as compared with the appearance after several days of operation. See Figures 27, 28 and 29.

Prior to breaking vacuum, the gallium in the model was frozen so that no rapid oxidation could take place when it was exposed to air. The gallium was frozen by passing cold nitrogen gas through the platen. Temperatures on the model were monitored and when it was determined that the gallium was frozen, the vacuum was broken and the chamber lid removed. The model and structure were again examined for evidence of ejected contamination in the back of the model or at the base of the structure. This examination showed that there was no ejected

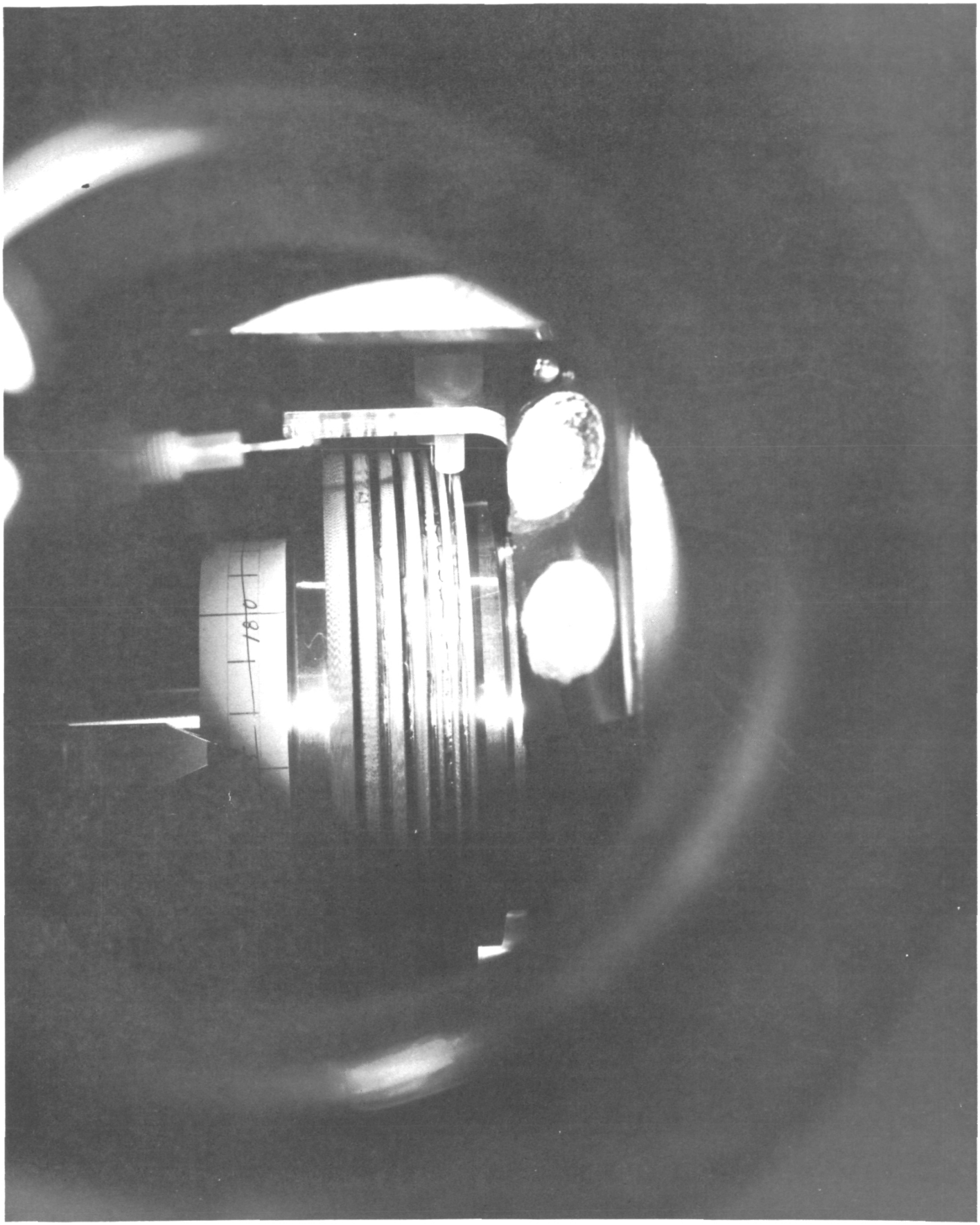

Fig. 27. Rings and Probes at Completion of Vacuum Tests

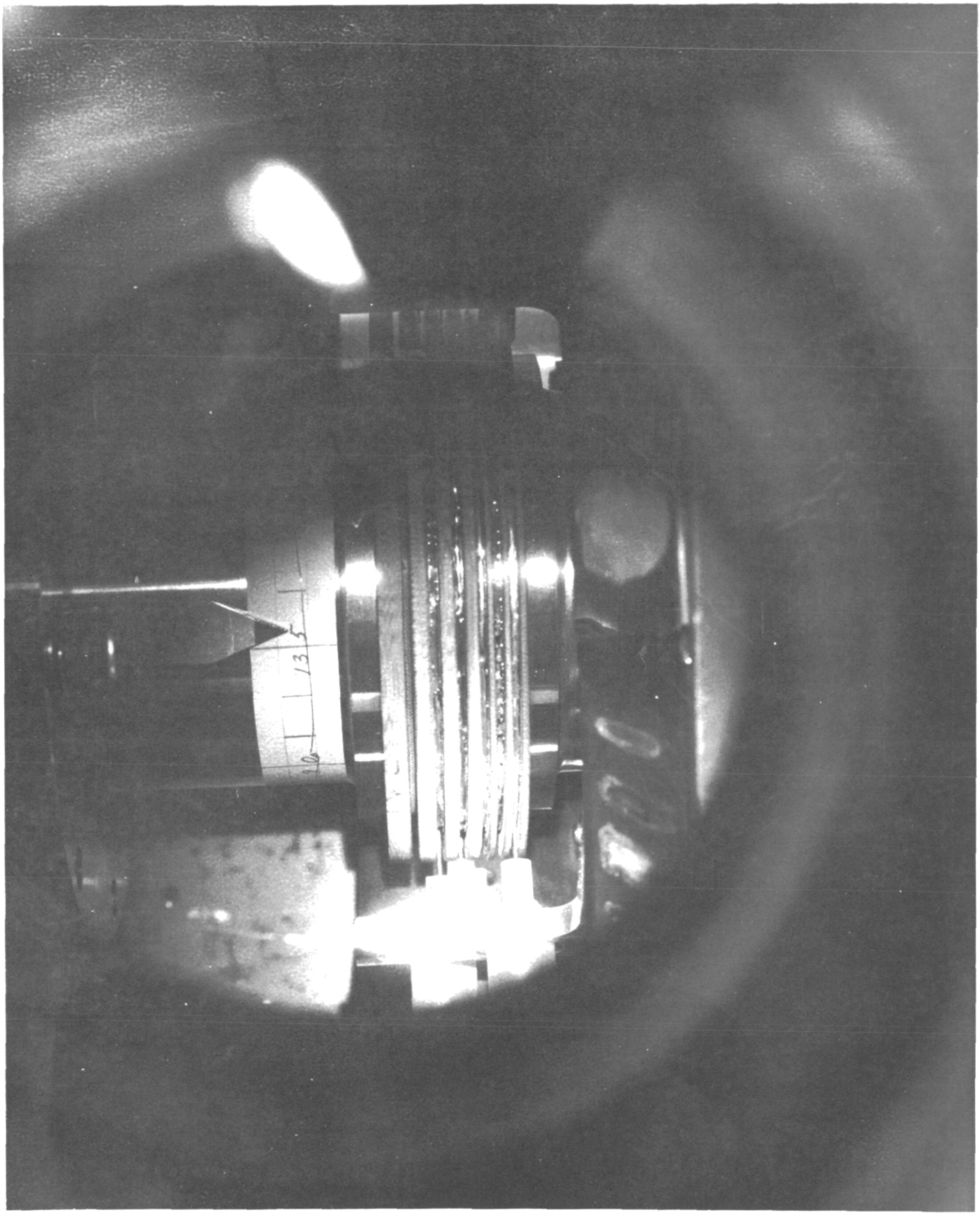

Fig. 28. Rings and Probes at Completion of Vacuum Tests

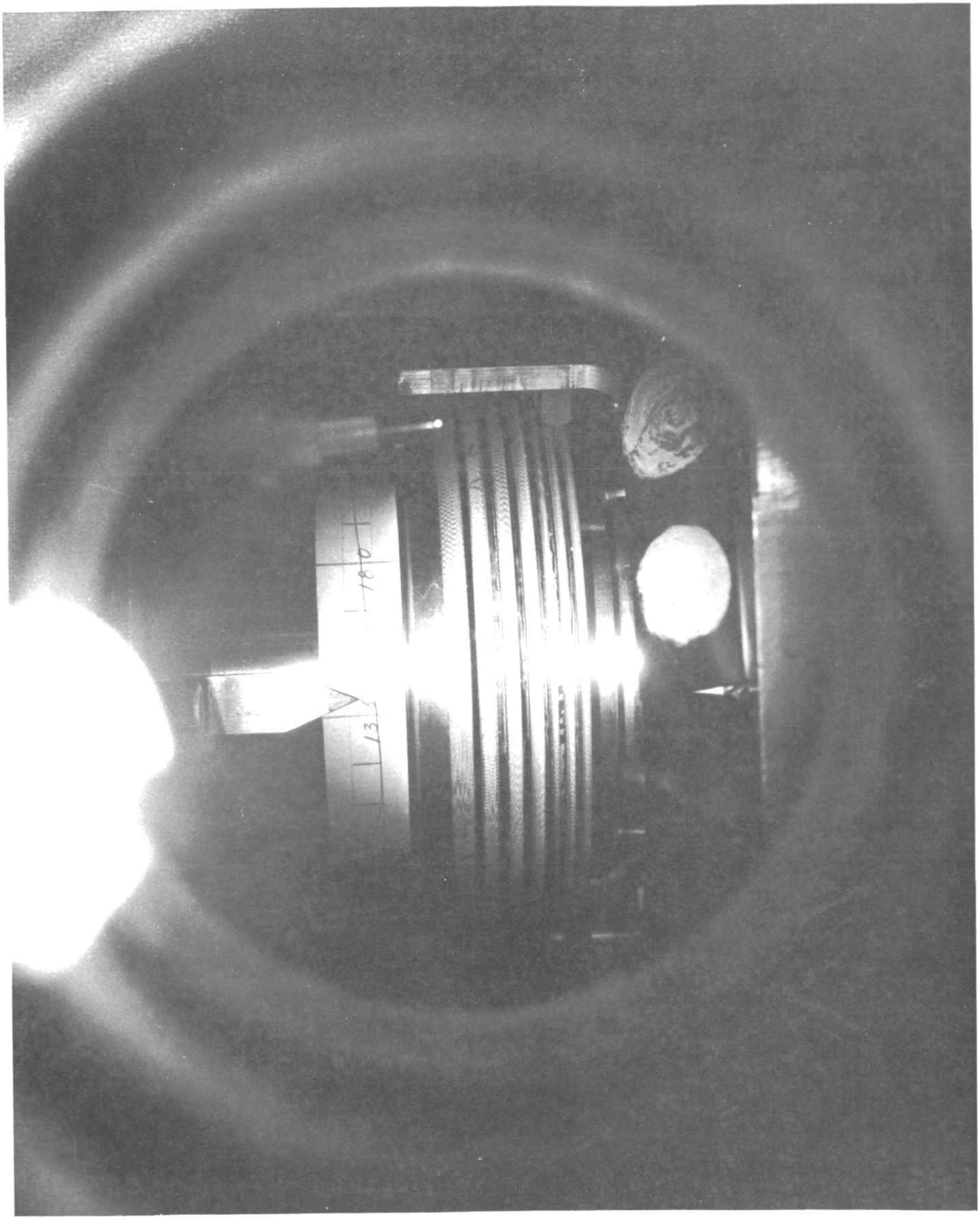

Fig. 29. Rings and Probes at Completion of Vacuum Tests

contamination anywhere. A closer examination of the gallium surface showed that it had a slightly ripple surface not substantially different from what it was initially. See Figures 30, 31 and 32.

One of the rings appeared to be dewet over approximately 3/4" of its periphery. The dewetting experienced with the nickel plated rings was substantially less than the dewetting observed with the stainless steel rings. This is consistent with the concept that dewetting is actually the result of incomplete wetting. Since nickel is easier to wet than stainless, there is less tendency towards incomplete wetting of the nickel. Improved wetting techniques greatly decrease the probability of dewetting.

The vacuum tests successfully demonstrated the probe concept for a liquid metal slip ring. During operation and post test examination, there was no evidence of failure or incipient failure of the slip ring.

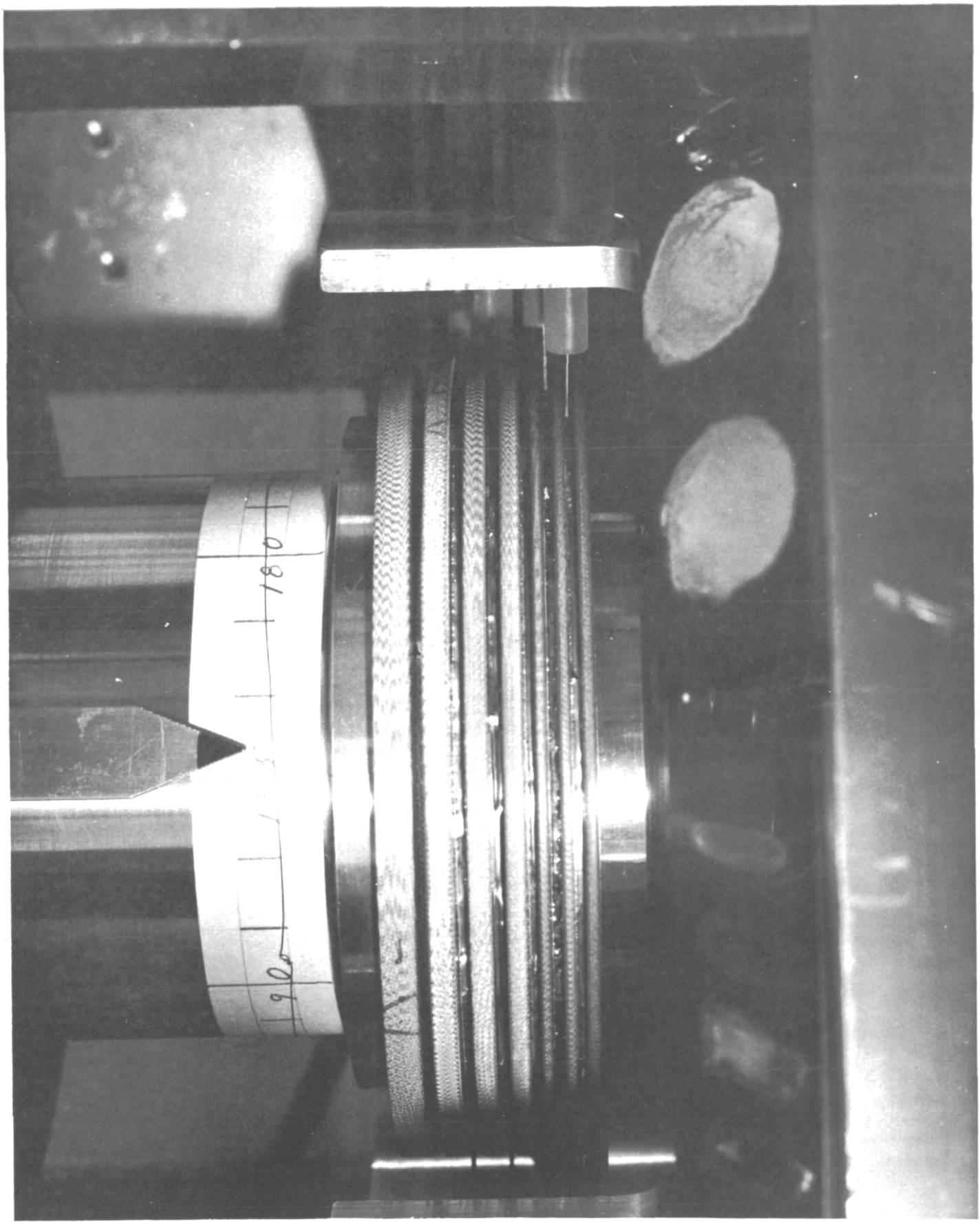

Fig. 30. Rings and Probes After Vacuum Tests

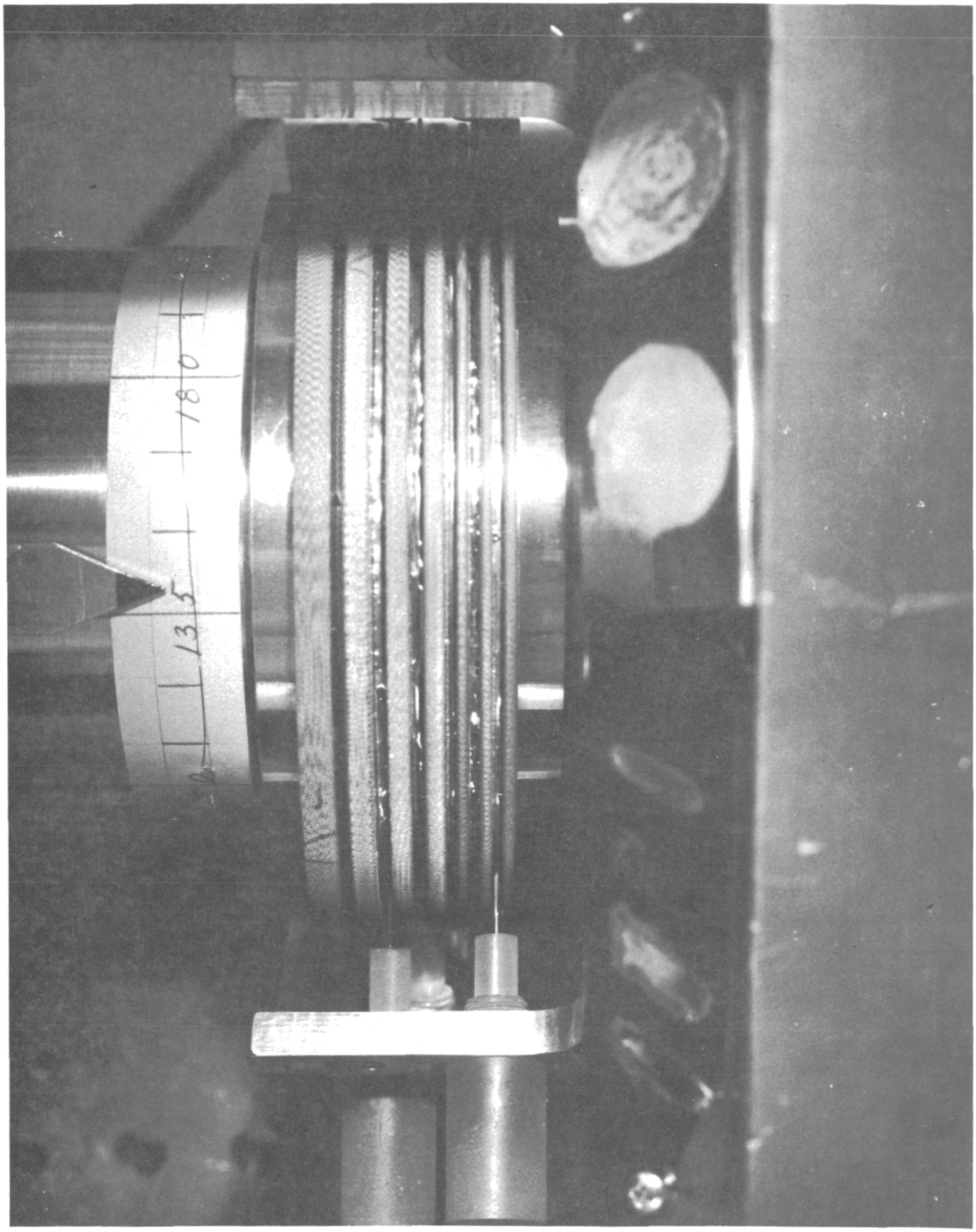

Fig. 31. Rings and Probes After Vacuum Tests

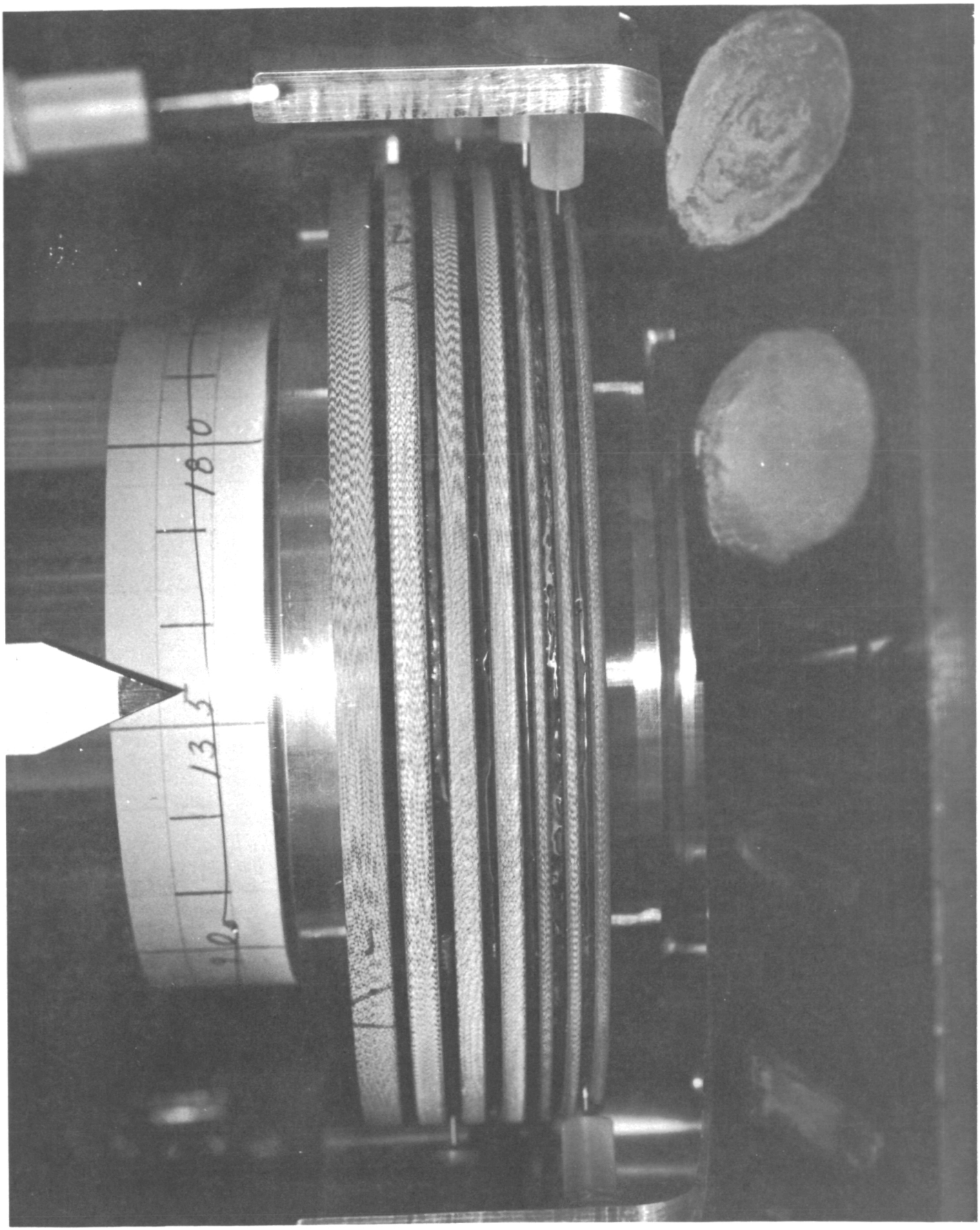

Fig. 32. Rings and Probes After Vacuum Tests

3.3.5 Summary and Conclusions

The results of the tests on the verification model are as follows:

a. A gallium liquid metal slip ring using the probe concept is feasible.

b. Nickel and 300 series stainless steel are satisfactory electrode materials for use with gallium.

c. The probe concept is tolerant of small amounts of contamination in the ring. There is no additional contamination build-up or ejection, in vacuum.

d. Contamination free gallium is not attainable in atmospheres containing several parts per million oxygen or water vapor. However, the amount of contamination produced can be accommodated by the probe design.

e. Gallium in the liquid state was retained by capillary forces under the anticipated orbital conditions of vibration and acceleration. There was no evidence of sloshing or instability of the liquid gallium.

f. Solid gallium showed no evidence of failing structurally because of the prelaunch or launch environments.

g. Liquid metal slip rings having a dielectric strength of 15,000 volts are feasible.

4.0 DETAIL DESIGN

Based on the work accomplished in the preliminary design study, the probe concept was selected for the detail design. The detail design consisted of a complete set of design drawings of the liquid metal slip ring/solar array orientation mechanism; the drawings were prepared in sufficient detail that an engineering unit could be fabricated from them. A detail design package was made which consisted of the following:

- Overall Assembly
- Slip Ring Assembly
- Subassemblies
- Details
- Parts List

In the detail design, the following were the major considerations:

- Fabrication of detail parts
- Assembly
- Component Selection
- Concentricities, position tolerances, size tolerances

Figures 33 and 34 show the assembly drawing of the LMSR/SAOM.

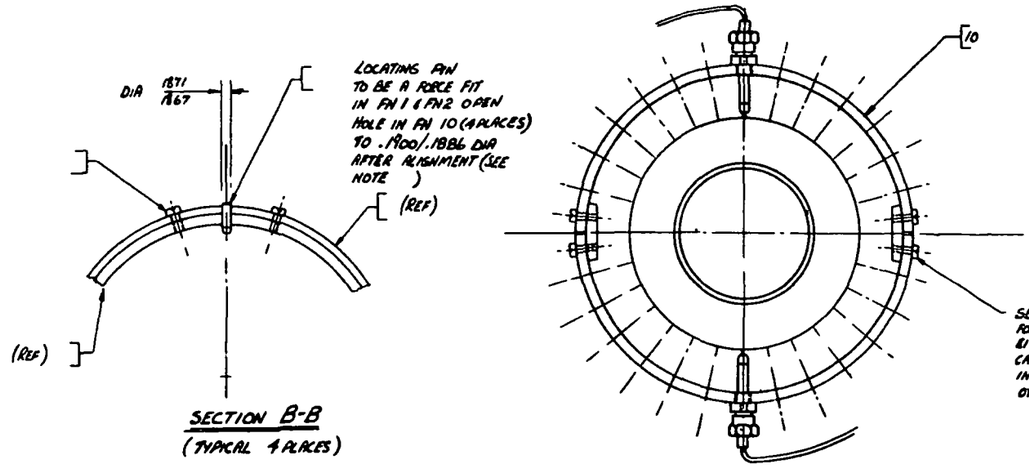

SECTION B-B
(TYPICAL 4 PLACES)

SECTION A-A

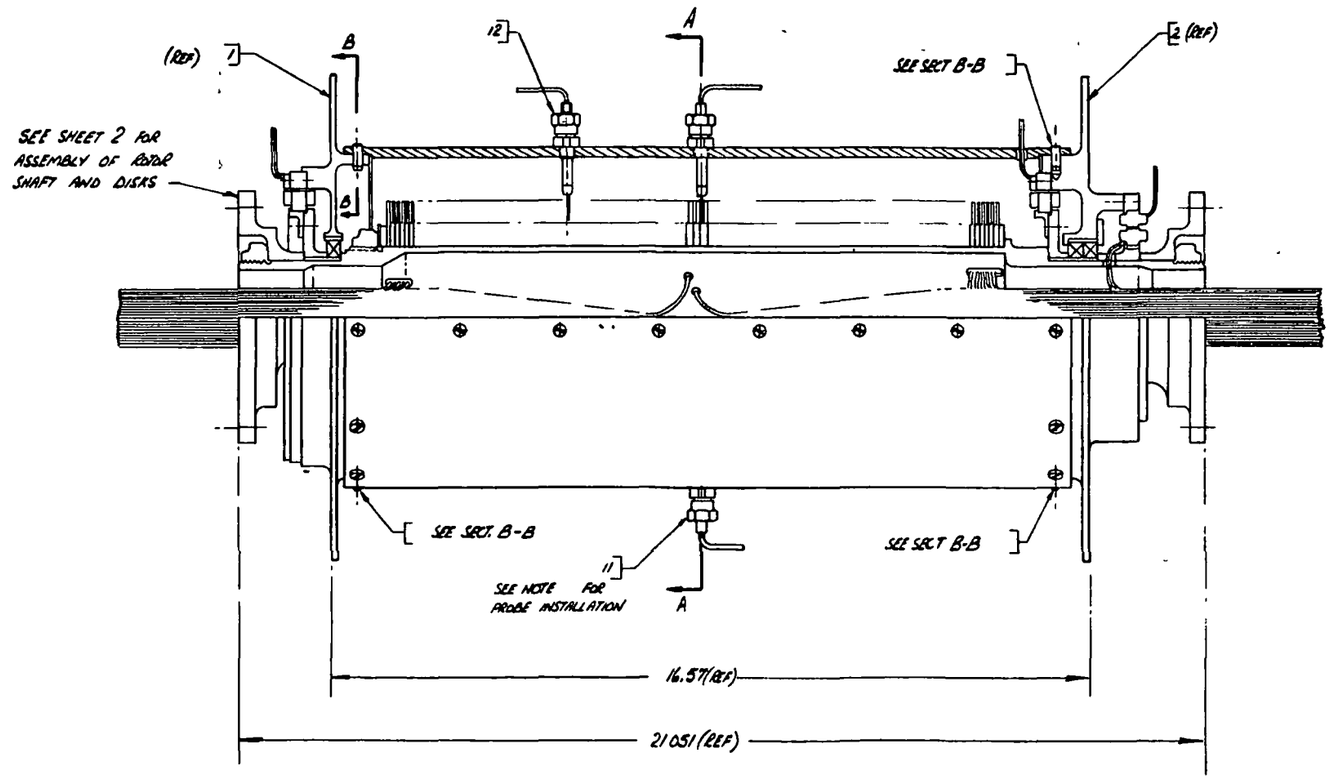

(G1) ASSY

GENERAL NOTES

1. INTERPRETATIONS OF DRAWING TERMS AND TOLERANCES PER GE SPEC 11BA1664
2. MARK PART "23991-47E223276 G1" PER GE SPEC 11BA1526 CLASS
3. TORQUER INSTALLATION -
   ASSEMBLE STATOR HALF OF TORQUER ON TO FN 1 AFTER TIGHTENING ASSEMBLY SCREWS FN 37 ASSEMBLE ROTOR HALF OF TORQUER ON TO SHAFT AND POSITION RELATIVE TO STATOR - ROTOR TO BE CONCENTRIC TO STATOR TO WITHIN .003 T.I.R - LOCK ROTOR IN POSITION BY PINS FN AFTER TIGHTENING SCREWS FN 30 IN RETAINING RING FN 5
   WARNING - KEEPER RING IS NOT TO BE REMOVED OR DISPLACED FROM ITS POSITION ON STATOR FOR ANY REASON UNTIL STATOR AND ROTOR ARE FULLY ASSEMBLED
4. RESOLVER INSTALLATION -
   ASSEMBLE ROTOR HALF OF RESOLVER ON TO MOUNTING RING FN 7 WITH FLEXIBLE TYPE ADHESIVE (SEE BELOW) RESOLVER ROTOR OUTSIDE DIA. SHALL RUN CONCENTRIC TO AXIS OF ROTATION TO WITHIN .0005 T.I.R
   ASSEMBLE STATOR HALF OF RESOLVER ASSY ON TO SUPPORT PLATE FN 2 WITH ATTACHMENT SCREWS FN 31 OUTSIDE DIA OF STATOR ASSY SHALL RUN CONCENTRIC TO ROTOR SHAFT TO WITH IN .0005 T.I.R.
   LOCK STATOR ASSY IN POSITION WITH PINS FN
   ADHESIVE TO BE EPON 828 CATYLIZED WITH TETA PER GE SPEC 171A9525
5. ANGULAR CONTACT BEARINGS FN 28 TO BE ASSEMBLED BACK TO BACK LUBRICATE WITH SS LUBE II PER GE SPEC 171A4636 (DRY FILM LUBRICANT)
   PRE-LOAD CALLOUT REQUIREMENT TO BE ADDED TO IDENTIFICATION NUMBER ON PARTS LIST LATER

SEE SEPARATE C/S AND P/L

REVISIONS			
ZONE	LTR	DESCRIPTION	DATE / APPROVED

UNLESS OTHERWISE SPECIFIED DIMENSIONS ARE IN INCHES	SIGNATURES	DATE	
TOLERANCES ON:	DRAWN		
3 PLACE DECIMALS ± .010	CHECKED		
2 PLACE DECIMALS ± .005 ALL SURF 125	ENGINEER		
ANGLES ± 0° 30'	MFG		
FINISH 125	PROJ. ENGR.		
MATERIAL			

GENERAL ELECTRIC
SPACE SYSTEMS DEPT. LOC. PHILA PA

SLIP RING - ASSEMBLY
LIQUID METAL

SIZE	DRAWING NO.	REV
E	23991 47E223276	

SCALE 1/1 SHEET 1 OF 2

47E223276

Figure 33

REVISIONS

ZONE	LTR	DESCRIPTION	DATE	APPROVED

38 REAM HOLE TO FOR FORCE FIT OF PIN AFTER FINAL LOCATION OF TORQUER PER NOTE 3

30 - 8 PLACES TORQUE BOLT TO 12-15 LBS

(REF) 39

4 PLACES 37

4

DISK ASSEMBLY SEE TABLE FOR PART NUMBER AND POSITION (ZONE F 2)

ELECTRICAL LEADS. THREAD LEADS THRU APPROPRIATE SLOT OR HOLE DURING ASSEMBLY OF DISK

38 REAM HOLE TO FOR FORCE FIT OF PIN AFTER FINAL LOCATION OF RESOLVER PER NOTE 3

31 - TYP 8 PLACES

(REF) 40

7

SECTION B-B

SECTION D-D

SECTION A-A

& SECTION C-C

TORQUE NUT TILL WAVE WASHER FN 29 IS 128 HIGH

SEE NOTE 3

POWER RINGS | SIGNAL RINGS | HIGH VOLT. RINGS | VERY HIGH VOLT RINGS | HIGH VOLT RINGS | SIGNAL RINGS | RESOLVER RINGS | POWER RINGS

SEE NOTE 3

29 36 33 1 32 5 24 39 6 27 3 26 24 2 28 SEE NOTE 5 8 - TORQUE BOLT TO 12-15 LBS 35 - 8 PLACES - SEE NOTE 9 SEE NOTE 4 34 40 25

DISK N°120

DISK N° 1

2.565 ± .001

5.030 ± .001

8.375 ± .001

10.840 ± .001

12.34 ± .035

TYPICAL 4 PLACES PEEL SHIM SIDE TO SUIT DIMENSIONED STATION POINTS INSTALL BETWEEN DISK No 24 AND 25 No 48 AND 49 No 72 AND 79 No 96 AND 97

ALL WIRING LEADS ON DISKS NOS 63 TO 120 TO BE ROUTED THRU THIS END OF SHAFT

ALL WIRING LEADS ON DISKS NOS 1 TO 62 TO BE ROUTED THRU THIS END OF SHAFT

TABLE OF DISK POSITIONS

DISK POS.	PART NUMBER	DESCRIPTION
1 THRU 2	470223277 G7	POWER RINGS
3 - 6	470223277 G8	RESOLVER RINGS
7 - 12	470223277 G2	SIGNAL RINGS
13 - 18	470223277 G1	" "
19 - 24	470223277 G4	" "
25 - 29	470223277 G5	" "
30	470223277 G3	HIGH VOLTAGE RING
31 THRU 36	470223277 G2	" " "
37 - 42	470223277 G1	" " "
43	470223277 G4	" " "
44 THRU 47	470223277 G6	" " "
48	470223277 G4	" " "
49 THRU 53	470223277 G3	" " "
54	470223277 G3	VERY HIGH VOLTAGE RING
55	470223277 G3	" " " "
56	470223277 G2	" " " "
57	470223278 G1	" " " "
58	470223278 G4	" " " "
59	470223278 G3	" " " "
60	470223278 G2	" " " "
61	470223278 G1	" " " "
62	470223277 G4	" " " "
63	470223278 G3	" " " "
64	470223278 G2	" " " "
65	470223278 G1	" " " "
66	470223277 G4	" " " "
67	470223277 G4	" " " "
68 THRU 78	470223277 G4	HIGH VOLTAGE RINGS
79	470223277 G5	" "
74 THRU 77	470223277 G5	" "
78	470223277 G3	" "
79 THRU 89	470223277 G2	" "
65 - 90	470223277 G1	" "
91	470223277 G4	" "
92 THRU 96	470223277 G4	SIGNAL RINGS
97 - 102	470223277 G5	" "
103 - 108	47 0223277 G2	" "
109 - 114	470223277 G1	" "
115 - 118	470223277 G4	" "
119 - 120	470223277 G7	POWER RINGS

UNLESS OTHERWISE SPECIFIED DIMENSIONS ARE IN INCHES TOLERANCES ON: 2 PLACE DECIMALS ± .010 ALL; 3 PLACE DECIMALS ± .005 SURF; ANGLES ±; FINISH; MATERIAL

GENERAL ELECTRIC SPACE SYSTEMS LOS ANGELES, CAL.

SLIP RING - ASSY LIQUID METAL

SIZE E | CODE IDENT NO. 23991 | 47E223276

SCALE 1/1 | SHEET 2 OF 2

47E223276

Figure 34

34

80

In the preliminary design of the probe concept, two Inland torque motors, each having an ouput of 11 ft. lbs. were used. It was subsequently decided that based on the solar panel torque requirements, smaller torque motors could be satisfactorily utilized on the slip ring and, therefore, 1.3 ft. lb. Inland torque motors were selected. This motor weighs approximately 1.2 lbs. and has an OD of 6.01 inches and an ID of 4.5 inches. As a comparison, the 11 ft. lb. motor has an OD of 9.0 inches and an ID of 5.37 inches. Thus, in addiition to the motor weight considerations, there is the advantage of a reduction in OD of 3.0 inches with an ID still sufficient to accept slip ring leads. This will reflect in a smaller slip ring size and weight.

A single speed resolver having an accuracy of 3 arc-minutes was selected for the position sensor. This was a Kearfott gimbal-type resolver which has a 4.68" OD and 3.12" ID. The resolver has a nominal accuracy of 5 arc-minutes, however, the vendor was contacted and could deliver one with 3 arc-minutes of accuracy in the same size.

These component changes were incorporated into the design. In addition, in order to reduce the bending loads on the outer shaft, two bulkhead-type mounting flanges, one at each end, will be used. This replaces the original design approach of providing a cantilevered support mounted from one end.

The disk placement on the shaft is symmetrical about the center with the exception of the 4 resolver disks which are located at the resolver end of the shaft. The power disks require 8 leads each because of their high current capacity. These are located at the ends of the shaft to minimize lead weight by reducing the length of lead required. The 15 amp high voltage disks, 8 total, requiring 4 leads per disk, are located between the signal disks and the center of the shaft. This location was necessary since there would have been an insufficient amount of material on the outer shaft to mount 4 probes required per disk adjacent to the 8 probe power disks. Table 1 lists the disk electrical characteristics, thicknesses, shaft location, leads requirements and quantity required.

The overall length of the disk assembly on the shaft is 13.130". The main shaft assembly includes torquers, resolvers, bearings, and support flanges in addition to the disk assembly. The overall length of the main shaft assembly is 20.75 inches.

The outer stator shaft will be made in two halves, split longitudinally and assembled as a clam shell. This will facilitate assembly, especially the assembly of the probes into the gallium. The assembly of the probes into the gallium will be as follows: The disks will be assembled on the rotor shaft without gallium. One half of the clam shell will be installed and the probes inserted and aligned to their correct position by rotation. The probes will be eccentric with an off-center rotation of .10 inch diameter to accommodate the tolerance build up within the disk groups and

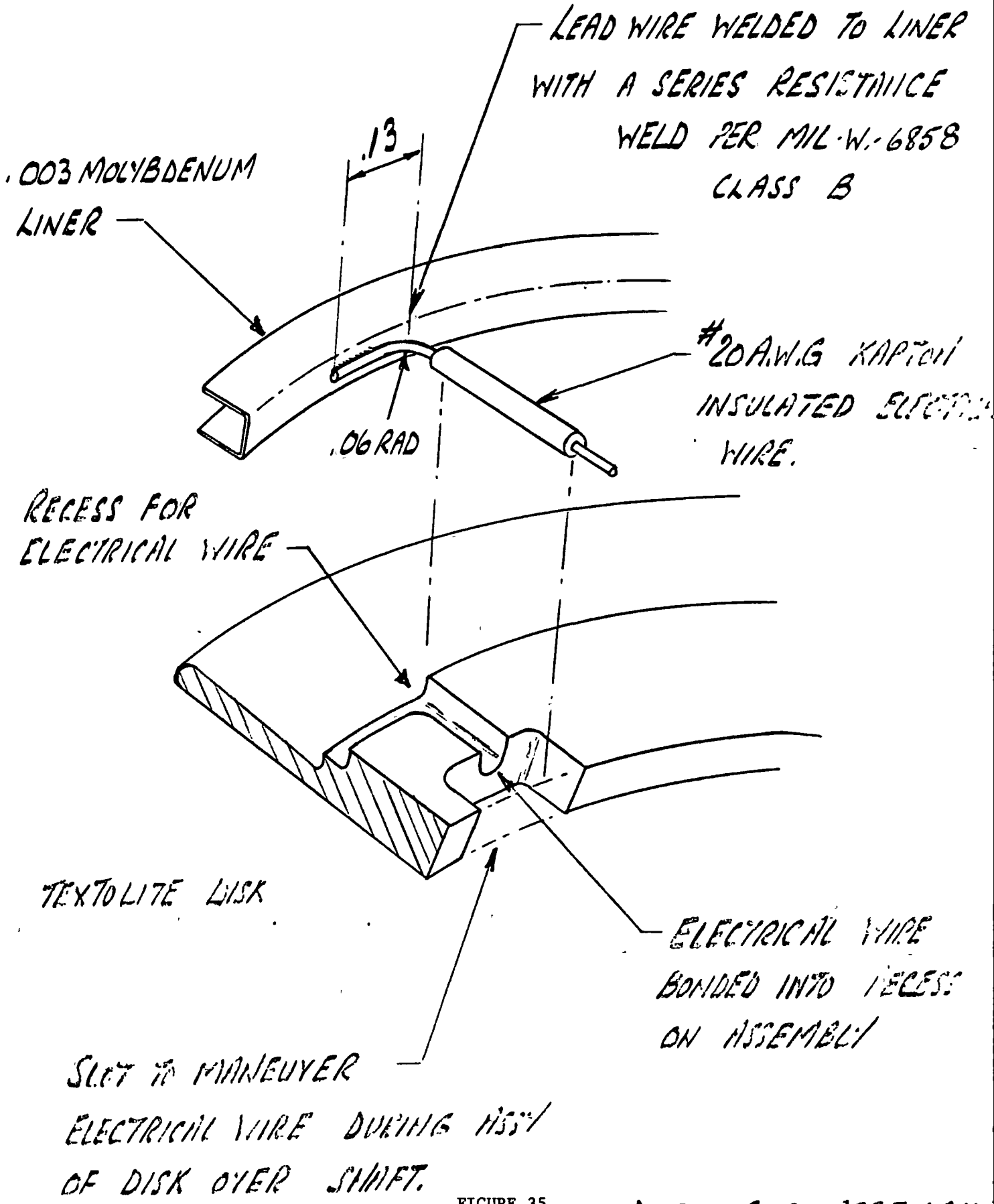

FIGURE 35

DISK SUB-ASSEMBLY

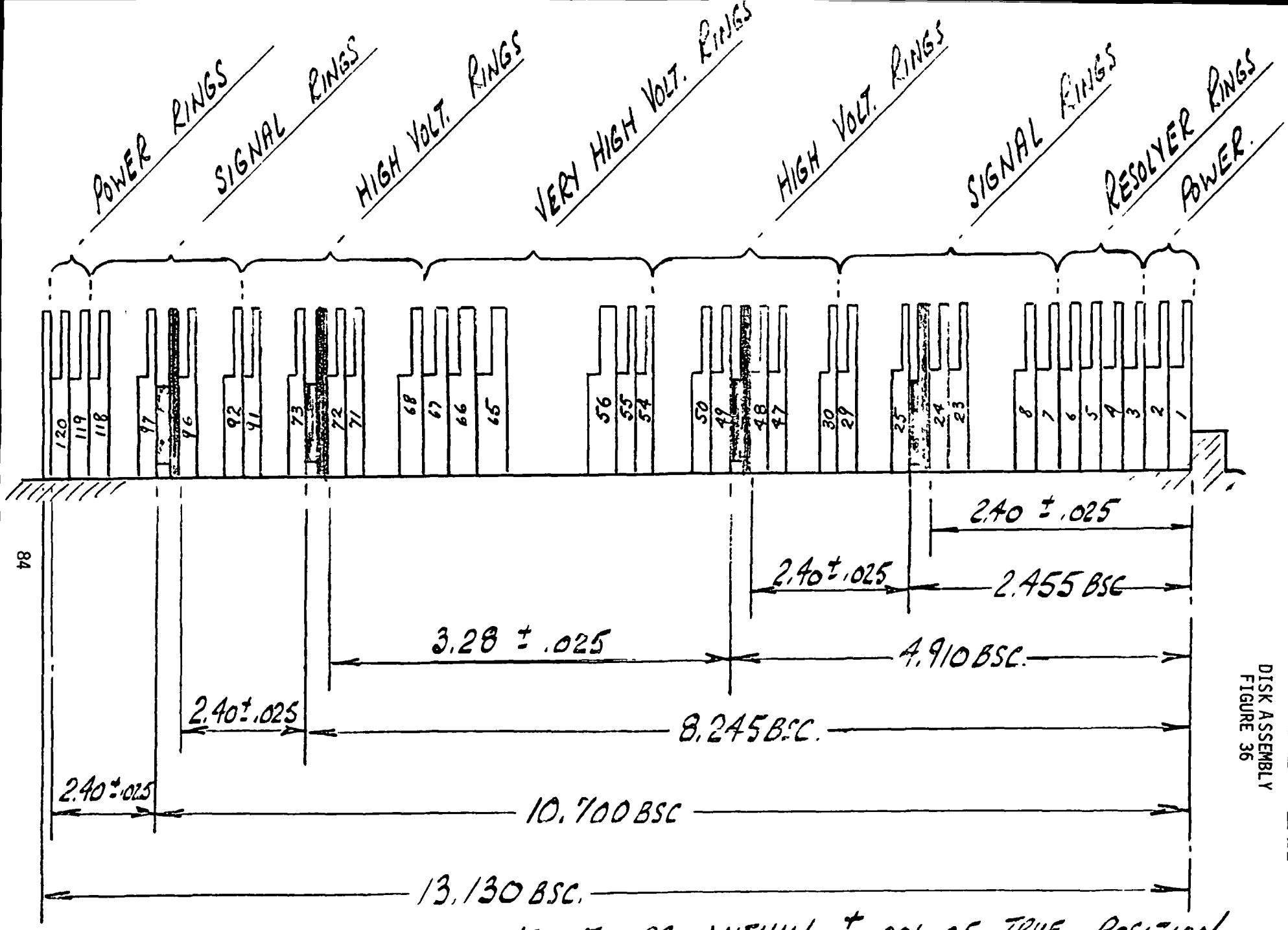

NOTE. BASIC DIMENSIONS TO BE WITHIN ± .001 OF TRUE POSITION.

DISK ASSEMBLY
FIGURE 36

TABLE 1. DISK TABULATION AND LOCATION

TYPE	LEADS	RING NO.	THICKNESS	VOLTS	AMPS	# REQUIRES
POWER	8	1, 2 119,120	.10	300	30	4
RESOLVER	2	3 - 6	.10	30	.135	4
SIGNAL	2	7 - 29 92 - 118	.10	300/2000	.20	50
HIGH VOLTAGE	4	30 - 33 88 - 91	.10	2000	15	8
	2	34 - 47 74 - 87	.10	2000	3	28
	2	48 - 53 68 - 73	.10	2000	1	12
VERY HIGH VOLTAGE	2	54, 67	.10	2000	.5	2
	2	55, 66	.10/.18	3000	.5	2
	2	56, 65	.18	6000	.5	2
	2	57, 64	.18	9000	.5	2
	2	58, 63	.18	12,000	.5	2
	2	59 - 62	.18	15,000	.5	4

the out-of-position tolerance of the tapered probe installation holes in the outer shaft. The probe position will be marked so that they can be removed if necessary to facilitate assembly. This procedure is then repeated with the other half of clam shell. With clam shells removed, gallium preforms are inserted into disk cavities and melted. The stator shaft halves (clam shells) are then reassembled.

It is contemplated that the stator shaft will be fabricated out of either aluminum or magnesium. However, some consideration is merited on the possibility of fabricating it out of Textolite. The major reason for using Textolite is to improve the dielectric characteristics by reducing the possibility of voltage breakdown either between electrodes, or between electrode and ground, especially for the very high voltage rings which have a 15,000 volt requirement.

The disks are being tapered by about 2° to provide for both gallium and contamination retention. The amount of taper is limited primarily by clearance and tolerance considerations. As discussed, in section B.9 "Dielectric Stress," it is possible to have a very high voltage gradients across the gap between the liner and the Textolite. These gradients can lead to corona or voltage breakdown which can cause degradation of the Textolite insulation. The voltage gradient can be eliminated by having an electrically conducting paint on the Textolite surface which is in proximity with the liner. A candidate material for this is Eccobond solder V-91 which is a good adhesive and has high electrical conductivity. It is important not to have the paint extend beyond the edge of the liner so as to substantially reduce the breakdown path between adjacent rings.

Resolver Installation

Due to the very high accuracy required from the resolver, special care has to be taken in assembly. The proposed method is as follows:

1. The resolver and outer mounting ring will be supplied by the vendor. A source control drawing will give specific envelope dimensions and tolerances to be adhered to.
2. The inner mounting ring will be separately detailed and need not be supplied by the resolver vendor.
3. At installation the inner mounting ring will be assembled onto the rotating shaft. The inner half of resolver can be set to required concentricity tolerances, with respect to the outer stator shaft. The outer mounting ring along with the outer half of the resolver as an assembly, will then be assembled to the stator side support flange. Positioning will be achieved by indicating the outside diameter of the mounting ring, with respect to the rotating shaft. The outer ring will have been machined concentric to the inside bore of the resolver stator. Attachment screws will then be tightened down and the mounting ring pinned.

5.0 CONCLUSIONS

The following conclusions can be made based on the results of this program:

1. A liquid metal slip ring/solar array orientation mechanism to transfer electrical power across a rotating gap is feasible.
2. A liquid metal slip ring having 116 rings operating at voltages up to 15,000 volts and currents up to 30 amps weighs less than 40 pounds and is approximately 9.0 inches in diameter and 20 inches long.
3. The probe concept slip ring design will operate in a vacuum with gallium for extended periods without building up or ejecting debris.
4. Gallium is feasible as the liquid metal, and nickel as the electrode material.
5. Contamination free gallium is not attainable in atmospheres containing several parts per million oxygen or water vapor.
6. Solid and liquid gallium can be successfully retained by cavity geometry under launch and orbital environments.

6.0 RECOMMENDATIONS

A liquid metal slip ring using gallium has been successfully demonstrated. There are, however, a number of topics which should be investigated further in order to achieve a higher level of confidence and understanding in the function of the slip ring. Topics include:

1. Determination of composition of gallium contamination.
2. Determine rate of formation of debris in air and under protective atmospheres when gallium is both liquid and frozen.
3. Development of contamination clean-up techniques.
4. Accelerated functional tests at 10 revolutions per day, 15,000 volts and 30 amps.
5. Functional tests at 1 revolution per day, 15kv and 30 amps.

APPENDIX A

PRELIMINARY DESIGN STUDY

A.1 Introduction

A design study was made in which a number of design concepts for the liquid metal slip ring/solar array orientation mechanism were evolved. Each design concept was based on meeting the functional, operational and environmental requirements imposed on the slip ring. Specific critical areas to the design, fabrication and test were identified. These were investigated in detail by design drawings and engineering studies. After the completion of the design phase, a complete in-depth study of the various concepts was performed and selection recommendation made. A very major consideration in the entire design study was the determination of techniques to reduce the formation and ejection of gallium contamination.

A.2 Slip Ring Design Requirements

A.2.1 Slip Ring Assembly

The basis slip ring functional requirements are to transfer electrical power and electrical signals across a rotating interface. A total of four sets of rings were required and were designated: power, signal, high voltage and very high voltage. The specific number of rings, current and voltage requirements of the slip ring are summarized in Table A-1. The most severe requirement was the 15,000 volts of the very high voltage rings. This requirement establishes such parameters

RING DESIGNATION	NUMBER	CURRENT CAPACITY (Amps)	VOLTAGE RATING (VOLTS)	ALLOWABLE POWER LOSS (Watts)
Power Rings	4	30.0	+300 Ring-Ring ±300 Ring-Ground	2 per ring
Signal Rings	50(min)	0.2	+300 Ring-Ring 2000 Ring-Ground	
High Voltage Rings	48 total		Ring-Ring & Ring-Ground	2 (total)
	12	1.0	2000	
	28	3.0	2000	
	8	15.0	2000	
Very High Voltage	14	.5	15,000 Ring-Ring 15,000 Ring-Ground	

TABLE A-1

SLIP RING REQUIREMENTS

as insulation thickness, electrode to electrode spacing, electrode geometry, lead insulation, etc., not only for these rings, but the entire slip ring assembly design is influenced by these requirements.

The 30.0 amp requirement for the power rings is not particularly severe because sufficient electrode surface area can be provided so as to have adequately low current density.

The entire assembly was to be less than 10 inches, diameter, 24 inches long, and weigh less than 40 pounds.

A.2.2 Torquer Requirements

The designs provided two redundant torque motors which produce a rotation of the center shaft relative to the housing. It was anticipated that the torquers would eventually be brushless; however, brush type torquers were used in the design because of their availability. The operational specifications of the torquer are:

Power Input	
Voltage	100 volts dc, maximum
Current	10 amps dc, maximum
Torquer Output	
Torque	10 ft. lbs., minimum
Torque Sensitivity	1 ft. lb. per amp ±10%, maximum
Operation	
Pulsed mode	
Pulse width	.01 to 0.4 seconds
Repetition frequency	2 pulses per second, maximum

A.2.3 Position Sensor Requirements

A position sensor is required to measure angular position of the center shaft. The sensor must be a non-contact type, frameless and capable of 360° of continuous rotation. The position sensor shall be capable of measuring shaft position within $\pm$ 3 arc-minutes.

A.2.4 Bearing Requirements

The LMSR/SAOM incorporated preloaded angular contact bearings. However, the design was such that it could accept unconventional bearings such as magnetic or fluid bearings without compromising the design concept. The friction level torque design requirements for the bearings were as follows:

Running friction torque at 1 earth rate	3 in-oz.
Variations in running friction torque at 1 earth rate	1 in-oz.
Starting friction torque	10 in.oz.

A.2.5 Shroud Requirements

A shroud is required to permit the circulation of a dry cold gas through thr LMSR/SAOM. The shroud shall also be capable of functioning as a magnetic or rf shield, if necessary.

A.2.6 Lead Requirements

Each slip ring terminates in a separate lead. The leads from each half of the rings extend through the shaft end closest to those rings. The voltage and current ratings of the lead insulation and wire are consistent with the ring requirements as well as the proximity to adjacent rings or leads.

A.2.7 Environmental Requirements

The following are the environmental requirements for the LMSR/SAOM.

A.2.7.1 Pre-Launch Environment (non-operative)

The applicable environments for the pre-launch condition cover the time from final assembly, shipping, storage and launch pad to launch.

The LMSR must be frozen and purged with a dry gas.

A.2.7.1.1 Vibration, Shock, Acceleration

The system is designed for vibration, shock, and acceleration levels expected during shipment via commercial air.

A.2.7.1.2 Temperature

-20°C to +70°C

A.2.7.1.3 Thermal Shock

10°C/minute

A.2.7.1.4 Pressure

One atmosphere to 50,000 feet

A.2.7.1.5 Humidity

95% @ 30°C for 1 month

A.2.7.1.6 Salt Spray

Seaside atmosphere

A.2.7.1.7 Corrosive Atmosphere

Propellant fumes from Titan III C or Centaur

A.2.7.1.8 Shelf Life

The shelf life shall be greater than 18 months.

A.2.7.2 Pre-launch Test Environment

The pre-launch test environment applies during ground systems testing of the LMSR/SAOM. The LMSR shall be considered operating; it shall not be considered frozen during these conditions.

A.2.7.2.1 Acceleration

1.5 g's on all axes.

A.2.7.2.2 Shock

10 g's peak with 1/2 sine wave waveform of 8 milliseconds duration on all axes.

A.2.7.2.3 Vibration

0.1 g's random in frequency range of 20 to 2000 Hz superimposed on 1g static acceleration; all axes.

A.2.7.2.4 Pressure

One atmosphere and 10^{-5} to 10^{-9} torr.

A.2.7.2.5 Temperature

-30°C to +80°C

A.2.7.3 Launch Environment

The LMSR/SAOM will not function during launch. Six hours coast time between thruster burns may be required to achieve desired synchronous orbit.

A.2.7.3.1 Acceleration

15 g's all axes

A.2.7.3.2 Shock

22 g's peak with 1/2 sine wave waveform of 11 millisecond duration on all axes.

A.2.7.3.3 Vibration

Sinusoidal

Axis	Frequency Range (Hz)	Level q,	Sweep Rate Octaves/Minute
All	5 - 10	0.9 in. D.A.	2.0
	10 - 50	± 4 g	
	50 - 200	± 3 g	

A.2.7.3.3 (Continued)

R a n d o m

Axis	Frequency Range (Hz)	PSD Level g^2/Hz	Acceleration	Duration
All	20 - 250	0.001 to 0.16 increasing from 20 Hz at a rate of 6 db/octave	17.0	4 min. each axis
	250 - 2000	.16 roll off above 2000 Hz greater than 40 db/octave		

A.2.7.3.4 Temperature

For high temperature, add 15°C to the worst case high temperature. For low temperature, subtract 15°C from worst case low temperature.

A.2.7.3.4.1 Radiation

Assume the LMSR/SAOM is exposed to the sun on all sides for high temperature. For low temperature, assume the system is radiating to dark space.

A.2.7.3.4.2 Conduction

Assume all interface mounting blocks are heat sinks at -10°C to +50°C.

A.2.7.4 Operating Environment

A.2.7.4.1 Acceleration

Linear accelerations of $\pm 10^{-3}$g continuous on any axis may be expected.

A.2.7.4.2 Vibration

Linear accelerations in the form of square waves (10^{-3}g's O-P) over the frequency range of .0004 to 4 Hz may be expected.

A.2.7.4.3 Shock

Shocks may arise from pyrotechnic releases. 10 g's peak with 1/2 sine wave waveform of 8 milliseconds duration on all axes.

A.2.7.4.4 Pressure

10^{-5} torr to hard vacuum. The system must be designed for freezing at one atmosphere and thawing in a hard vacuum.

A.2.7.4.5 Temperature

For high temperature, add 15°C to the worst case obtained below and for low temperature subtract 15°C.

A.2.7.4.5.1 Radiation

Assume the system is exposed to the direct sun on all sides continuously. During shadow, assume shadow entry in 1 minute radiating to dark space on all sides for 75 minutes. The system must rotated during shadow.

A.2.7.4.5.2 Conduction

Assume all interface mounting blocks are heat sinks at -10°C to +50°C.

A.2.7.5 Magnetic Fields

The system shall meet all design specifications in the presence of a 0.5 gauss magnetic field oriented in worst case direction.

A.2.7.6 RF Fields

The system shall meet all of the design specifications in the presence of the following rf field: .01 watts/m^2, 800 MHz to 15 GHz.

A.3 Design Concepts

During the preliminary design phase, design concepts were evolved and studied in detail with the objective of meeting the requirements of the slip ring and to determine the optimum design. Some of the specific areas which were considered for each design included:

a) Electrode design for gallium containment under dynamic environments; ease of filling with gallium, fabrication and assembly; size and weight.

b) Methods for minimizing gallium contamination formation and ejection from slip ring.

c) Disk design for ease of fabrication and assembly.

d) Methods for connecting wire to electrodes and wire routing.

e) Packaging and assembly of motors, resolver, bearings.

f) Provisions for assembly to solar array.

The following design concepts were generated during the design study:

Flat disk

Stacked disk

Slotted disk

Post

Probe

Side Electrode

Integrally wound

The results of the preliminary design study are summarized in Section A-4.

The approach recommended was the probe concept. The basis for recommending the probe concept were:

1. Excellent low contamination generation characteristics.
2. Excellent configuration for contamination containment.
3. Ease of gallium filling.
4. Ease of fabrication, assembly and inspection.
5. Meets size and weight requirements.

A.3.1 Flat Disk Design

The flat disk design consists of a number of rotating disk assemblies mounted on a central shaft with stationary disk assemblies interleaved between them. Rotating disk assemblies and stationary disk assemblies consists of separated substrates fabricated from an insulating material to which electrode rings are bonded. Leads which are connected to the electrode rings pass between the substrates. A volume of gallium is placed between adjacent electrode rings to complete the electrical path. The flat disk design is shown in Figure A-1.

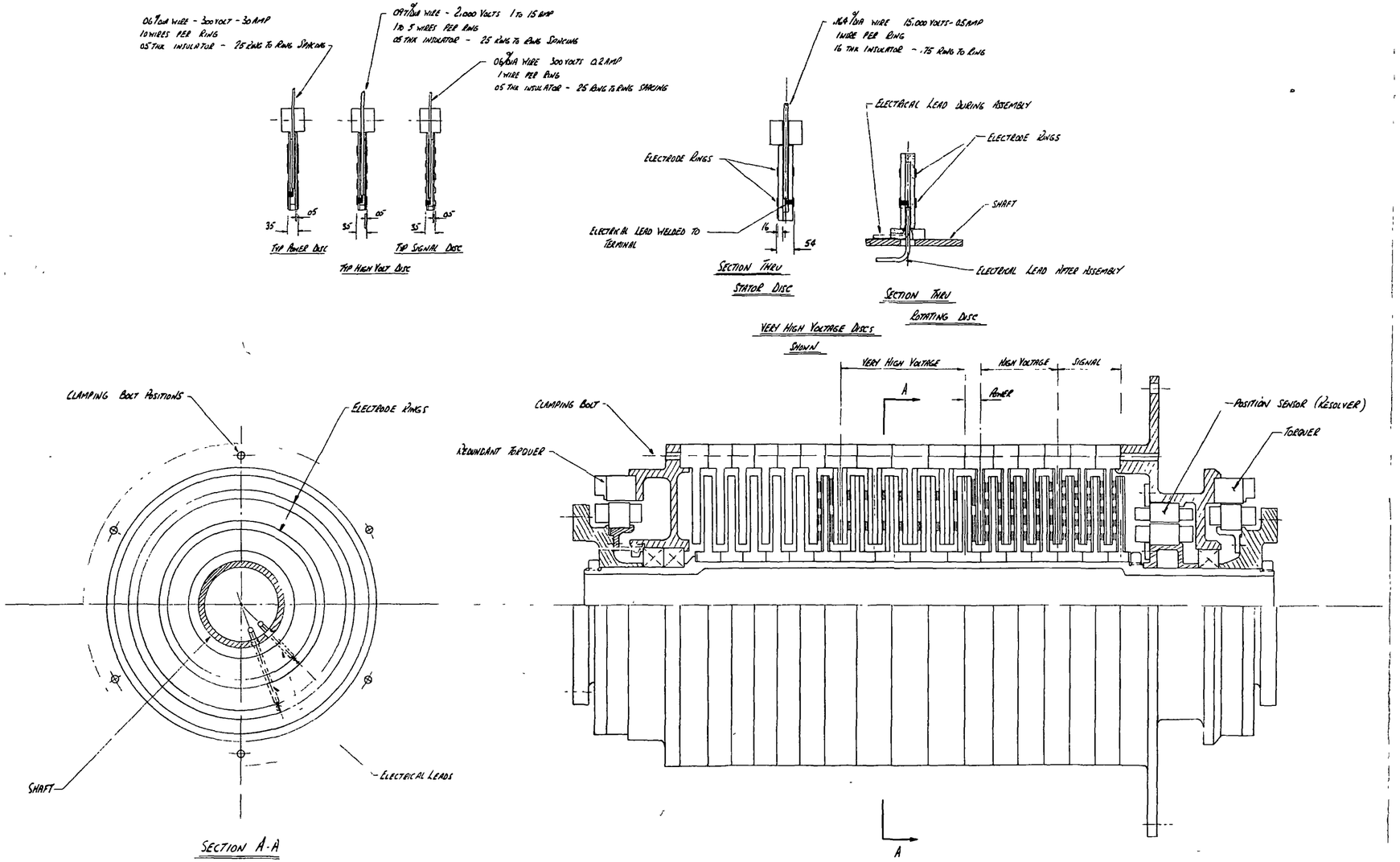

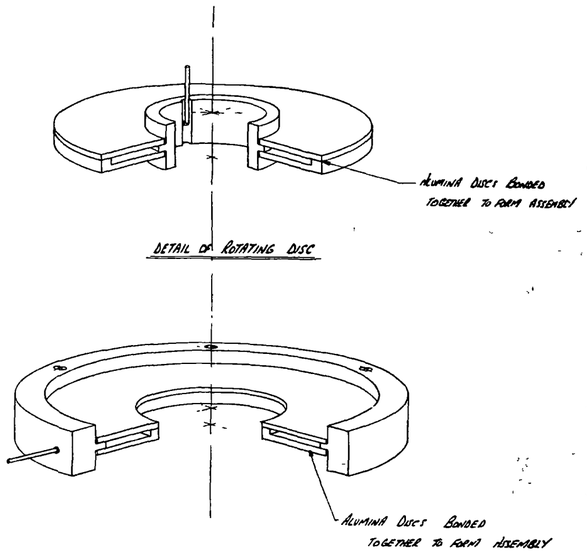

FIGURE A-1
FLAT DISC CONCEPT

In the initial approach to the flat disk design as shown in Figure A-1 four different disk assemblies were used to accommodate the different voltage and current requirements of the slip ring groups. Figure A-2 shows a disk assembly incorporating revised assumptions for electrode sizing. These revised assumptions consider that the current flow is shared by the gallium and electrodes proportional to their respective electrical resistances, and that the gallium fill is continuous with no voids. The original assumption was more conservative in that the electrodes were sized so that they could individually carry full current without causing excessive power losses. The revised assumptions allow five high voltage electrode rings and four power electrode rings to be bonded to each insulating substrate. The number of signal and very high voltage electrode rings bonded to each substrate was not changed since the number was determined primarily by the dielectric breakdown characteristics.

Figure A-2 shows raised circumferential rings of insulating material which was considered for a number of reasons: to help in the containment of possible contamination, increase the length of surface dielectric breakdown path, and to reduce the possibility of electrode to electrode breakdown. However, this added more weight to the design which would have to be evaluated if the approach were to be considered.

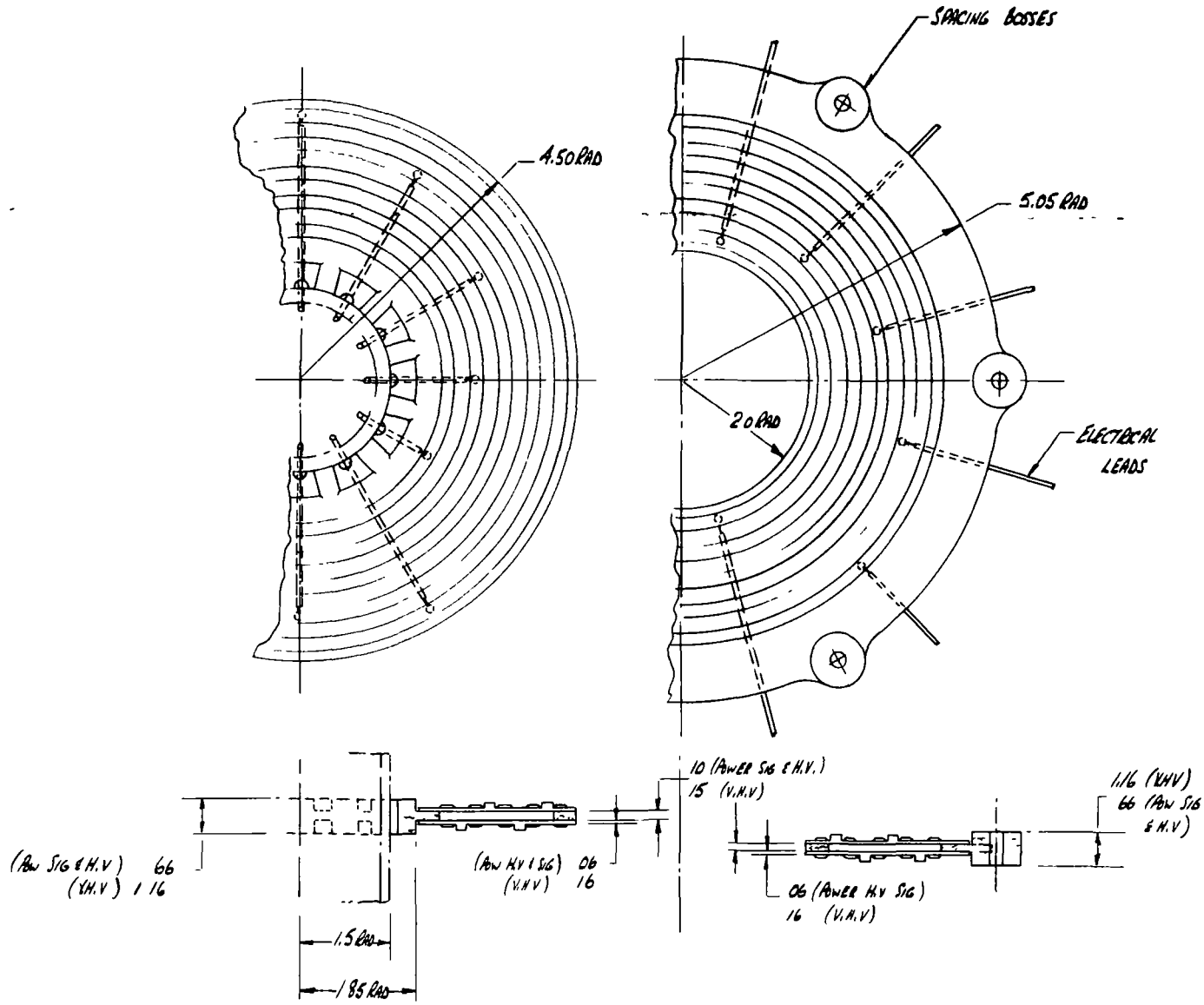

ROTATING DISC

FIXED DISC

NOTE. 1. SUPPORT STRUCTURE BASED ON AL ALLOY - MAGNESIUM WILL REDUCE WEIGHT BY 40%

2. DIELECTRIC BREAK DOWN ASSUMED MARGINAL FOR TEXTOLITE AT 16 THK ALUMINA DISCS USED FOR THIS WEIGHT CHK

MATERIAL	ALUMINA				TEXTOLITE			
	INDIVIDUAL DISCS		NO POSITIONS	TOTAL WT	INDIVIDUAL DISCS		NO POSITIONS	TOTAL WT
	ROTATING	FIXED			ROTATING	FIXED		
DISC (H.V. SIG & POWER)	1 80	1.60	11 EACH	30.8	57	75	11 EA	14.5
DISC (V.H.V)	1.50	2 02	4 EACH	14.08	*	*	*	13.0
ELECTRODE (H.V. SIG & POWER)	35	35	102 EA	7.14	-	-	-	7 14
" (V.H.V)	25	25	4 EACH	2.00	-	-	-	2 00
					-			
WIRE (POWER & SIG)	-	-	-	.112				.112
" (H.V.)	-	-	-	216				216
" (V.H.V)	-	-	-	040				.040
				54.388				37.008
SHAFT & SUPPORT STRUCTURE				15 00				15.00
RESOLVER & BEARINGS				2 25				2.25
MOTORS				20 6				20 6
				92 238				74.858

DISK DESIGN CONFIGURATION

FIGURE A-2

The electrode rings would be bonded to the insulating substrate with an adhesive and the excess material chem-milled away. This is a standard technique which is used in the manufacture of printed circuit boards and this technique is directly applicable to the size and geometry required.

In order to reduce weight and to facilitate the assembly of the stationary disks, these disks would be designed so that when clamped together, they would also form the outer housing of the slip ring. This is shown in Figure A-1 with the clamping accomplished with six longitudinal bolts.

The major advantage of the flat disk design is its length being shorter than any of the other concepts studied. It has two major disadvantages: contamination retention and gallium filling. Electrodes are adjacent to each other, not separated by a labryinth or a cavity that would contain possible contamination. The build-up of contamination in inter-electrode spaces could result in a voltage breakdown between adjacent electrodes. Gallium filling would be accomplished by casting gallium into performed segments and frozen. These preformed segments would be placed between electrodes and then melted.

Gallium filling is difficult because there are multiple rings on each disk with no external access to the inner rings so that the position of the gallium preforms can be observed and adjusted.

A.3.2 Stacked Disk Design

The stacked disk design was evolved primarily to facilitate the gallium filling procedure by permitting filling after the completion of the slip ring assembly. The basic design concept consists of a series of flat, two-thickness, disks assembled on a rotating central shaft; the stationary disk assembly would be similar with mating disks extending into the slots formed by the rotating disks. Electrodes would consist of rings placed around the outer periphery of the rotating disks and at the base of the slots of the stationary disks. Gallium would be placed between wetted electrodes to complete the electrical path. With the stacked disk concept, the slip ring can be filled with liquid gallium and visually checked after the completion of assembly. This would be accomplished by having the outer disk a thin section with local bosses only in the area of the clamping bolts or by using a spacer section. This would leave a gap through which individual slip ring cavities could be filled with gallium by using a hypodermic. In addition, a continuous visual check could be maintained by observations through this gap.

Figures A-3 and A-4 show several stacked disk concepts. Figure A-3 shows two types of disk construction, the right hand portion of the layout shows disks all having the same diameter. With this fabrication and assembly technique, there was concern that there could be surface dielectric breakdown between adjacent outer electrodes. In order to provide a longer surface breakdown path, a staggered disk configuration, as shown on the left, was devised. Figure A-4 shows additional revisions to the basic approach with a minimum length concept and a minimum diameter concept.

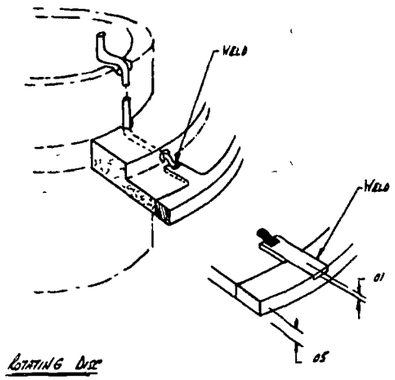

ROTATING DISC

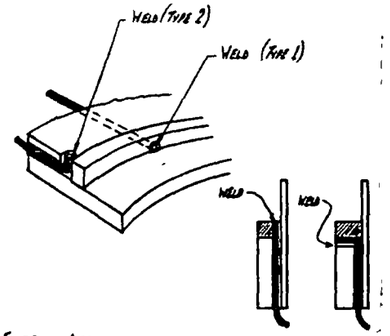

FIXED DISC

TYPE A — WELD IN CONTACT WITH GALLIUM

TYPE B

TYPE 2 — NON-STANDARD DISC DIA. - VARYING THICKNESS

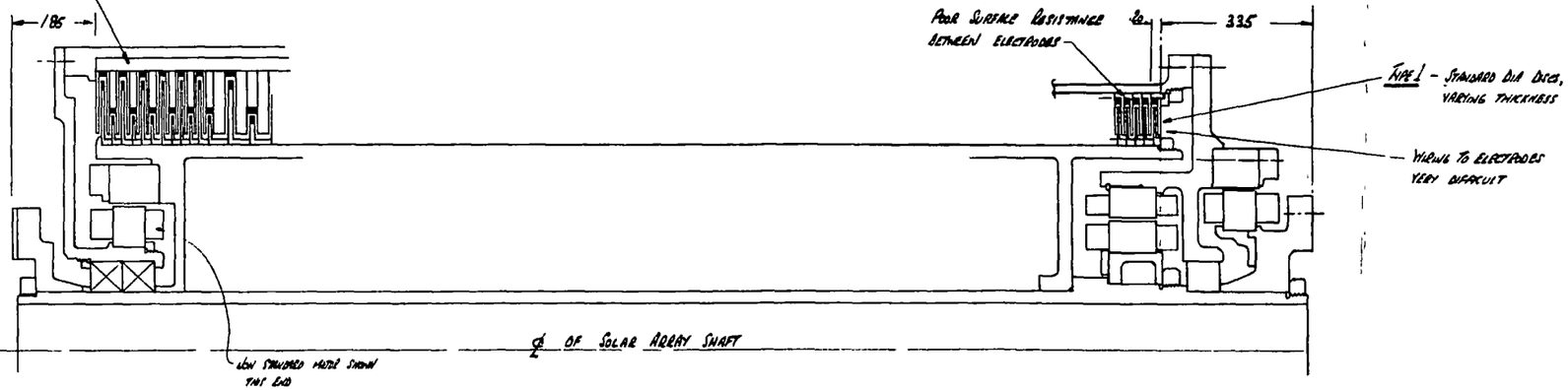

- WIRING TO ELECTRODES VERY DIFFICULT
- TOLERANCE BUILD UP ON DISCS CRITICAL
- NO CONTROL ON GALLIUM FILL

TYPE 3 STRUCTURAL DISCS

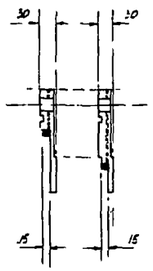

ALTERNATE DISCS

2,000 VOLT DISCS

108 DISCS AT 25 THICK = 25.50

15,000 VOLT DISCS

14 DISCS AT .45 THICK = 6.30

TOTAL BUILD UP = 31.80

OVERALL LENGTH = 37.00

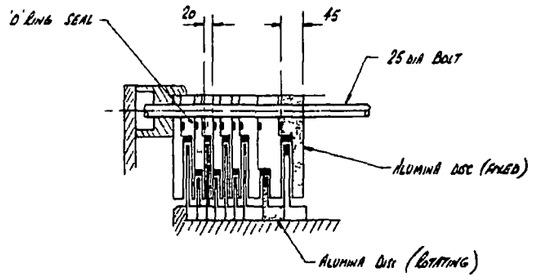

2000 VOLT DISCS

108 DISCS AT .20 THICK = 20.4

15,000 VOLT DISCS

14 DISCS AT .45 THICK = 6.30

TOTAL BUILD UP = 26.70

OVERALL LENGTH = 31.90

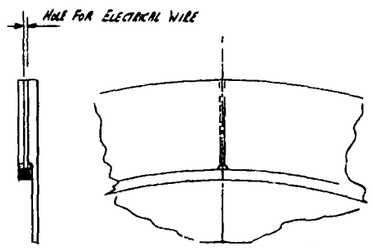

LIQUID METAL SLIP RING

STACKED DISC CONCEPT

FIGURE A3

SCALE 1/1

JULY 70

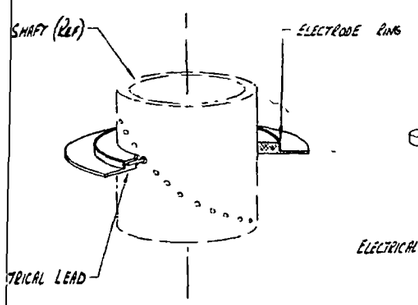

DETAIL A
SHOWING ROTATING DISC

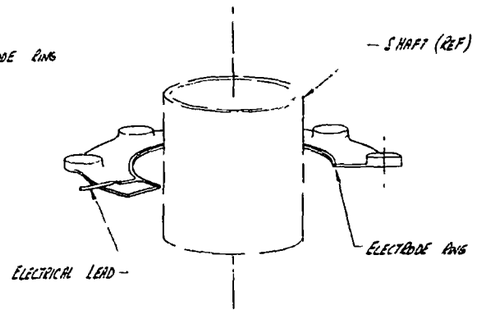

DETAIL B
SHOWING FIXED STATOR DISC

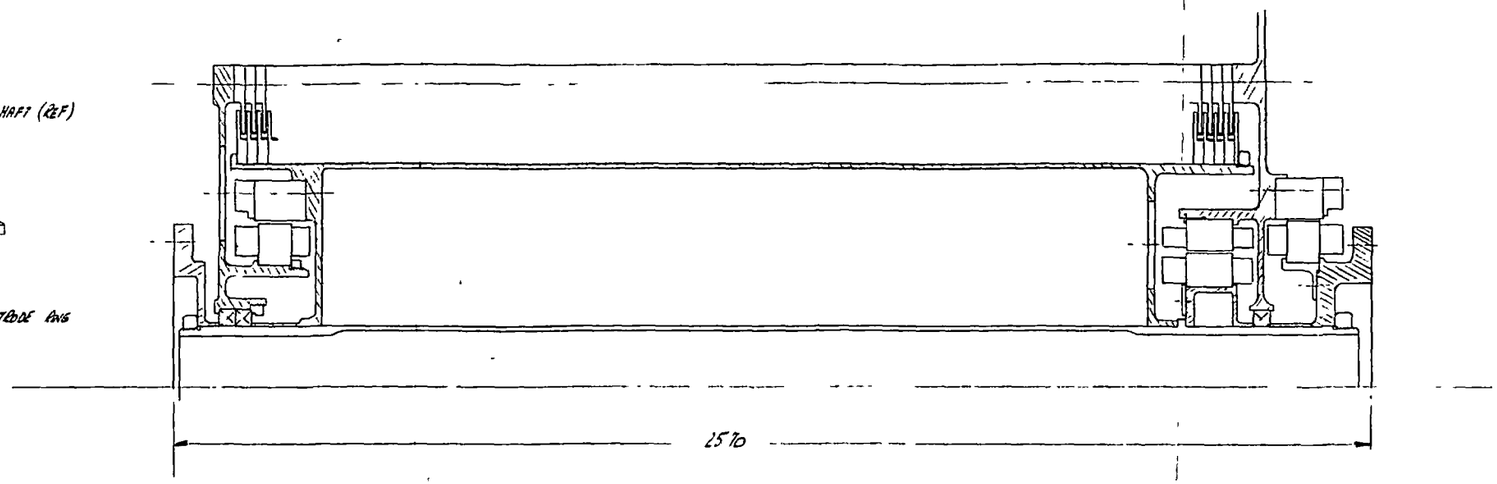

MINIMUM LENGTH CONCEPT

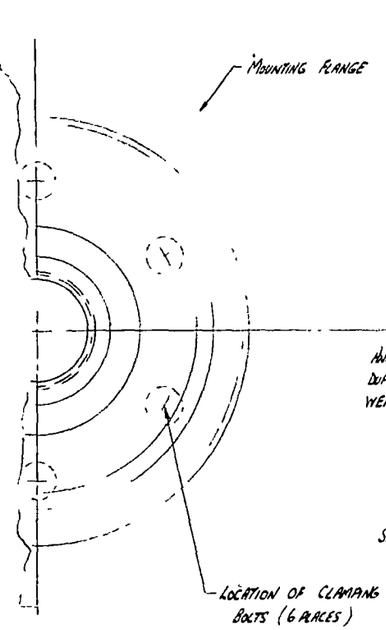

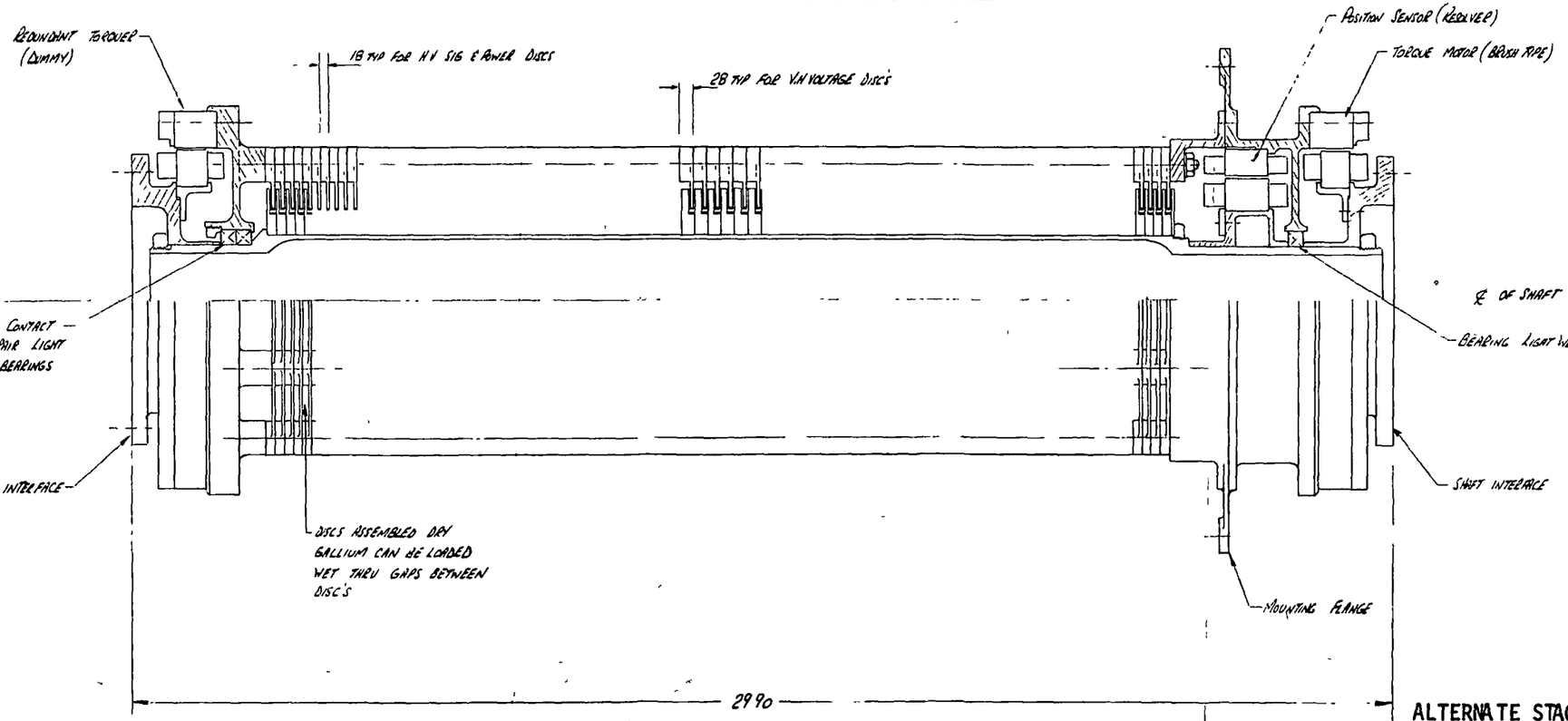

MINIMUM DIA CONCEPT

ALTERNATE STACKED DICS CONCEPT

LIQUID METAL SLIP RING

SCALE 1/4 1/20 1/5

REVISION A

FIGURE A4

Length is inherently a key factor in this concept. As designed, the gallium ring spacing is .12"; this is based on a .06" wide stationary electrode ring with .03" gaps on either side for rotating clearance. Overall length is therefore entirely dependent on the working clearance gap, stationary electrode thickness and insulation film thickness.

In this concept, gallium is allowed to fill the bottom of the circumferential slot allowing contact between the gallium and insulator material. The capillary forces that are established at the insulation material-gallium interface maintain gallium retention. Because of the uncertain stability of this interface with insulator materials, and possible reactions between the gallium and the insulator, metallic or insulator coatings might be considered to provide a stable and compatible interface. These coatings could be sputtered on the base insulation material forming a tenacious and continuous protective barrier.

Manufacturing and assembly tolerances will probably be a serious restraint with this concept. Because of the very narrow gaps, thickness and flatness tolerances will be very tight, and due to potential gallium leaks, "O" rings will probably be required between each stacked disk on the rotating shaft.

Figure A-5 shows detail disk design and a weight analysis for the stacked disk concept.

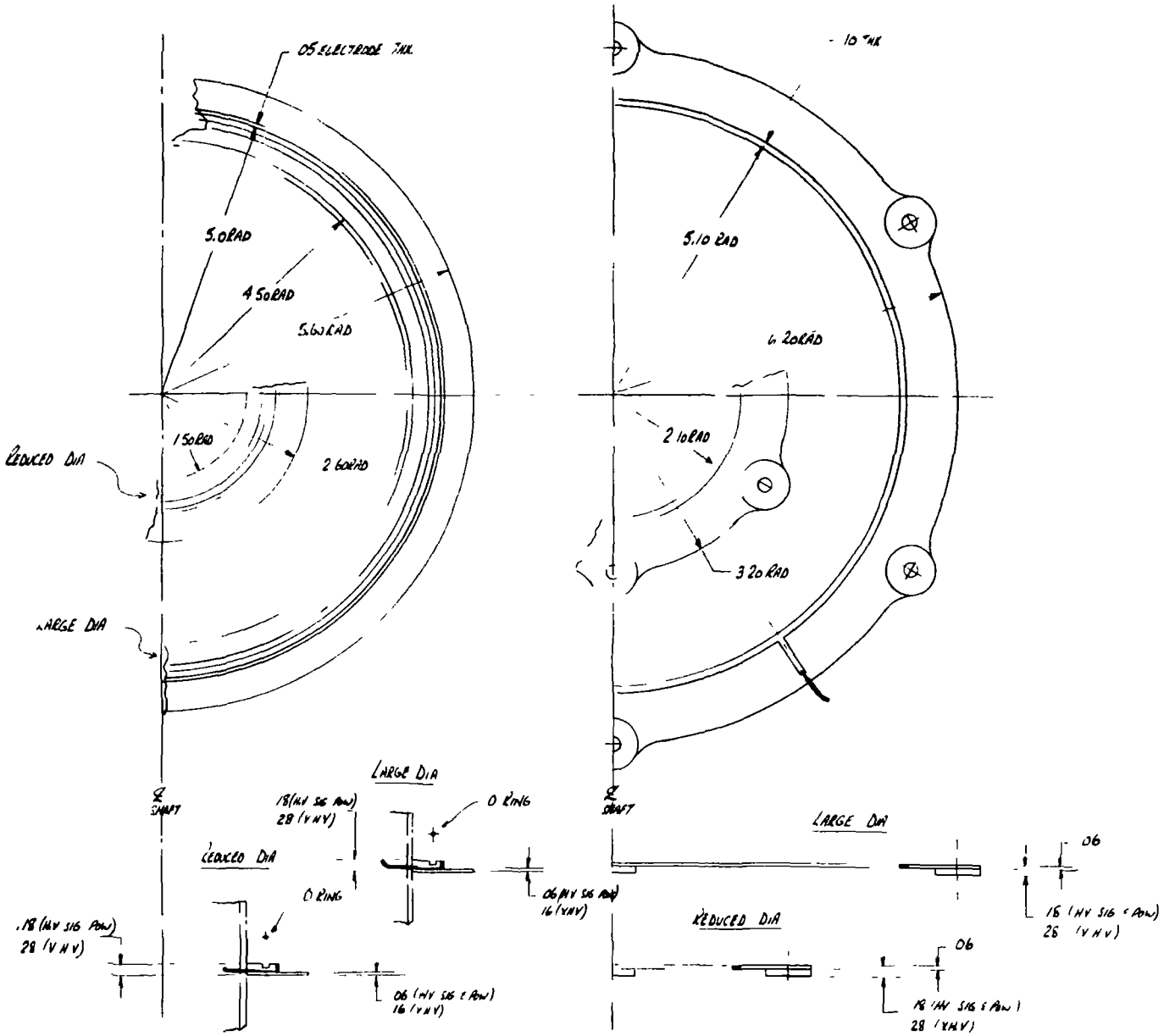

ROTATING DISC

FIXED DISC

MIN LENGTH (MAX # FAIRINGS BURIED) LARGE DIA

MATERIAL	ALUMINA				TEXTOLITE				REDUCED DIA	
	INDIVIDUAL DISCS		N° POSITIONS	WT TOTAL	INDIVIDUAL DISCS		N° POSITIONS	WT TOTAL	WT WEIGHT	
	ROTATING	FIXED			ROTATING	FIXED			ALUMINA	TEXTOLITE
DISC (HV SIG & POWER)	48	29	102 EA	78 6	226	136	102 EA	36 0	35 2	16 5
DISC (V H V)	95	33	14 EA	17 9	"	"	"	17 9	8 1	8 1
ELECTRODE (HV SIG & POW)	056	.059	102 EA	11 7	-	-	-	11 7	4 9	4 9
ELECTRODE (VHV)	056	059	14 EA	1 6	-	-	-	1 6	66	66
WIRE (POWER & SIG)	-	NEG	-	10	-	NEG	-	10	10	10
(HV)	-	NEG	-	18	-	NEG	-	18	18	18
(VHV)	-	NEG	-	03	-	NEG	-	03	.03	03
				111 11				77 57	49 19	30 49
SUPPORT STRUCTURE *				28 0				28 0	17 0	17 0
BEARINGS & RESOLVER				8 25				8 25	2 25	2 25
MOTORS				20 6				20 6	20 6	20 6
				142 96				98 30	89.04	70 34

DISC DESIGN & WEIGHT ANALYSIS

NOTE 1 * SUPPORT STRUCTURE BASED ON HI ALLOY - USING MAGNESIUM WILL REDUCE WT BY 1/3 TO

2 * DIELECTRIC BREAK DOWN ASSUMED MARGINAL AT .16 THK ALUMINA DISCS USED FOR THIS WEIGHT CHECK

FIGURE A5

The major advantage of the stacked disk design is its contamination retention capability. The stacked disk has excellent contamination containment characteristics since the design inherently provides a cavity to retain any contamination build-up. The major disadvantages are lead attachment and assembly considerations. Lead attachment is somewhat difficult but will probably be accomplished by electron beam welding techniques. Because "O" rings may be required to preclude gallium leakage, tolerance build-ups may cause some assembly problems.

A.3.3 Slotted Disk Design

The slotted disk design was conceived primarily to improve the retention capability of the liquid gallium and the possible contamination that might be present during ground handling.

The concept consists of a number of concentric circular channel disk assemblies mounted on a rotating central shaft with their mating stationary disk assemblies clamped together to form an outer housing. Disk assemblies having different wall thicknesses as a function of ring-to-ring voltage requirements are utilized to minimize the overall size and weight of the slip ring. When assembled, the rotating and stationary disks mesh, retaining the gallium in the channels. Slotted disk configurations are shown in Figures A-6 and A-7.

Channels are formed by machining circumferentially concentric slots in a single piece of insulating material, the number of slots per disk varying from 7 to 10, depending upon voltage requirements. Ten ten-ring assembly pairs would be required for each of the high voltage and signal rings, one pair for the power rings and very high voltage rings, and two pairs for the remaining very high voltage rings. Many variations can be assumed for ratio of slot width to slot depth to provide the optimum weight to dielectric strength trade-off balance.

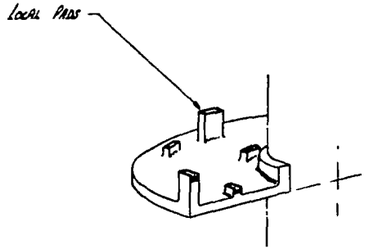

ALTERNATE ROTATING RING ASSY

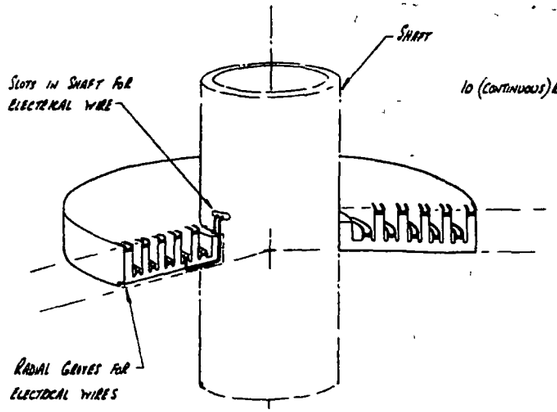

VIEW OF ROTATING RING ASSY
(CONTINUOUS RINGS)

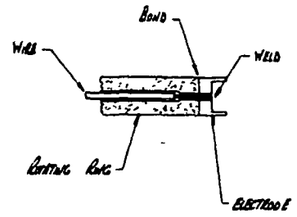

DETAIL OF ROTATING ELECTRODE
SCALE 4/1

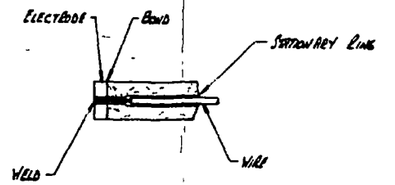

DETAIL OF STATIONARY ELECTRODE
SCALE 4/1

ALTERNATE SCHEMES

1 CONTINUOUS RINGS (ROTATING & FIXED)-AS SHOWN
2. LOCAL PADS ON ROTATING SHAFT -
CONTINUOUS RINGS OF FIXED SIDE
AS SHOWN ABOVE
3 CONTINUOUS RINGS ON ROTATING SHAFT
LOCAL PADS OR BUTTONS ON FIXED SIDE

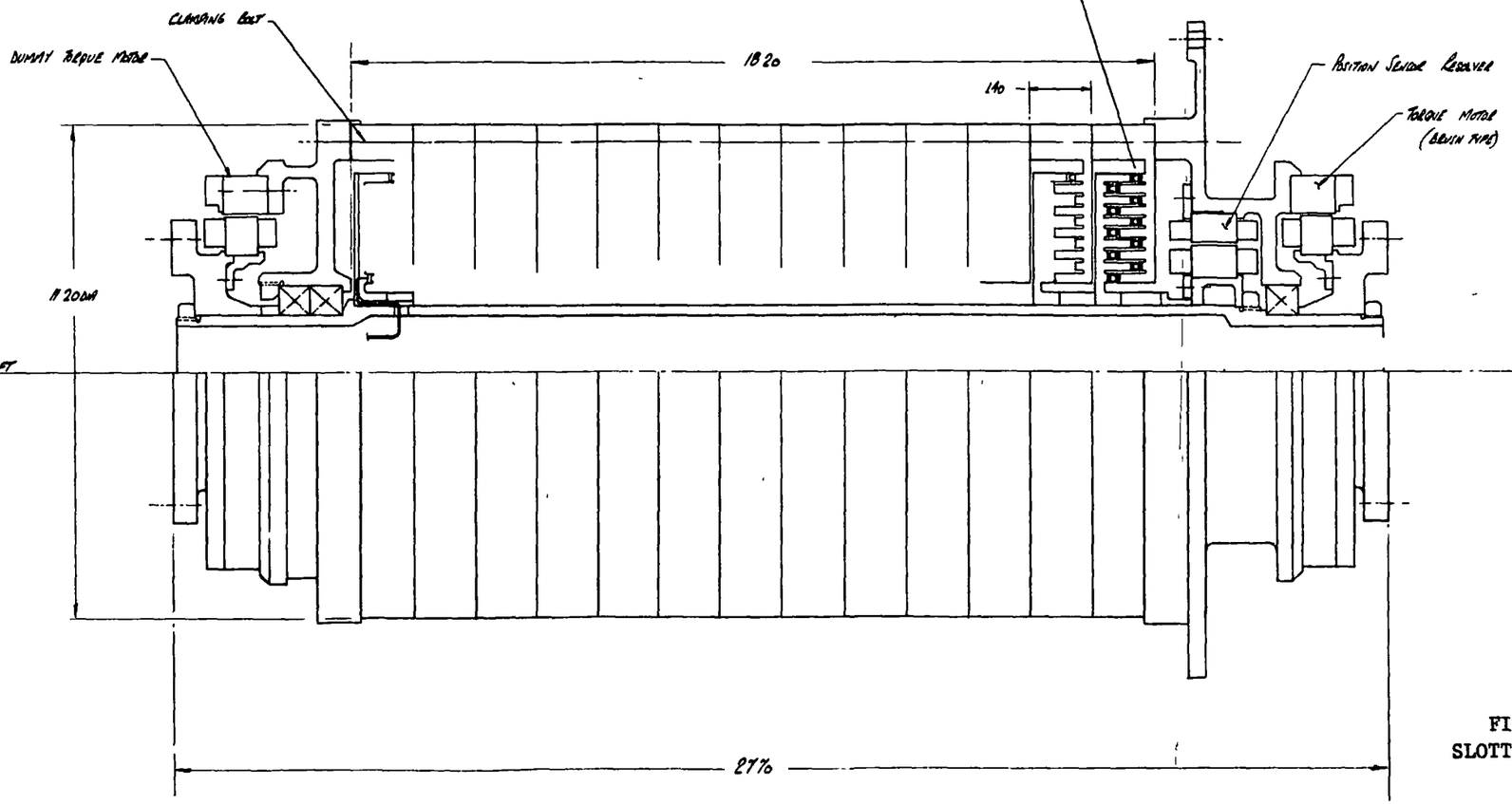

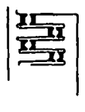

ALTERNATE RING DESIGN

FIGURE A6
SLOTTED DISC CONCEPT

LIQUID METAL SLIP RINGS

SCALE: 1/1 RDO JULY '70

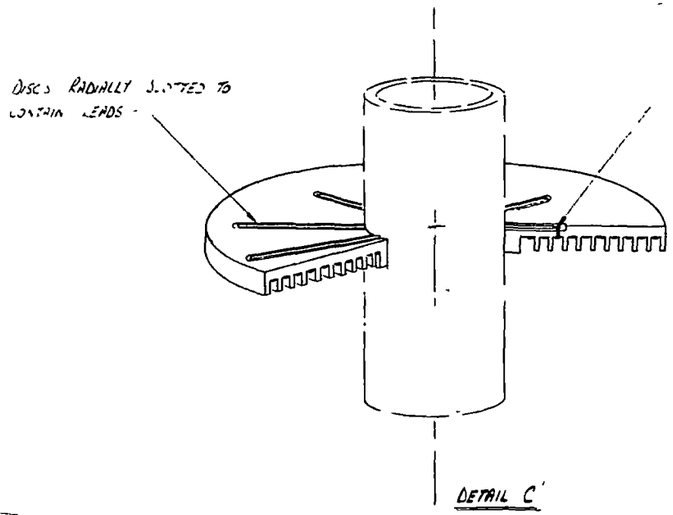

DETAIL C'

SHOWING ROTATING STATOR DISC

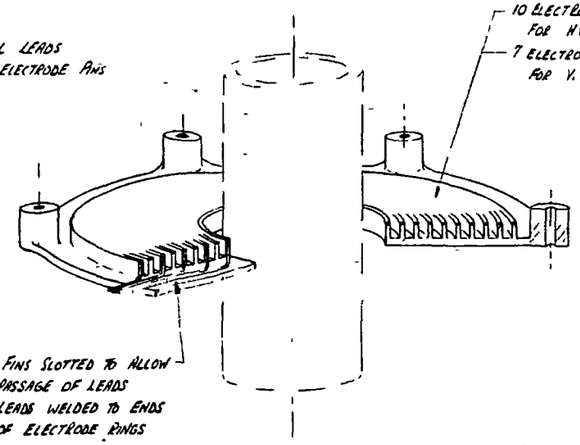

DETAIL B

SHOWING FIXED STATOR DISC

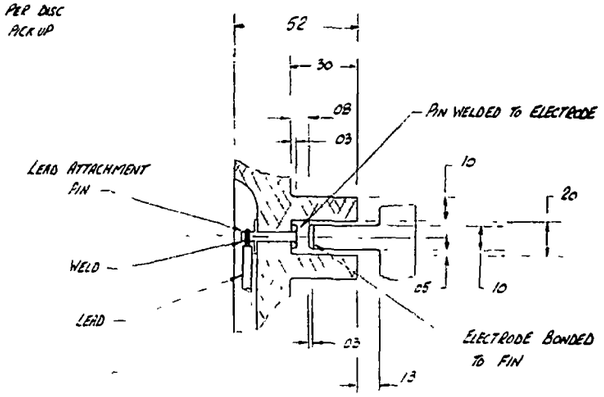

DETAIL A

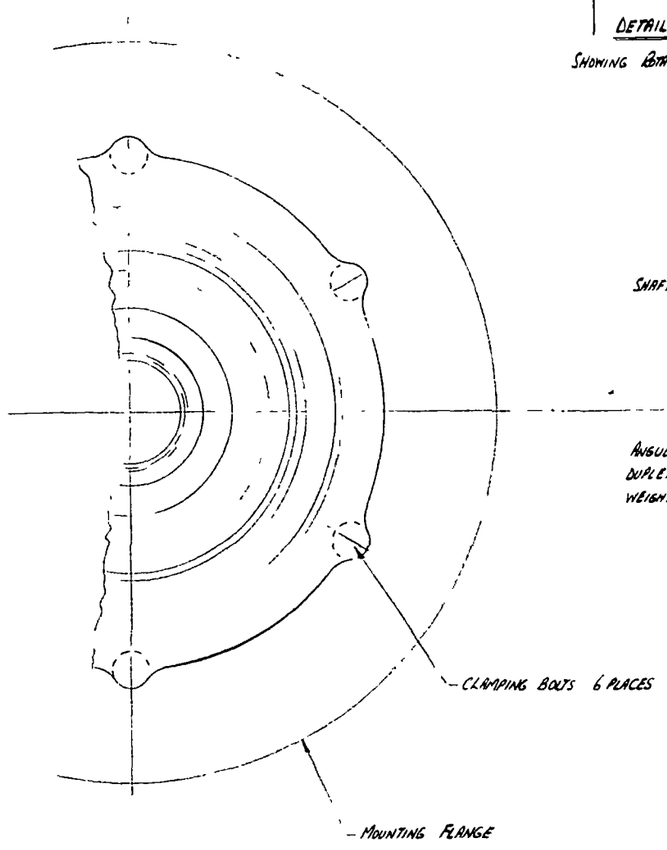

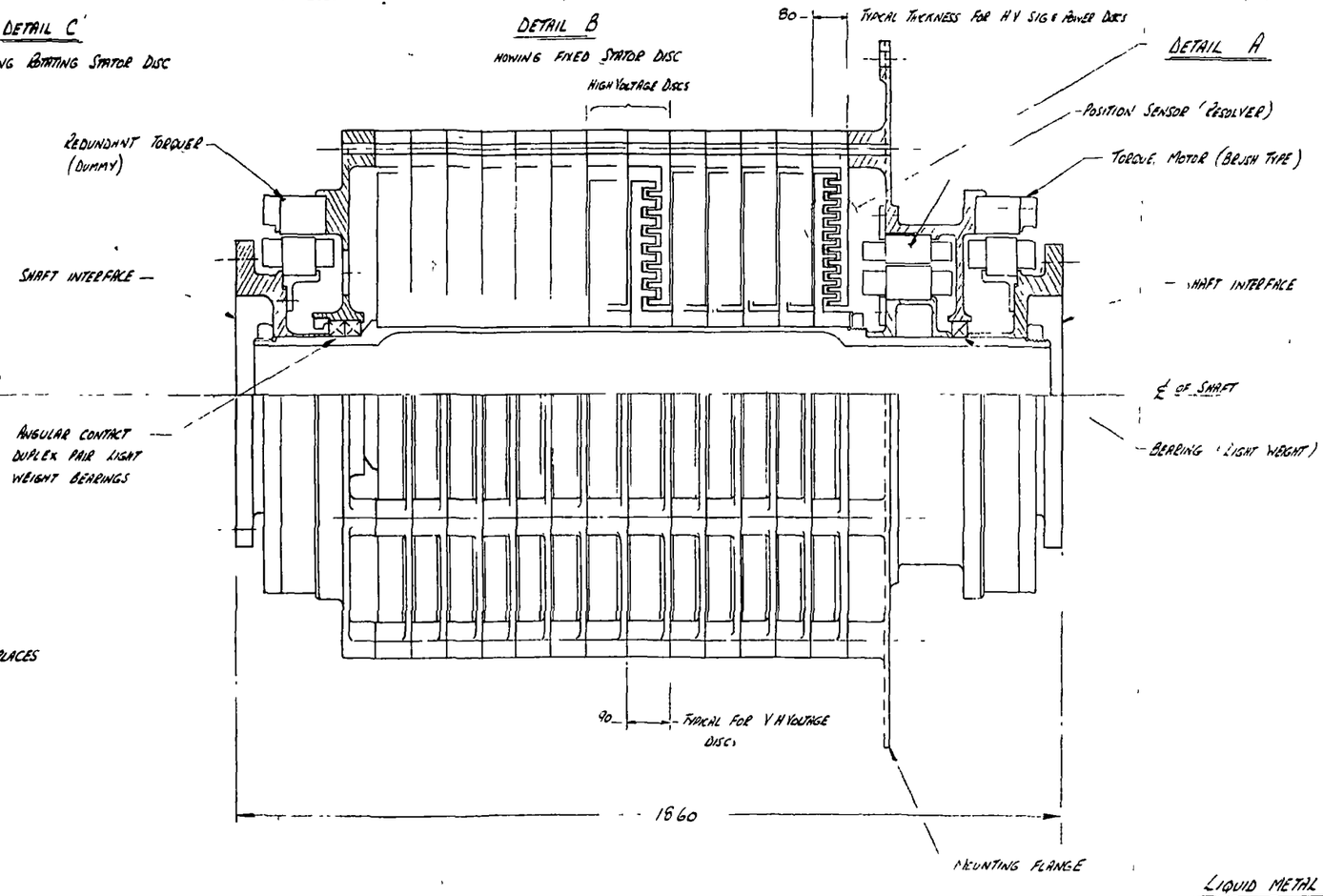

SLOTTED DISC CONCEPT

LIQUID METAL SLIP RING

SCALE - 1/1 = 5/1 A3 SIZE

FIGURE A7

REVISION A

The flat electrode rings assumed for this concept allow gallium to come in contact with the insulator material and the insulator material-gallium interface provides the capillary forces for gallium retention. See detail A in Figure A-7. Because of the uncertainties of gallium interaction with the insulator material (similar to stacked disk concept), it may be desirable to utilize the electrodes to contain the gallium. This is not presently possible with the flat machined electrodes because of the narrowness of the electrode ring channel and the need for maintaining the overall length. An alternate to using electrodes to retain the gallium would be to utilize coatings of insulator materials which are known to be non-reactive and stable with gallium. These coatings would be deposited on the basic insulator material by such techniques as sputtering or thermo-spray. See Figure A-8.

Electrical lead attachments are relatively simple with this concept. On the rotating disk assembly, radial slots will be machined into the underside of the disk. Pin terminals will be inserted through the bottom of the slots and welded to the electrode rings. Weld techniques, however, must be developed because of the thinness, .003", of the electrodes. The terminals will extend from the back side, allowing attachment of the leads via the radial slots. On the fixed disk assembly, two methods of lead attachment have been considered: (1) Extend leaders by chem-milling from the electrode to the base of each fin carrying an electrode, attach a pin terminal through the base material, attach leads to the terminals on the back side and run

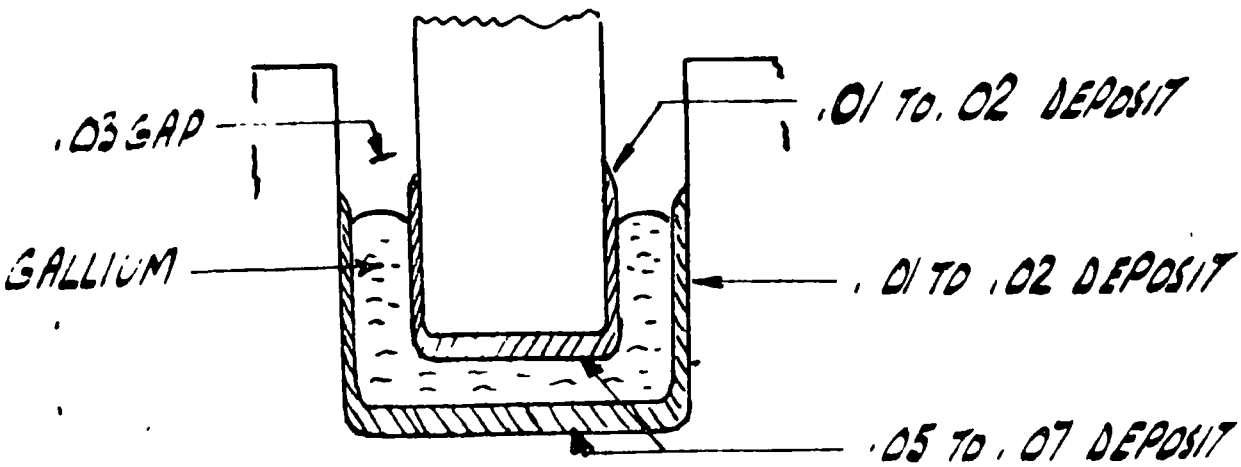

FIG. A8
CAVITY CONFIGURATION

wires radially outboard in grooves machined into the disk. (2) Cut through the electrode fins on the fin side of the disk and attach the electrical leads to the cut electrodes, routing the wires radially outboard until clear of the disk assembly.

The ten-ring design, Figure A-7 was chosen for a detailed weight analysis. Fig. A-9 shows the details and a weight analysis of the slotted disk for the design concept.

The major advantages of the slotted disk design are gallium filling and contamination retention. Gallium filling during assembly can be accomplished two ways: using solid preforms or liquid filling. Preforms are self-positioning, which eliminates the uncertainty of their exact position or whether they might have inadvertently moved during assembly. In addition, if desired, liquid filling of the slip ring is possible during assembly. Liquid filling may not be desirable from the aspect of contamination formation but might be easier than using preforms which entails additional casting and handling operations.

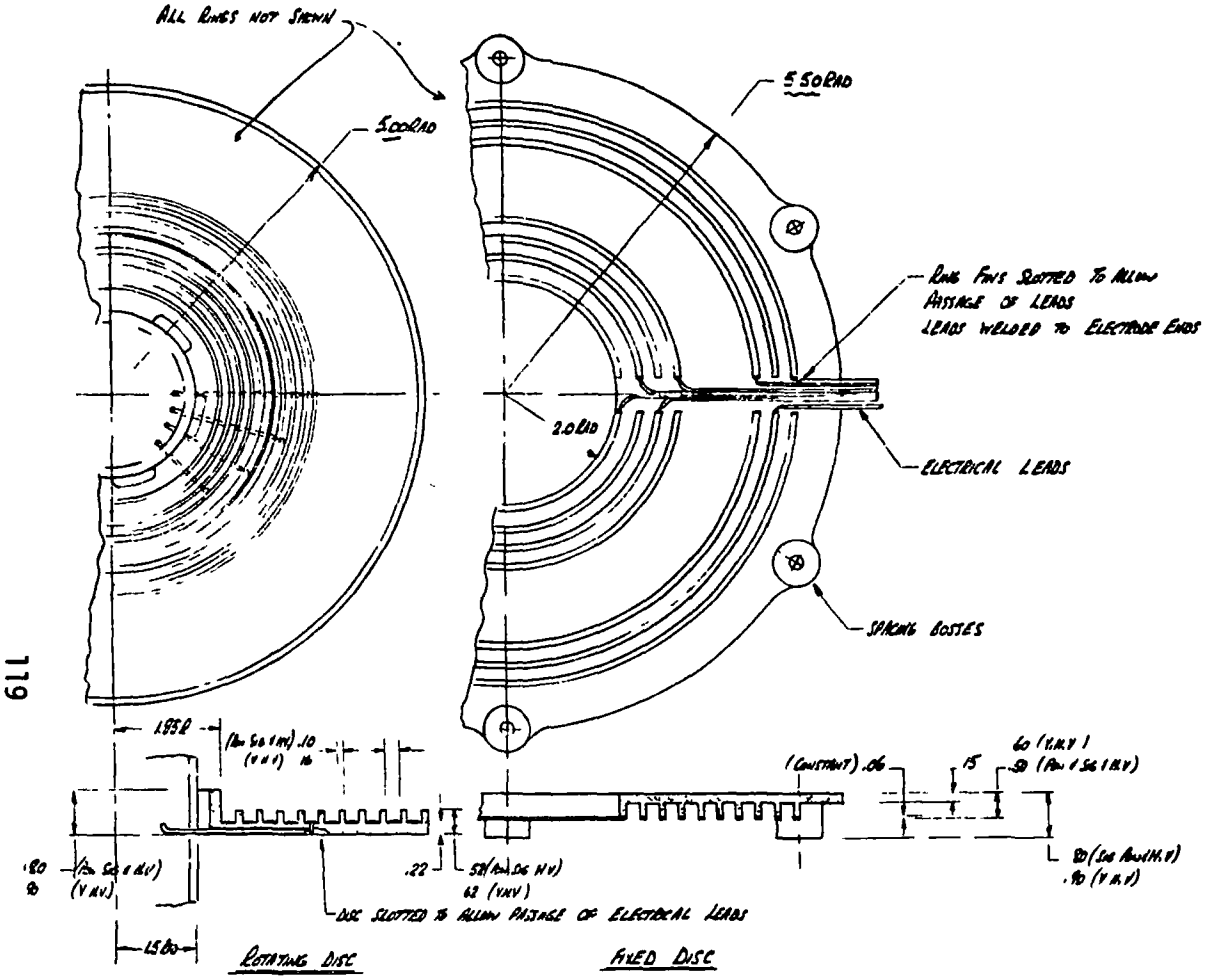

MATERIAL	ALUMINA				TEXTOLITE			
	INDIVIDUAL DISCS ROTATING	INDIVIDUAL DISCS FIXED	NO. POSITIONS	TOTAL WT	INDIVIDUAL DISCS CUTTINGS	INDIVIDUAL DISCS FIXED	NO. POSITIONS	TOTAL WT
DISC (INV SUB & POWER)	1.65	2.50	11 EACH	45.65	77	1.17	11 EACH	21.4
DISC (V.N.V)	2.50	2.80	2 EACH	10.2	"	"	"	10.80
ELECTRODES (INV SIG PAIR)	40	40	109 EACH	8.16	-	-	-	3.16
ELECTRODE (V.N.V)	28	28	2 EACH	1.12	-	-	-	1.12
WIRE (POWER & SIG)	-	-	-	1.12	-	-	-	1.12
WIRE (INV)	-	-	-	2.16	-	-	-	2.16
WIRE (V.N.V)	-	-	-	0.8	-	-	-	0.8
				65.498				41.248
SHAFT & SUPPORT STRUCTURE				14.50				14.50
RESOLVER & BEARINGS				2.25				2.25
MOTOR				20.00				20.00
				102.648				72.548

NOTE 1. SUPPORT STRUCTURE BASED ON AL ALLOY — MAGNESIUM WILL REDUCE WEIGHT BY 40%

2. * DIELECTRIC BREAK DOWN ASSUMED MARGINAL AT 1KV IN TEXTOLITE ALUMINA DISCS USED FOR THIS WEIGHT CALC

DISC DESIGN & WEIGHT ANALYSIS

FIGURE A9

A.3.4 Post Design

The objective of the post design was to reduce the susceptibility of the gallium to shock and vibration and to improve the maintainability of the slip ring. The susceptibility to shock and vibration is a concern since the capillary forces resulting with gallium between two parallel surfaces separated by .050" is approximately 1 inch of head. If a slip ring has a gallium ring approximately 4" in diameter, then the capillary force can sustain a shock or acceleration load of less than 1/4 g across the plane of the gallium. During handling, it is conceivable that the slip ring will be subjected to this level of shock or vibration.

The design consists of a series of electrode rings assembled on an insulated rotating shaft. In order to minimize the possibility of dielectric breakdown, separation, insulated disks or fins could be placed between electrode rings; or the electrodes could be mounted at the base and top of the insulating fins. Assembled over the inner shaft would be an outer stationary tube through which posts could be inserted. The post would be an insulating material except for the tip which would be an electrode button with a hemisphere cut into it. The gallium would be contained in the recessed hemisphere and by the continuous electrode on the rotating shaft. The configuration is shown in Figure A-10.

The post design is inherently long. Design studies indicated that even by staggering the posts radially on the outer tube, the length

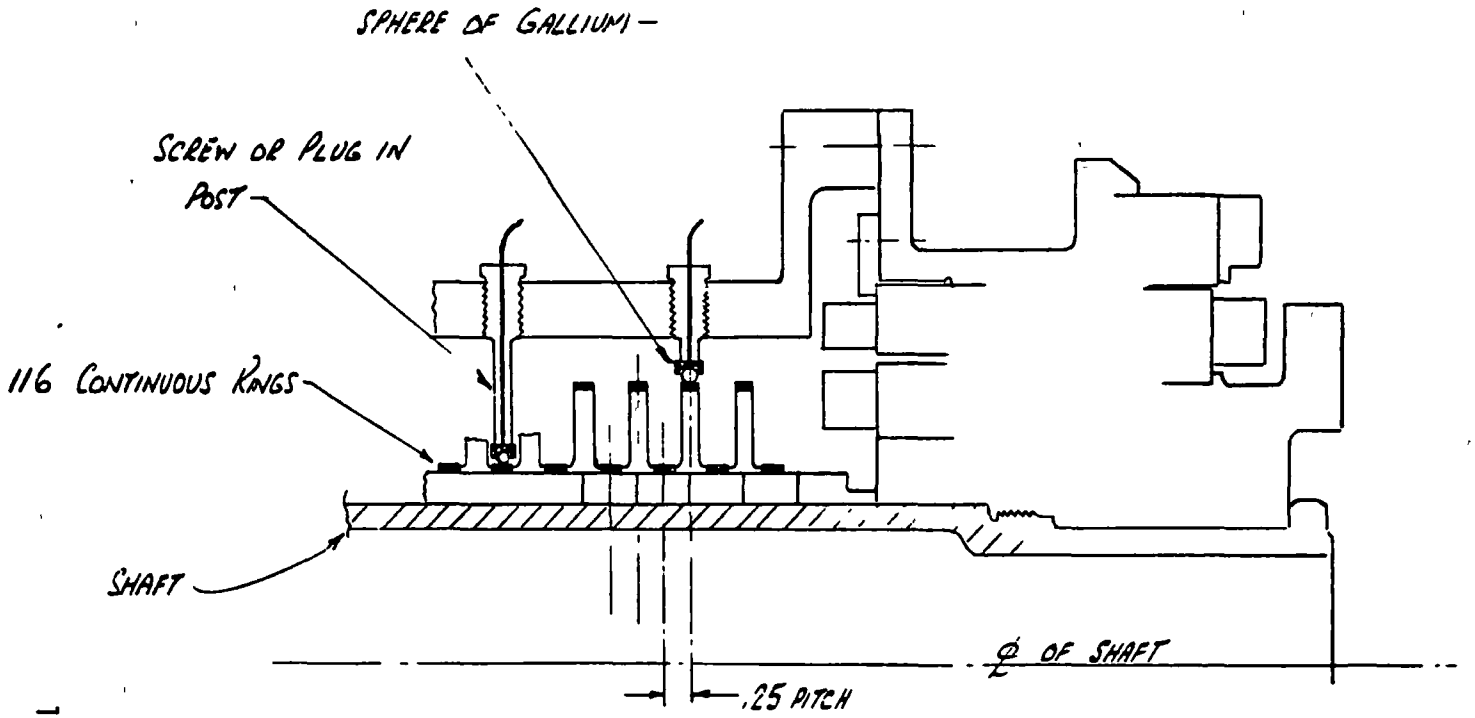

FOR 2,000 VOLT RINGS = 25.5

.50 PITCH
FOR 15,000 VOLT RINGS = 7.0

32.50 —— OVERALL LENGTH APPROX = 41.0

POST DESIGN CONCEPT

LIQUID METAL SLIP RING

SCALE. 1/1 RGS JULY '70

FIG. A-10

of the slip ring was in excess of 40 inches. In an attempt to reduce the overall length, a double-tiered rotating assembly was studied, as shown in Figure A-11. However, this resulted in excessive structural weight and an extremely mechanically complex approach.

The post design has a number of very important advantages, as well as disadvantages. The major advantages to this approach are gallium retention, gallium filling, and shock and vibration considerations. The gallium retention capability is excellent because it is held in shaped electrodes. In addition, since it is not in the form of a continuous ring, it can withstand high lateral shock and vibration. Gallium filling is simplified because the quantity of gallium is small and it can be inserted into its electrode external to the slip ring.

A potential major disadvantage of this approach is a possible gallium wipe-off consideration. The gallium-wetted electrodes continuously rotate against the sphere of gallium. There is concern that after a long period of time some of the gallium will be wiped off this sphere and deposited on the electrode, resulting in an open circuit. Since the post concept has not been tested, it is not certain that this wipe-off will actually occur; however, it is a consideration in the design selection.

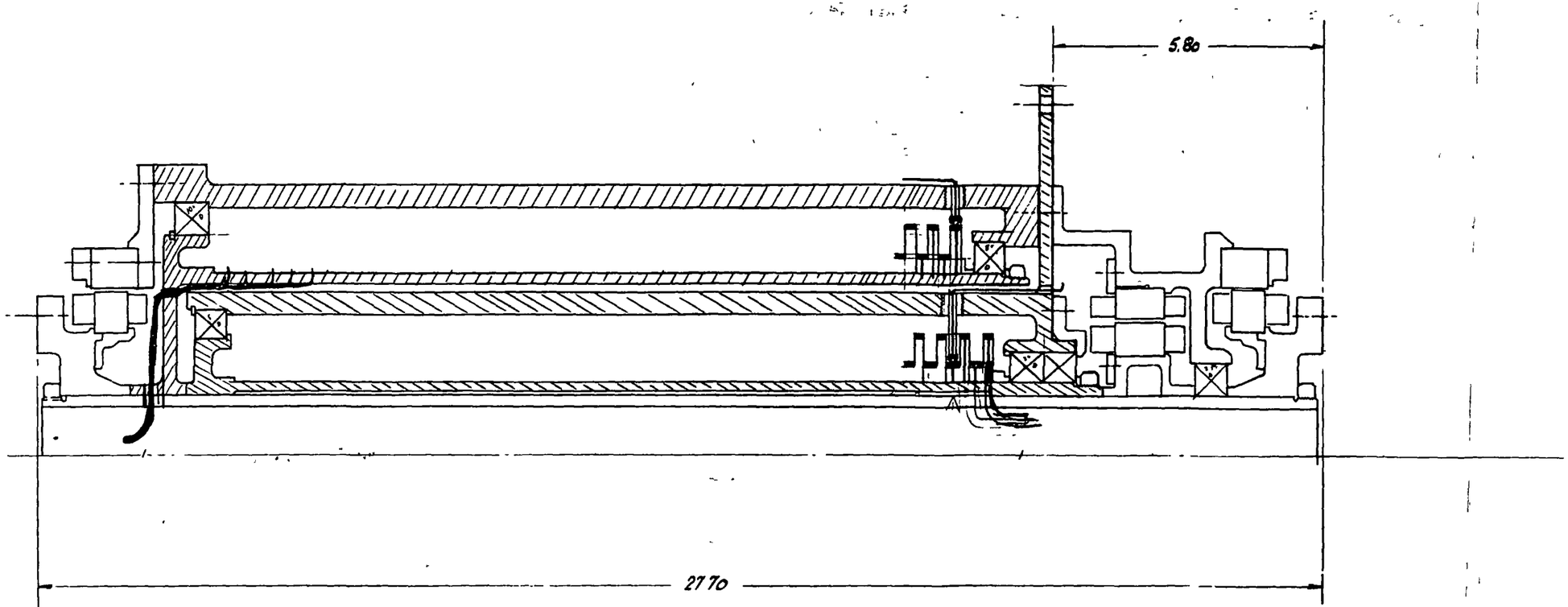

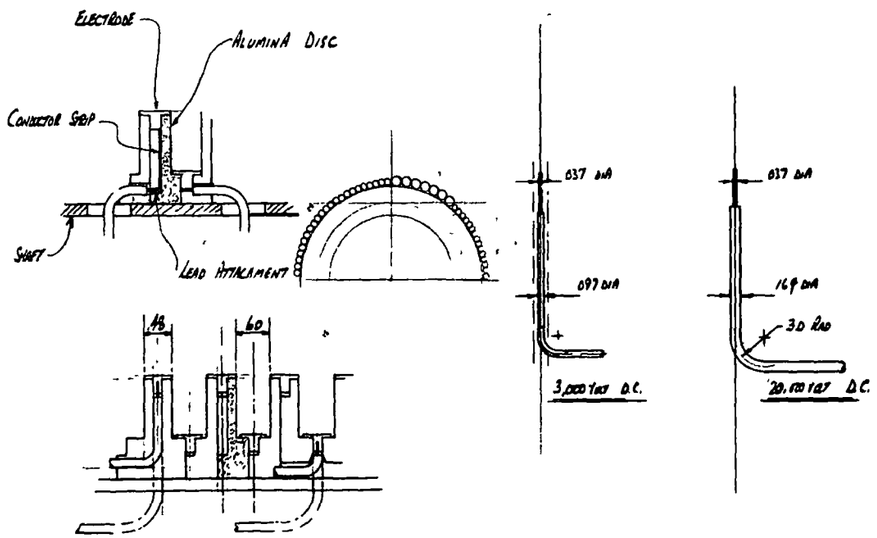

FIGURE A-11
LIQUID METAL SLIP RING
DOUBLE TIERED POST CONCEPT

A.3.5 Probe Design

The probe design concept consists of probes of wire which projected into a cavity of gallium. The configuration and construction of the gallium cavity is similar to that of the stacked disk concept in which flat machined disks are assembled together on a central shaft. The wire probes can be fabricated of such materials as molybdenum, stainless steel or nickel which are molded into a plug for installing into the outer shaft. This design readily lends itself to electrical circuit checks on both the rotor and stator sides of the slip ring. In addition, the probe concept is relatively simple and easily assembled, as compared with the stacked disk approach. Figure A-12 shows the probe concept. Figure A-13 shows the disk detail design and lead connections.

The major advantages of the probe design are related to contamination formation and retention. It has been hypothesized that the continuous disruption of the gallium surface causes a continuous formation of contamination. The rotating element in this design is a gallium pool as compared with a continuous cylindrical surface in the other design concepts. Since there is less surface rotating in relation to the probe, there could be much less surface disruption of the gallium to create contamination. The contamination retention characteristics of the probe design are excellent since the contamination can be retained

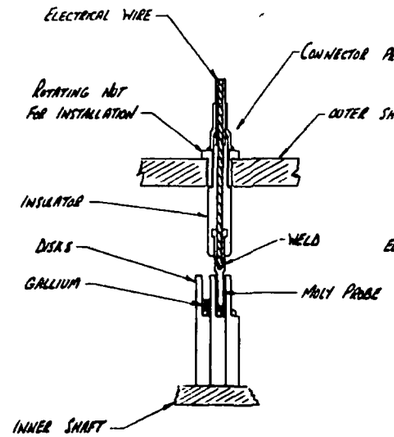

DETAIL A
SCALE 3/1

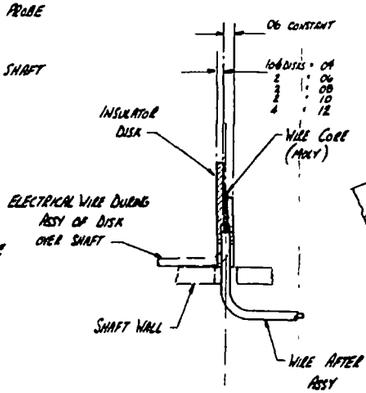

SECTION C-C

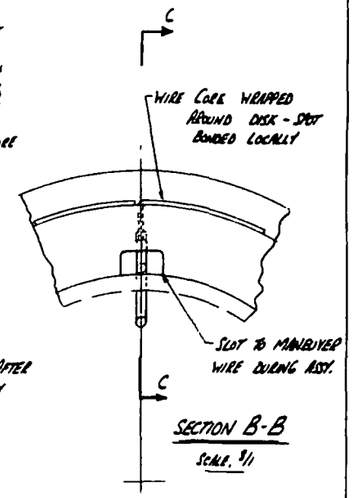

SECTION B-B
SCALE 9/1

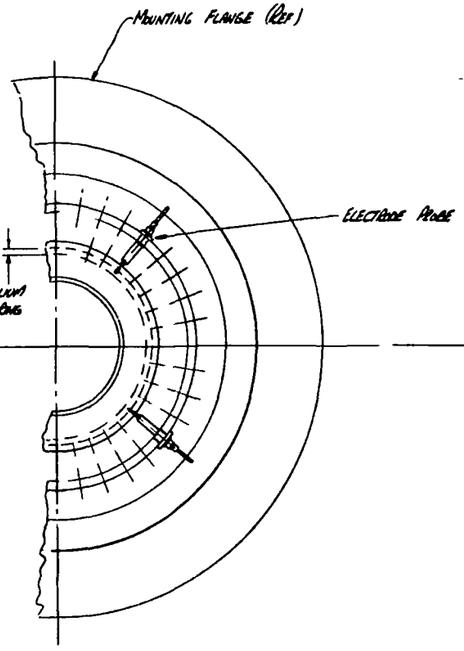

PART SECTION D-D

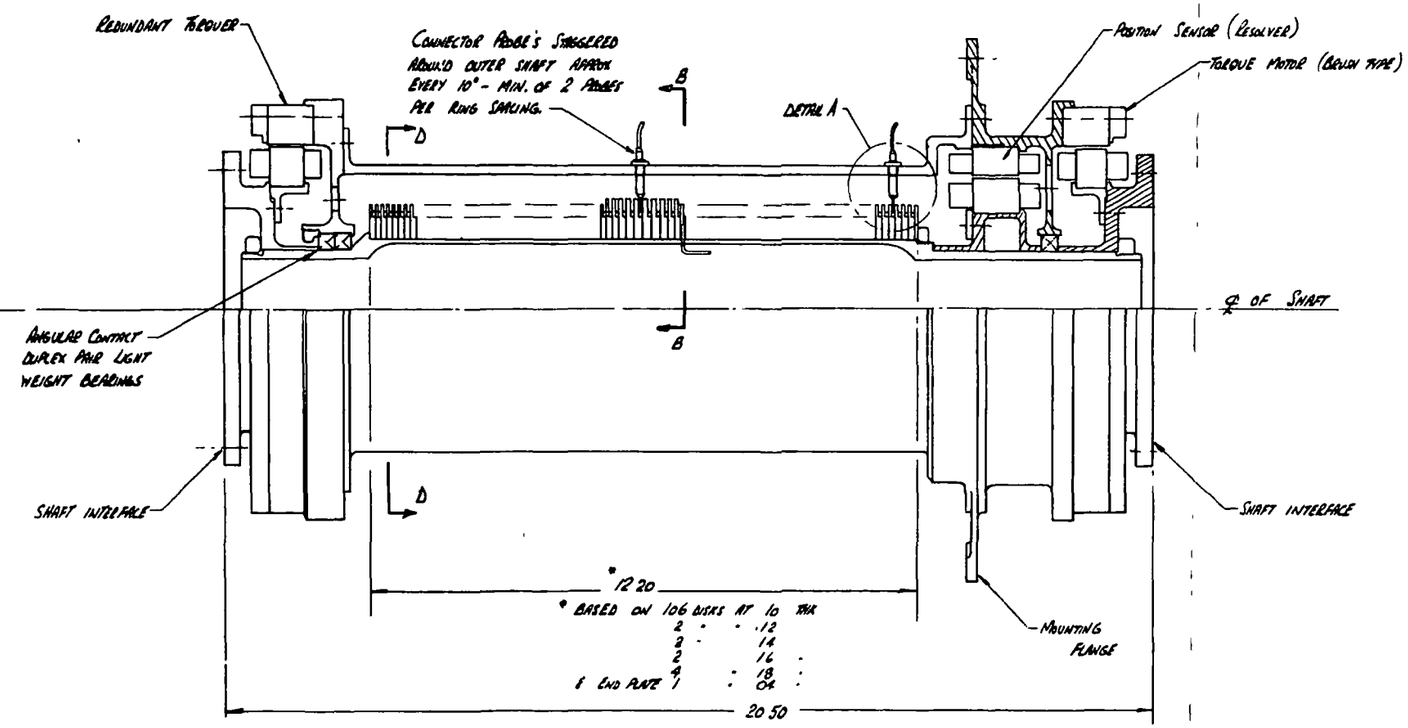

WEIGHT TABLE

		LBS	Sub Total LBS
DISK	116 REQD	6.9	
PROBE	348 REQD COLLECTED	1.8	
			8.7
ELECTRODE	PROT WIRE INCLUDED	0.3	
GALLIUM		2.7	
ELECTRICAL WIRE		4.0	
			7.0
STRUCTURE		13.5	
BEARINGS		0.4	
RESOLVER		1.8	15.7
MOTORS	2 @ 10.3 EA.	20.6	
MISC.		3.0	23.6
			53.2

LIQUID METAL SLIP RING

PROBE CONCEPT

SCALE 1/8 3/1

SEPT '70

FIGURE A-12

in the electrode cavity. A very important operational constraint for the probe design is to prevent movement of the shaft which might cause the wire to shear off or bend it the gallium is frozen. In the other designs, there is much surface area of gallium and electrodes in contact so as to prevent any movement of the shaft unless extremely large torques were applied.

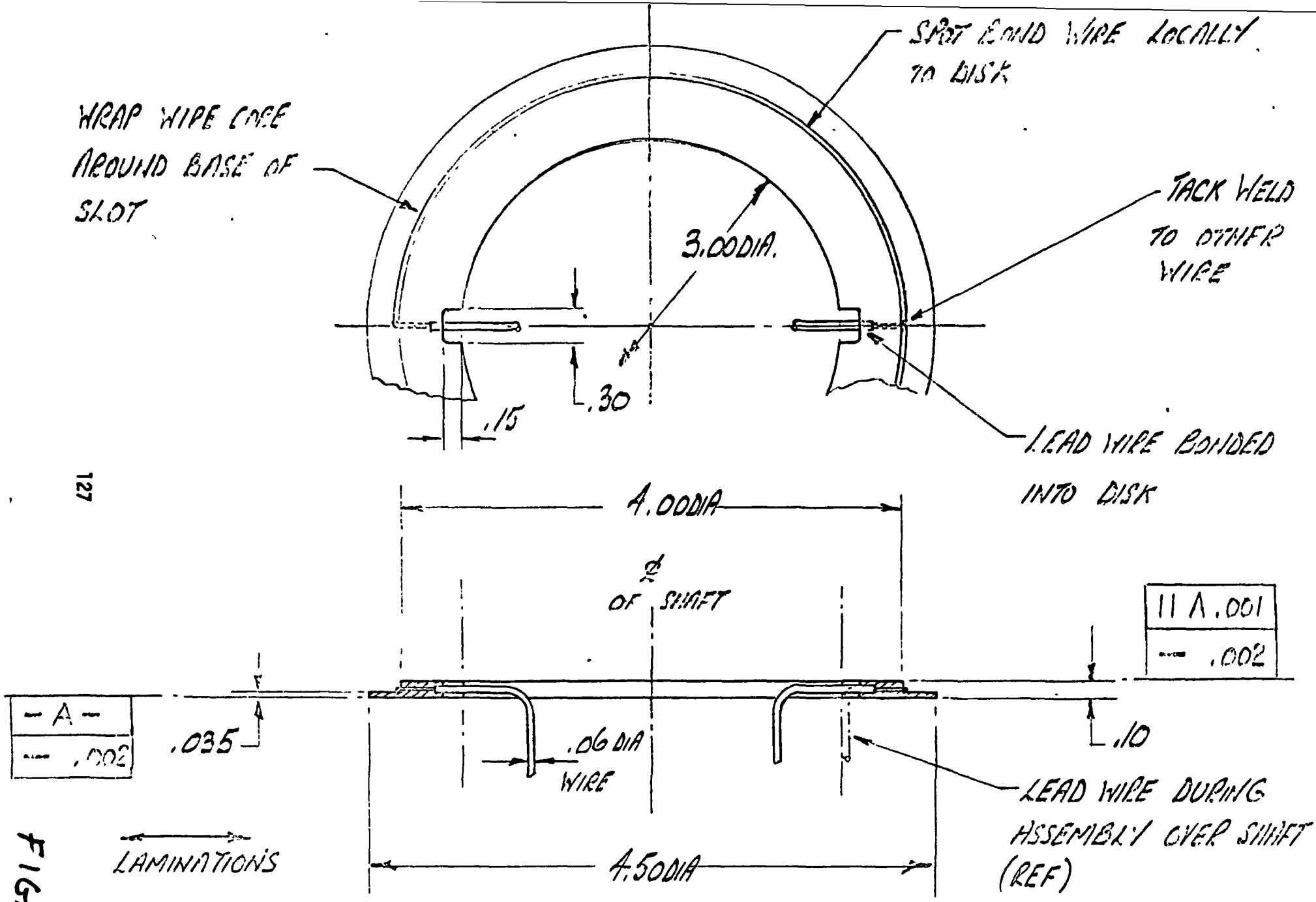

127

FIG A13

MATERIAL - TEXTOLITE (GR. 11584)

DISK REGION - PROBE CONCEPT

A.3.6 Side Electrode Design

The configuration of the side electrode concept is quite similar to that of the stacked disk design with the exception of the electrodes which are placed on the sides of the insulator disks rather than at the base of the rotating disks and at the outer periphery of the stationary disks. See Figure A-14. The back-to-back electrode design permits a significant reduction in overall slip ring length, as compared with the stacked disk design. The disk thicknesses vary in accordance with the dielectric requirements of the various rings. The electrodes are made by bonding the electrode material to this disk and removing the excess by chem-milling or photo-chemical etching. Lead attachments are made to tongues that are left remaining on the electrodes. After the complete assembly of the slip ring, the gallium in all rings as well as the stationary lead attachments are visible, facilitating inspection.

The major advantages of the side electrode design are weight and gallium retention capabilities. The gallium retention is very favorable since non-wetted electrode surfaces retain the gallium rather than the insulator surfaces as in some of the designs. The major disadvantages of the side concept are gallium filling and lead attachment. Lead attachment entails the use of electron beam welding. Gallium filling is troublesome because of potential difficulty in maintaining the preformed rings in the desired position during assembly.

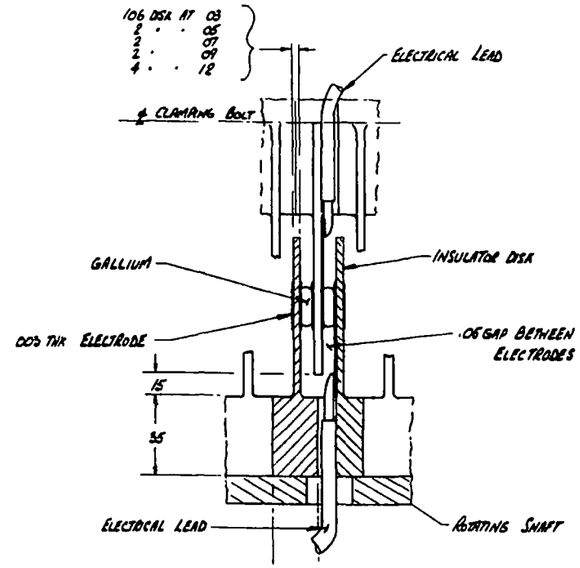

DETAIL A
SCALE 4/1

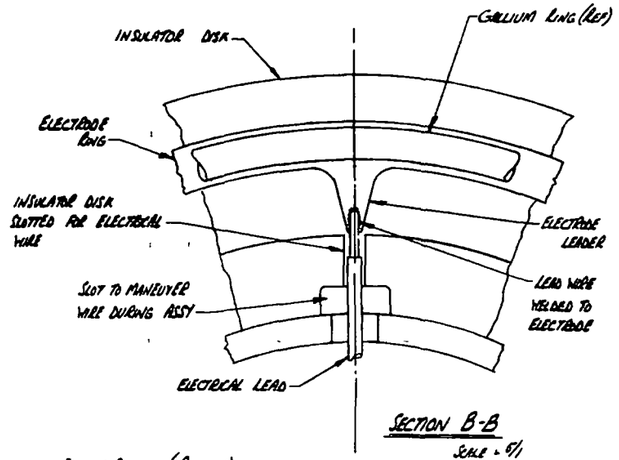

SECTION B-B
SCALE 4/1

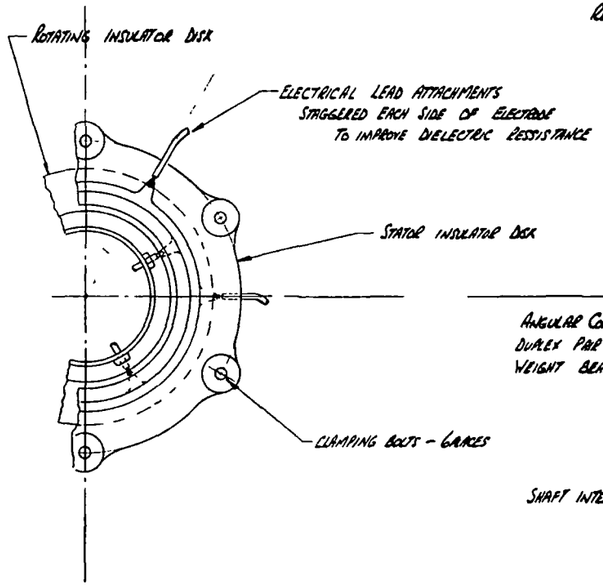

PART SECTION C-C

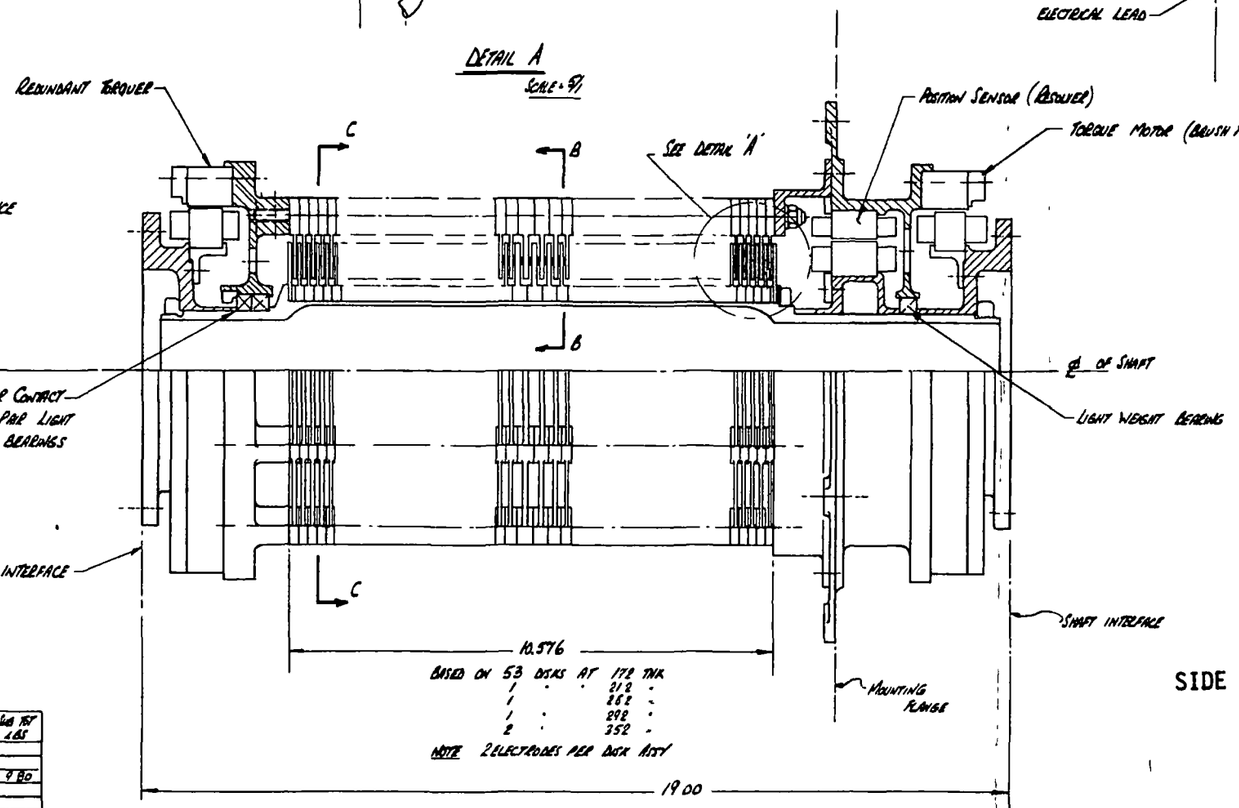

BASED ON 53 DISKS AT 172 THK
1 . 212 "
1 . 282 "
1 . 292 "
2 . 352 "

NOTE 2 ELECTRODES PER DISK REQ'D

WEIGHT TABLE

	LBS	Sub TOT LBS
DISK - 53 STATOR	5.30	
DISK - 68 ROTOR	4.50	
		9.80
ELECTRODE - 003 THICK DISKS	0.65	
GALLIUM	3.50	
ELECTRICAL WIRE	4.0	
		8.15
STRUCTURE	15.25	
BEARINGS	0.40	
RESOLVER	1.80	
		17.45
MOTORS 2 @ 10.3 LBS EA.	20.6	
MISC.	3.0	23.60
		59.00

NOTE 1 WEIGHT BASED ON BEST (MIN) MANUFACTURING THICKNESS
2. AL ALLOY SUPPORT STRUCTURE

SIDE ELECTRODE CONCEPT
FIGURE A-14

SK 56197-893

LIQUID METAL SLIP RING

SCALE: 1/1 & 4/1 SEPT '70

GENERAL ELECTRIC CO - S.T.C. VALLEY FORGE

A.3.7 Integrally Wound Concept

The integrally wound concept is essentially the same as the stacked disk except in the manner in which it is fabricated. The design consists of a one-piece glass or composite fiberwinding, rotating inner assembly and a two-piece clam-shell outer assembly. The inner assembly is a one-piece single winding, externally-finned, rotating shaft of 117 fins. The electrode rings are wound into the assembly. The outer assembly is a one-piece single winding internally finned stationary shaft, with the electrode rings bonded to the tips of the fins. The outer assembly is split longitudinally, assembled over the internal shaft, and clamped together. The design is shown in Figure A-15 and A-16.

The integrally wound approach is not presently recommended because of anticipated manufacturing problems in winding the thin barriers. These problems can be solved but require developmental effort.

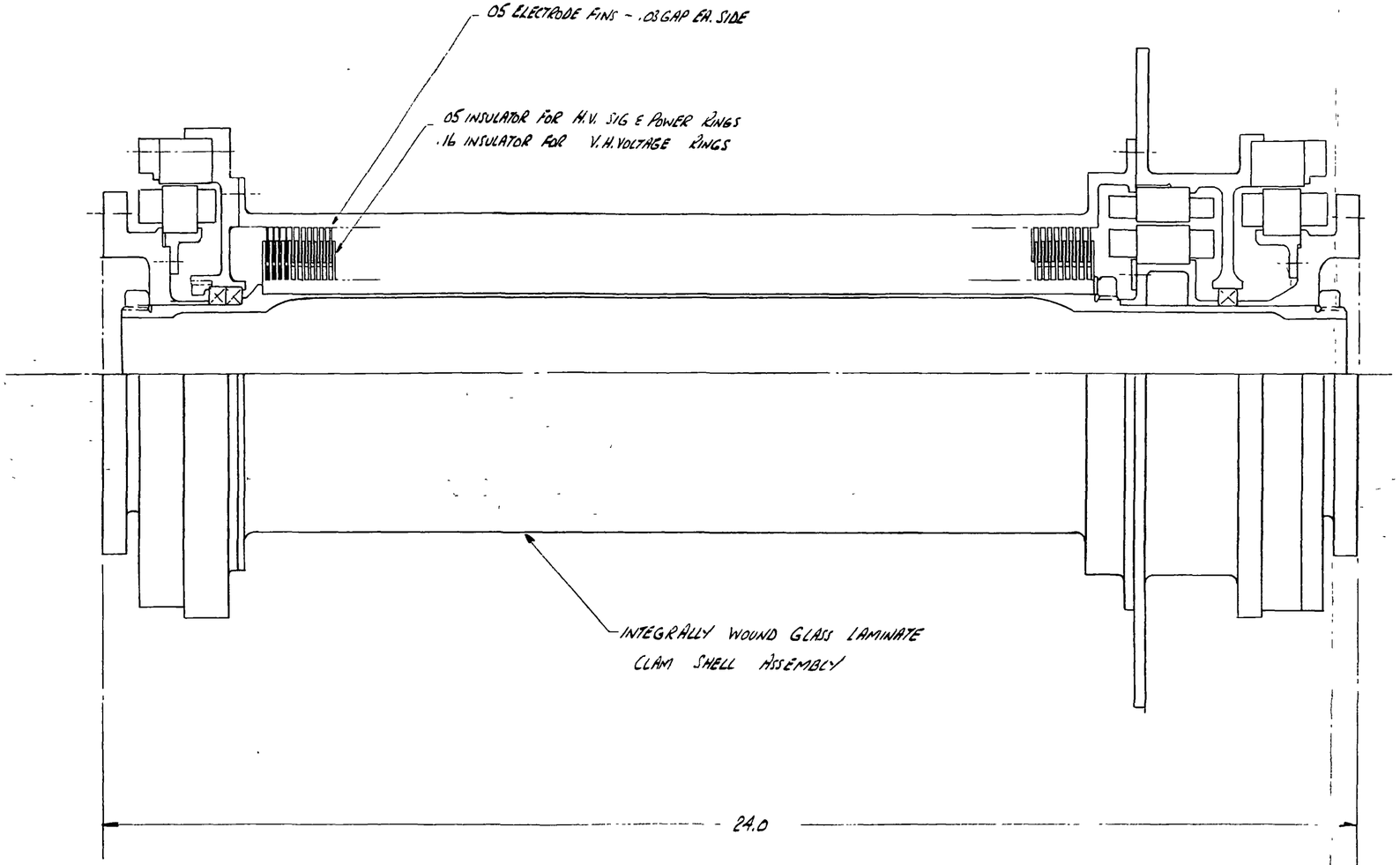

FIGURE A-15
LIQUID METAL SLIP RING
INTEGRALLY WOUND CONCEPT

SCALE 1/1 AUG '70

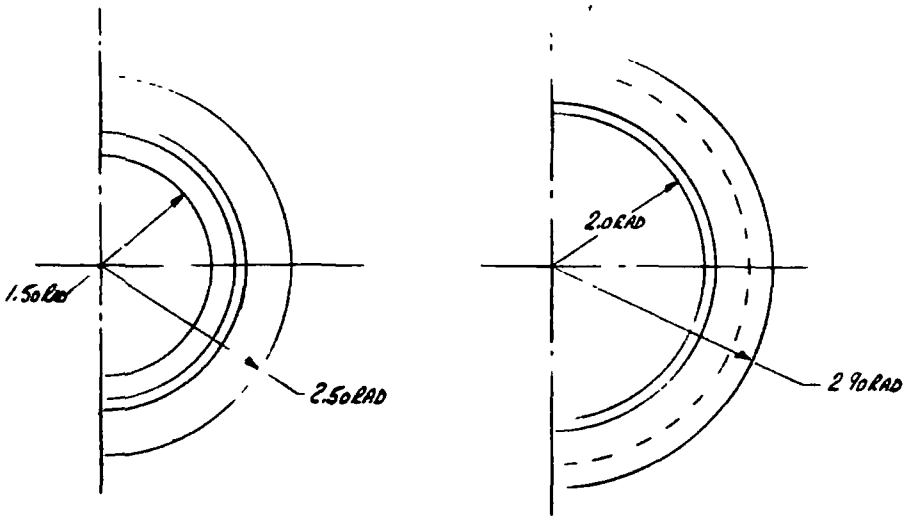

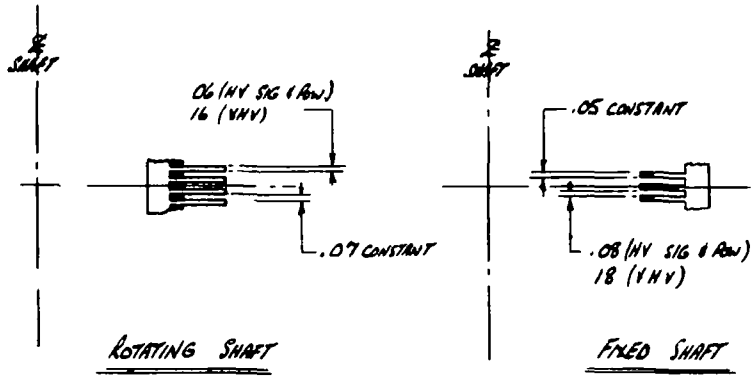

ROTATING SHAFT

FIXED SHAFT

MATERIAL	GLASS WEAVE COMPOSITE		
	ROTATING ASSY	FIXED ASSY	TOTAL WT
HV. SIG & POWER PORTION	8 85	5 50	11 35
V.H.V PORTION	1 95	1.35	3 30
ELECTRODES - (ALL)	2 35	2 81	5.1 6
WIRE (ADDED)	-	-	.25
			30.06

SUPPORT STRUCTURE ⊕		15 20
BEARINGS & RESOLVER		2.25
MOTORS		20 60
		68.11

INTEGRALLY WOUND CONCEPT DETAIL

NOTE. SUPPORT STRUCTURE BASED ON NI. ALLOY USING MAGNESIUM WILL REDUCE STRUCTURE WEIGHT BY 40%

FIGURE A-16

A.3.8 Weight & Size Study

A detailed weight and size study was made of the design concepts. The purpose of this study was to determine if there were significant differences in size and weight of the various configurations. The following assumptions were made:

1. Electrodes

   Material - Molybdenum

   Thickness - .003"

   Spacing - Minimum dielectric requirements

2. Structure - Magnesium

3. Torque Motors

   Number - 2

   Type - Inland, T-5003

   Torque Output - 6 ft. lbs., each

   Weight - 5.7 lbs. each

4. Insulation

   Textolite, Epoxy Glass

   NEMA Grade, G-10

Based on these assumptions, the sizes and weights of the various design concepts were determined. The weights were determined two ways, minimum design weight and optimum manufacturing weight. The

minimum design weight is a minimum weight based upon the design requirement of the slip ring. The optimum manufacturing weight represents a design which can be manufactured without any undue fabrication problems. The major difference between the design weight and the manufacturing weight is in the disk thickness. If the disk thickness is based upon dielectric requirements, the disks for signal, power and high voltage rings can be thin and light, but difficult to manufacture. Thus the optimum manufacturing weight will result in disks which are relatively easy to fabricate but at the same time will have more than the required dielectric capabilities.

The results of the size and weight studies are summarized below.

Concept	LMSR Dia. (Inches)	LMSR Length (Inches)	Minimum Design (lbs.)	Optimum Manufacturing (lbs.)
Flat Disk	11.0	15.0	46	49
Stacked Disk	9.1	23.7	47	50
Slotted Disk	8.9	15.5	48	69
Post	10.0	40.0	56	56
Probe	9.1	20.5	37	42
Side Electrode	9.1	19.0	38	43
Integrally Wound	9.1	24.0	58	58

A detailed analysis was made to determine the weight distribution between two slip ring concepts, probe and side electrode. The probe and side electrode designs were selected since they appeared to be the most promising approaches and in addition their configurations were quite dissimilar. The weight of these designs was determined using the same sizing assumptions for each, and was calculated based on the weight that could be manufactured with some moderate degree of difficulty. Since 6 ft-lb. torque motors were considered to be more than required, 3 ft-lb. torque motors were assumed. This weight breakdown is as follows:

	WEIGHT (lbs)	
	Probe	Side Electrode
Disks	11.3	9.8
Electrodes	0.3	0.7
Gallium	2.5	3.5
Total	14.1	14.0
Motors (3 ft.-lb)	6.0	6.0
Resolver	2.0	2.0
Bearings	0.5	0.5
Leads	4.0	4.0
Miscellaneous	3.0	3.0
Total	15.5	15.5

	Aluminum	Magnesium	Aluminum	Magnesium
Structure	13.0	7.8	13.5	8.0
Total	42.6	37.4	43.0	37.5

A number of interesting aspects can be noted. First, that although the design concepts are quite dissimilar physically, there is relatively little total weight difference between them. Second, of the total weight, approximately 1/3 is in the disks, electrodes and gallium, while the remaining 2/3 is in the structure, motor, leads, etc. The greatest sources of weight are the disks, motors, leads and structure.

A-4 Design Concept Summary

The characteristics and parameters of all the design concepts are summarized in Table A-2. A weighting table, Table A-3, was worked out in order to quantitize the various selection criteria of the design approaches. These sets of criteria were established, from primary to tertiary, and weighting factors applied to each.

DESIGN CONCEPT SUMMARY
TABLE A-2

DESIGN CONCEPT MATRIX

Criteria	Flat Disk	Stacked Disk	Slotted Disk	Post	Probe	Side Electrode	Integrally Wound
Size Diam. - outside Length - between flanges	11"D x 15"L	9.1"D x 23.7"L	8.9"D x 15.5"L	10.00"D x 40.0"L	9.10"D x 20.56"L	9.10"D x 19.06"L	9 10"D x 24 06"L
Weight (min. design) Weight (best manufacture)	46 lbs. 49 lbs.	47 lbs. 50 lbs.	48 lbs. 69 lbs	56 lbs 56 lbs	37 lbs 42 lbs.	38 lbs. 43 lbs.	58 lbs 58 lbs
Contamination Retention	Poor - electrodes in proximity; no inherent cavity.	Excellent - cavity for containment.	Very good - cavity; less volume than stack disk.	Very good - potential volume of contamination very small. Contamination can fall into adjacent electrode or to bottom of slip ring.	Excellent - less gallium in contact with rotating surface Less potential contamination.	Very good - cavity; not as good as stacked disk because cavity is shared with adjacent electrode.	Excellent - cavity for containment.
Gallium Retention	Excellent - non-wetted electrode surfaces retain gallium.	Good - insulation retains gallium; material must be determined.	Good - insulation retains gallium; material must be determined.	Excellent - shaped electrodes retain gallium, high shock capability, all axes, gallium wipe-off potential problem.	Good - insulation retains gallium; material must be determined.	Excellent - non-wetted electrode surfaces retain gallium.	Good - insulation retains gallium, material must be determined
Gallium Filling	Poor - preformed gallium rings. Multiple rings per disk, no access to inner rings, position cannot be verified.	Good - preformed gallium rings, self positioning.	Very good - preformed rings, self positioning; liquid filling possible during slip ring assembly.	Excellent - small quantities of gallium, can be filled external to slip ring, gallium on non-rotating electrode.	Good - preformed rings, self positioning; liquid filling possible, after slip ring assembly	Fair - preformed rings, position can be verified.	Good - preformed gallium rings, self positioning.

DESIGN CONCEPT MATRIX

Criteria	Flat Disk	Stacked Disk	Slotted Disk	Post	Probe	Side Electrode	Integrally Wound
Manufacture	Good - electrode sheet material bonded to insulation, chem-etched.	Good - electrode bonded or sputtered.	Poor - slots machined; electrodes preformed and bonded, fixtures required.	Good - intricate machining of moly post.	Good - may require insulated moly wire.	Good - electrodes bonded and chem-etched.	Poor - integrally glass wound technique must be developed for this size winding.
Lead Attachment	Good - leads welded to terminals, terminals sonic welded, to moly electrodes or spot welded, to stainless electrodes.	Fair - (a) electron beam weld lead to electrode, or (b) electron beam weld lead to moly electrode tab, or (c) if electrode is moly wire, lead electron beam welded.	Fair - (a) electron beam weld lead to electrode, or (b) electron beam weld lead to moly electrode tab, or (c) if electrode is moly wire, lead electron beam welded.	Good - rotating electrode, same as stacked disk; post electrode, lead welded to moly. tip.	Good - rotating electrode, same as stacked disk; probe electrode, lead welded to moly wire.	Good - lead electron beam welded to moly electrode tongue.	Poor - lead wire integrally wound with glass cord; wire to electrode attachment must be developed.
Assembly	Poor - bulky wiring; lead bending away from welds; gallium containment during assembly.	Fair - tolerance, build-up due to "O-rings", lead bending close to welds.	Fair - lead bending away from welds; bulky wiring.	Good - can be assembled and checked prior to installation of posts and gallium.	Good - can be assembled and checked prior to installation of posts and gallium.	Fair - lead bending close to welds; gallium containment.	Good - stationary disks fabricated in halves, tolerances critical.
Inspection	Poor - cannot see past outer rings; no separate check of electrical circuits can be made.	Good - gallium visible from outside; check of separate rotor and stator electrical circuits possible.	Poor - cannot see inside, lead attachments on gallium; no separate check of electrical circuits can be made.	Fair - can see lead attachments, not gallium; separate checks of electrical circuits possible.	Good - can see gallium; separate checks of stator and rotor electrical circuits possible	Good - can see gallium and stationary lead attachments.	Poor - cannot see inside slip ring.

DESIGN CONCEPT MATRIX

Criteria	Flat Disk	Stacked Disk	Slotted Disk	Post	Probe	Side Electrode	Integraily Wound
Shock and Vibration	Good	Good	Good	Excellent	Good	Good	Good
Other Considerations	Hard to vent.	--------	--------	When gallium frozen, less shear restraint to shaft rotation, stator electrode can fail.	When gallium frozen, less shear restraint to shaft rotation, stator electrode can fail. Button electrodes can replace wire electrodes on stator.	----------	Approach not recommended, manufacturing technique not developed.

TABLE A-3

DESIGN CONCEPT WEIGHTING TABLE

CRITERIA	DESIGN CONCEPT						
	FLAT	STACKED	SLOTTED	POST	PROBE	SIDE	INTEGRAL
PRIMARY CRITERIA							
Contamination							
Formation	7	8	7	10	9	8	8
Containment	6	8	7	9	9	7	8
Gallium Retention							
During - Assembly	6	9	10	8	9	7	8
- Handling & S/C Ass'y	7	8	10	7	7	8	8
- Ground Operation	7	8	10	9	8	8	7
- Space Operation	7	8	7	*	8	7	8
Capillary Force	10	7	8	10	7	10	7
Environmental Requirements							
Shock, Vibration, Thermal, etc.	9	9	7	8	9	9	9
SECONDARY CRITERIA							
Manufacture							
Electrodes	8	7	4	7	7	8	4
Disks	7	6	4	6	6	5	4
Wiring							
Wire to Electrode Connection	8	6	8	7	7	8	4
Assembly							
Lead Wire Bending	7	5	7	6	6	7	8
Tolerance Build-up	8	6	8	7	7	6	5
Inspection							
Gallium Fill	4	7	4	6	8	7	6
Electrodes	4	6	4	8	8	7	4
Lead to Electrode Connections	4	6	5	7	7	6	4
Gallium Filling							
Fabrication of Preforms	6	5	4	7	8	7	5
Positioning During Ass'y	4	8	8	7	8	6	7
Miscellaneous							
Venting	4	8	5	7	7	6	7
Shaft Rotation with GA Frozen	7	7	7	4	5	6	7
Specification							
Size - Length & Diameter	8	5	8	**	6	7	5
Weight	6	7	4	5	8	8	6
TERTIARY CRITERIA							
Rework							
Replacement of Gallium, Electrode, etc.	1	2	1	4	4	3	1
	145	156	147	149	168	161	140
				*			
				**			

* Gallium wipe off - unknown factor.
** 50% longer than spec. max. length.

WEIGHTING FACTORS

Primary Considerations		Secondary Considerations		Tertiary Considerations	
10	Excellent	8	Excellent	5	Excellent
9	Very good	7	Very good	4	Very good
8	Good	6	Good	3	Good
7	Fair	5	Fair	2	Fair
6	Poor	4	Poor	1	Poor

A-5 Recommendation & Selection

Based upon the design and engineering studies made of the seven design concepts, the recommended concepts, in order of preference, were as follows:

Primary Recommendations

a. Probe

b. Side Electrode

c. Stacked Disk

Secondary Recommendations

a. Slotted Disk

b. Flat Disk

c. Post

d. Integrally wound

The first choice was that of the probe concept. This is based primarily upon its excellent contamination formation and retention characteristics inherent in its geometry, as can be seen in Tables A-2 & A-3.

In addition, the probe concept has advantages in dielectric characteristics, ability to withstand shock, vibration and acceleration with gallium liquid and solid, ease of fabrication and test.

The recommendation of the probe concept was reviewed and then directed by NASA Lewis, and a verification model and a detail design was made of this approach.

APPENDIX B
TECHNICAL ANALYSIS

B.1 Introduction

A number of technical topics relevant to the characteristics of the slip ring were analyzed during the preliminary design effort, and are presented in this appendix. The topics that were investigated include the following:

1. Magnetic forces
2. Electrostatic forces
3. Gallium contamination
4. Low melting temperature alloys
5. Thermodynamics of oxide formation
6. Gallium oxide formation
7. Dielectric characteristics of gases and electrode spacing
8. Dielectric stress
9. Fluid flow characteristics
10. Venting Analysis
11. Normal stress - Weissenberg effect
12. Hydrodynamic considerations
13. Rate of gallium oxidation

B.2 Magnetic Forces

The order of magnitude of magnetic forces that could potentially exist in the slip ring were determined and compared with the capillary forces. The force between parallel, co-axial circuits is given by:

$$f = \frac{4\pi a d I_1 I_2}{(a-b)^2 + d^2}$$

where:

f	=	force, dynes
a,b	=	radii of current loops, cm
d	=	spacing of loops, cm
I_1 I_2	=	currents, abamps

If we assume

$a = b = 2$ inches

$d = 0.1$ inch

$I_1 = I_2 = 30$ amps

$$f = \frac{4\pi(2 \times 2.54)\ (.1 \times 2.54)\ (3)\ (3)}{(.1 \times 2.54)^2}$$

$$= 2260 \text{ dynes}$$

The force on a current carrying conductor in a magnetic field is

$$f = Bl\ I$$

where f = force, dynes

l = effective length of conductor, cm

I = current abamps

B = flux density, gauss

Letting B = 100 gauss

I = 30 amps

l = 4 inches

$$f = 100\ (4 \times 2.54)\ 3 = 3040 \text{ dynes}$$

The capillary force on a fluid between two parallel plates is

$$f = h\ d\ g\ \delta$$

where f = force, dynes

d = separation, cm

g = acceleration of gravity

h = capillary depression

$$h = \frac{4\sigma \cos \theta}{d\delta g}$$

θ = contact angle

σ = surface tension, dynes/cm

δ = density, grams/cm^3

For gallium and refractory metals

$$\sigma = 735 \text{ dynes/cm}$$

$$\theta = 135°$$

$$\delta = 6.1 \text{ grams/cm}^3$$

Therefore, f = 1470 dynes.

The capillary force is somewhat less than the magnetic forces calculated, 1470 dynes as compared with 2260 dynes and 3040 dynes. This indicates that care must be exercised in the detail design so that the magnetic forces are not greater than the capillary forces resulting in the gallium being forced out of the retaining gap.

B.3 Electrostatic Forces

The order of magnitude of electrostatic forces that could potentially exist between gallium rings in the slip ring was determined.

The force between large parallel plates is given by:

$$f = \frac{k}{8} \frac{V^2 A}{\pi d^2}$$

where: f = force, dynes

k = dielectric constant

V = voltage, statvolts

A = plate area, cm^2

d = plate separation, cm

Taking, k = 4.5 for Textolite

V = 15,000 volts, very high voltage rings (50 statvolts)

A = .1 x 4 π x 6.45 = 8.1 cm^2

d = .187"

The resulting force is approximately 16,000 dynes.

The electrostatic force is quite high as compared with the electromagnetic force of approximately 2000 dynes and capillary force of 1500 dynes, as shown in Section B.2.

B.3.1 Non-Polarized, Non-Conducting Particles

An analysis was made to determine the magnitude of the electrostatic force that would be exerted by an electrostatic field upon a non-conducting, non-polarized particle. The electrostatic field would be established between an electrode or the gallium to ground, the dielectric particle could be a particle of gallium oxide.

The force on dielectric particle in an electrostatic field is given by

$$f = \frac{k-1}{4\pi} \left(E \; V \right) \frac{d\,E}{d\,S}$$

where

f = force, dynes

k = dielectric constant

V = volume of particle, cm^3

E = electric field intensity, statvolts/cm

$\frac{d\,E}{d\,S}$ = electric field gradient

The geometry shown will be assumed:

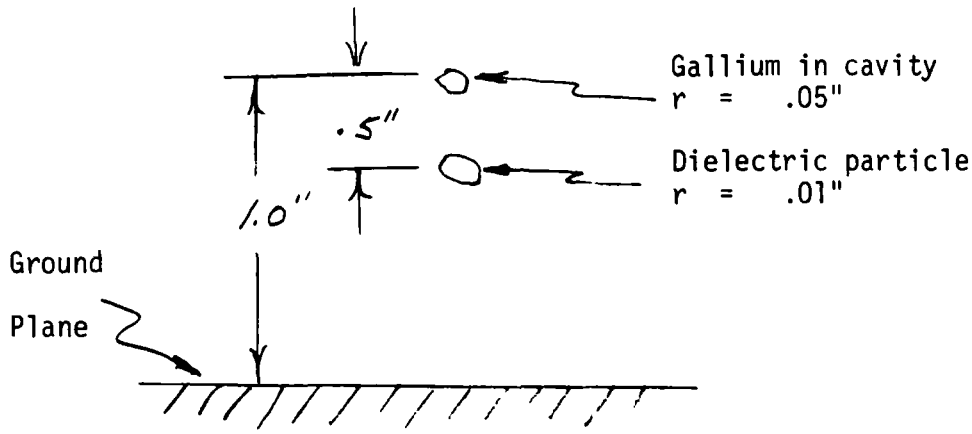

The electric field intensity produced by an infinitely long wire in air or vacuum is

$$E = \frac{2Q_S}{S}$$

where Q_S = conductor charge per cm, esu

S = distance from conductor, cm.

Also,

$$Q_S = C_S V$$

where

C_S = capacitance of wire, statfarads/cm

V = potential, statvolts

$$C_S = \frac{k}{2 \ln \left(\frac{h}{r}\right)}$$

where h = distance to ground, cm

r = radius of conductor, cm

From the geometry shown

$$C_S = \frac{1}{2 \ln \frac{1}{.05}} = .167 \text{ statfarads/cm}$$

Assuming the potential to ground is 15,000 volts,

$Q_S = 50\ (.167) = 8.3$ statcoulombs

and $E = \frac{2(8.3)}{1(.5)} = 33$ statvolts/cm

$$\frac{dE}{dS} = \frac{-4Qs}{S^2} = \frac{-4(8.3)}{1\ (.5x2.54)^2}$$

$$= 20.4$$

$$V = \frac{4}{3}\ \pi\ r^3 = 4.2 \times 10^{-6}\ \text{in.}^3 = 69 \times 10\text{-}6\ \text{cm}^3$$

Assuming a dielectric constant of 7, and negligible depolarization, the force will be:

$$f = \frac{6}{4\pi}\ (33)\ (69 \times 10^{-6})\ 20.4$$

$$= .022 \text{ dynes}$$

The acceleration experienced by the particle will be approximately

$$a = \frac{f}{m} = \frac{.022}{69x10^{-6} \times 6}$$

$$= 53\ \text{cm/sec}^2$$

The forces and accelerations imparted by electrostatic fields to dielectric particles appear to be appreciable. They increase substantially as the particle gets closer to the electrode where the field is greater.

B.3.2 Polarized, Non-Conducting Particles

The electrostatic force on a non-conducting, non-polarized particle in an electric field was analyzed. In that analysis, it was assumed that depolarization effects of the dielectric were negligible This assumption leads to somewhat higher force levels being calculated than are actually present. To be more precise, an analysis was made to determine the effects of depolarization upon the force exerted on a spherical dielectric particle . When a dielectric material is placed in an electric field, changes are induced on the surface of the particle. The polarity of these changes is such as to oppose the applied field. The result is that the internal field in the material is less than the external field. Mathematically, this can be expressed as

$$E_i = E_o - NP$$

where E_i = internal field intensity in particle

E_o = external field intensity

N = depolarization factor

P = electric polarization of material

Since $P = \dfrac{(D_i - E_i)}{4\pi}$

where D_i = dielectric flux

$$E_i = E_o - \frac{N (D_i - E_i)}{4\pi}$$

It can be shown for a sphere that

$$E_i = \frac{3}{k + 2} E_o$$

where k = dielectric constant of particle

Thus, the internal field will be reduced because of depolarization by an amount which is a function of the dielectric constant. The following table shows how the internal field in a sphere varies for the normal range of dielectric constants,

k	$\frac{E_i}{E_o}$
1	1
3	.6
7	.33
10	.25

The force on a dielectric particle was computed neglecting depolarization. This force can now be determined considering depolarization.

It was found that there was a force of 0.022 dynes on a particle of a dielectric constant of 7. If the particle was considered to be spherical, the force would be reduced by depolarization effects to

$$f = .022 \times (.33)^2$$

$$= 2.44 \times 10^{-3} \text{ dynes}$$

The acceleration would also be reduced, by the same factor, giving

$$a = 5.9 \text{ cm/sec.}^2$$

It should be noted that the depolarization of spherical particles is much higher than that of elongated particles. The depolarization effect of an ellipsoidal particle having an aspect ratic of 10:1 and a dielectric constant of 7 is approximately 0.9 along the major axis as compared with .33 for a spherical particle. The force on the ellipsoidal particle considering depolarization would thus be .81 of that not considering depolarization.

B.3.3 Conducting Particle

Electrostatic forces are exerted on conducting particles, as well as non-conducting particles, in electric fields.

The force on a conducting particle in an electrostatic field can be found based on the force on an electric dipole being

$$f = M \frac{dE}{dS}$$

where M = electric dipole

E = electric field intensity

For a conducting spherical particle

$$M = r^3 E$$

where r = radius of particle

Therefore

$$f = r^3 E \frac{dE}{dS}$$

It is of interest to note that the force on a dielectric sphere is less than that on a conducting sphere, primarily because of depolarization, Considering depolarization, the force on a dielectric sphere is

$$f_d = 3\left[\frac{k-1}{(k+2)^2}\right]\left(r^3E\right)\frac{dE}{dS}$$

and a conducting sphere is

$$f_c = r^3 E \frac{dE}{dS}$$

and

$$\frac{f_d}{f_c} = .37$$

Rough laboratory tests performed on conducting as well as dielectric material placed in an electrostatic field appear to indicate that the force acting on conducting materials are higher than the force on dielectrics.

B.4 Gallium Contamination

In order to obtain additional insight into the characteristics of gallium contamination, a number of organizations which work with gallium or produce it were contacted for their opinions. The groups contacted were:

Bell Labs.	- Murrary Hill, New Jersey
Cominco	- Clarkson, Canada; Spokane, Washington; Trail, British Columbia
Monsanto	- St. Louis, Missouri
Alcoa	- E. St. Louis, Illinois

Their comments are summarized below.

Bell Labs.

- Gallium oxide which is formed at room temperature will show amorphous x-ray diffraction patterns. Aluminum oxide, which is chemically similar to gallium oxide, also shows amorphous pattern unless it is heated to 800°.
- Contamination could be oxide or hydrated oxide.
- Argon might be better than nitrogen to prevent formation of oxide.
- Oxidation can be prevented by using phosphorous oxy-chloride getter.
- There should not be much dissolved oxygen in gallium.

Monsanto

- Gallium oxide is probably Ga_2O_3 not likely to be GaO. Do not know if it is hydrated.
- They keep gallium frozen at all times, and melted only under a vacuum. A "crud" still is formed which they have not been able to eliminate. They decant the liquid gallium using the middle portion.
- "White material" is formed in the presence of moisture.
- Know of no way of stopping oxidation, know of no alloy of gallium which will not oxidize.
- Pure argon should be satisfactory.
- Oxygen cannot be present in gallium, will react.
- GaO may be present.
- There are not many dark salts of gallium.

Cominco

- Surface contamination is gallium plus oxide.
- Gallium oxide very tenacious, adheres to sides of plastic containers for gallium.
- Gallium oxide actually is globules of gallium surrounded by oxide.
- Oxidized gallium can be cleaned with dilute HCl. A "more" stable technique consists of HCl dissolved in glycerol.
- Oxide can be reduced by slightly heating in presence of hydrogen.
- Do not think oxide is in hydrated form.
- Gallium does not react with nitrogen at room temperature. Oxygen and water could be present in "ordinary" nitrogen which could react.
- Dry, deoxidized nitrogen satisfactory. Dry, deoxidized argon satisfactory.
- Have not observed any vaporization of gallium GaO could be present and is very volatile.
- Oxide probably β-Ga_2O_3.

Alcoa

- Surface oxide is Ga_2O_3.
- Is not hydrated because of rapid formation.
- Impurities tend to concentrate in oxide film.
- Bubbling air through gallium causes a gray foamy matter.
- Black oxide has been observed, do not know what it is, may be Ga_2O_3.
- Store gallium under 1% HCl, "this argues against hydrated form".
- They supply gallium under nitrogen environment "because customer wants it", "seems advantageous".
- Would not expect dry nitrogen to react with gallium.
- Gallium-indium-tin alloy might have lower oxidation rate then pure gallium.
- Black deposit above gallium may be GaO which is volatile. However, do not expect GaO.
- Would not expect any gallium reaction with epoxy, or change in wetting characteristics.

Although there were points of disagreement, there were a number of points of general agreement. The major point of agreement include the following:

1. A gallium contamination has been observed and it is probably Ga_2O_3.
2. Both argon and nitrogen, preferably argon, will prevent formation of oxide contamination. Gas must be dry and deoxidized.
3. Black deposits have been observed above liquid gallium. This could be GaO.
4. No dissolved oxygen can exist in liquid gallium.

The major point of disagreement was whether the contamination could be the hydrated form of gallium oxide. Cominco and Alcoa did not think it could be the hydrated form while Bell Labs. and Monsanto thought that it could be hydrated.

B.5 LOW MELTING TEMPERATURE ALLOYS

An investigation was made to determine the melting temperatures and composition of alloys which could be utilized as a liquid metal and as a potential replacement for gallium in the slip ring. In addition to these characteristics, the vapor pressure and surface tension were ascertained for the element constituting the alloys.

The melting temperature and composition of low melting temperature alloys is given below:

Melting Temp. °C	Composition
3	61 Ga, 25 In, 13 Sn, 1 Zn
5	62 Ga, 25 In, 13 Sn
10.7	62.5 Ga, 21.5 In, 16 Sn
10.8	69.8 Ga, 17.6 In, 12.5 Sn
13	67 Ga, 29 In, 4 Zn
16	76 Ga, 24 In
17	82 Ga, 12 In, 6 Zn
20	92 Ga, 8 Sn
25	95 Ga, 5 Zn
27.3	99.5 Ga, .5 Tl
46.5	40.6 Bi, 22.1 Pb, 18.1 In
	10.7 Sn, 8.2 C_d
47	44.7 Bi, 22.6 Pb, 19.1 In, 8.3 Sn
	5.3 Cd (Cerrolow 117, Indalloy 117)

Melting Temp. °C	Composition
57.7	49 Bi, 18 Pb, 21 In, 12 Sn, (Cerrolow 136, Indalloy 136)
60.5	32.5 Bi, 51.0 In, 16.5 Sn
64	48 Bi, 25.6 Pb, 4 In, 12.8 Sn, 9.6 Cd (Cerrolow 147, Indalloy 147)
70	50 Bi, 26.7 Pb, 13.3 Sn, 10 C_d (Cerrobend, Indalloy 158, Lipowitz's metal)
70	50 Bi, 25 Pb, 12.5 Sn, 12.5 Cd (Wood's metal)
93	44 In, 42 Sn, 14 C_d
117	52 In, 48 Sn
125	70 In, 15 Sn, 9.6 Pb, 5.4 Cd
	56 Bi, 44 Pb
	50 In, 50 Sn

Of these alloys, those containing zinc and cadmium would probably be unsatisfactory from the aspect of vapor pressure since their vapor pressures are many order of magnitude greater than gallium. Bismuth and lead have vapor pressures approximately 5 orders of magnitude higher than gallium, indium is two orders of magnitude higher, while tin is about one order of magnitude lower. It should be noted that the rate of evaporation of these alloys is not only a function of vapor pressure but the molar concentration by virture of Raoult's law. This latter factor may permit small concentrations of high vapor pressure elements. Calculations indicate that alloys containing bismuth, gallium, indium, lead and tin would probably have

evaporation rates low enough to allow their usage. Alloys containing cadmium and zinc are probably unsatisfactory unless it can be demonstrated that the evaporation rates of the cadmium and zinc are low enough to be tolerated because of their low concentration.

The surface tension of the constituent elements of the various alloys are as follows:

	Surface Tension (dynes/cm)	Temperature (°C)
Bismuth	370	271
Cadmium	666	320
Gallium	735	30
Indium	554	170
Lead	480	330
Tin	480 - 662	232
Zinc	773	420

It appears that the surface tension of the elements constituting the alloys are sufficiently high to permit retention by capillary forces.

B.6 THERMODYNAMICS OF OXIDE FORMATION

In order to gain insight into the oxidation phenomenon, the thermodynamics of oxide formation was studied. Unfortunately, the thermodynamics does not define the entire phenomenon since the kinetics of the reaction must also be studied in context with the thermodynamics. However, the objective was to determine whether there were any great differences in the heats of formation of the oxides of the elements in low melting temperature alloys. As a comparison, the heats of formation of gold and silver oxides are given.

	Heat of Formation k gram calories/mole
Ga_2O	-83
Ga_2O_3	-258
In_2O_3	-220
Bi_2O_3	-142
SnO	-69
SnO_2	-143
CdO	-62
Pb O	-53
Pb O_2	-56
Au_2O_3	-2
Ag_2O	-8
Ag_2O_3	-6

It will be noted that the heats of formation of the various oxides are of the same orders of magnitude except for gold and silver which are substantially less. It would appear from this that lacking kinetic data, that low oxidation rates can be achieved only with elements having extremely low heats of formation and that the oxidation characteristics of the element used in low melting temperature alloys are about the same.

B.7 GALLIUM OXIDE FORMATION

If the gallium reacts with oxygen to form gallium oxide, Ga_2O_3, the weight of the oxide can be determined as:

$$4\ Ga + 3\ O_2 \longrightarrow 2\ Ga_2\ O_3$$

$$W_{Ga_2\ O_3} = \frac{2\ (140 + 48)}{3\ (32)}\ W_{O_2}$$

$$= 3.92\ W_{O_2}$$

Thus, the weight of gallium oxide is 3.92 times the weight of oxygen reacting with it, assuming complete reaction.

The weight of the oxygen and gallium oxide formed in the slip ring will be calculated two ways: first, as an outgassing of the Textolite and second, as being present in a protective nitrogen atmosphere.

Based on the extrapolated test data taken by General Electric, if Textolite is outgassed for 100 hours as a sheet and then assembled in bulk, the total remaining gas, probably water vapor, will outgas from the bulk for a total of 550×10^{-6} grams per sq. cm.

For the slip ring, the total cylinder area is approximately

$A_1 = 5\ \pi \times 12 =$ $188\ in^2$

$A_2 = .785\ \ (25)\ (2) =$ $\frac{39}{227}\ in^2$

Total $227\ in^2 = 1460\ cm^2$

Assuming $1500\ cm^2$, and that the outgas is all oxygen, the weight of gallium oxide is

$W = 550 \times 10^{-6} \times 1500 \times 3.92$

$= 3.26$ grams

or .0281 grams per ring

If the oxide is assumed to have a density of 6 grams/cm^3 and the cavity width is .06 inches, the oxide depth will be

$$d = \frac{.0281 \times 6}{.06 \times 5\pi \times 6.45} = .0277 \text{ cm}$$

$$= .011 \text{ inches}$$

This depth is not excessive considering that the available depth of cavity is .5 inches, although all of the depth cannot be utilized for contamination containment because of dielectric breakdown considerations.

If the "open" volume of the entire slip ring is assumed to be .2 $ft.^3$, there are 5 nitrogen changes per hour for 500 hours while the gallium is liquid, and that the oxygen content of the nitrogent is 10 ppm, the total oxygen flowing through the slip ring will be

$$V = .2 \times 5 \times 500 \times 10 \times 10^{-6}$$

$$= 5 \times 10^{-3} \text{ ft.}^3 = 140 \text{ cm}^3$$

The weight of oxygen will be

$$W = 140 \times 1.5 \times 10^{-3}$$

$$= .21 \text{ grams}$$

based on an oxygen density of 1.5×10^{-3} grams/cm^3. If this weight of oxygen reacts completely with the gallium, there will be .82 grams of gallium oxide produced resulting in a depth of .00275 inches.

Based on the above, the implication is clear: the formation of gallium oxide will not be severe as long as it is not allowed to build up in a small area but is kept spread over the entire circumference of the cavity.

B.8 DIELECTRIC CHARACTERISTIC OF GASES AND ELECTRODE SPACING

Since the liquid metal slip ring may be run in gases other than air in order to prevent the formation of gallium contamination, it is important to know the dielectric characteristics of these gases. Two dielectric characteristics were studied: the breakdown voltage at standard temperature and pressure, and the minimum breakdown voltage. Three gases were considered: air, nitrogen and argon.

The breakdown voltage between electrodes is a complicated phenomenon dependent upon such factors as electrode size, geometry spacing, material, surface finish, gas impurities in the gas, gas pressure, etc. The breakdown voltage for air at standard conditions is approximately 30,000 volts per cm or 75,000 volts per inch between large electrodes spaced at 1 cm. Comparable values for argon and nitrogen are given below:

	Breakdown Voltage	
	Volts/cm	Volts/inch
Argon	7500	19,000
Nitrogen	27,000 to 35,000	67,000 to 87,000
Air	30,000	75,000

The minimum breakdown voltage as well as the pd (pressure x separation) point on Paschen's curve is also a characteristic of the gas. These values for parallel plate electrodes are as follows:

	Minimum Breakdown Voltage	pd (mm Hg x cm)
Air	340	.57
Nitrogen	250	.67
Argon	275 160	1.5

Thus, the dielectric properties of nitrogen and air are approximately the same while argon is significantly poorer with about 25% the dielectric strength of air. The use of argon had been considered for the slip ring in order to

prevent the formation of gallium contamination. It does not appear possible with the present design to run the slip ring in an argon atmosphere at voltages in excess of 4000 volts. In order to run at 15,000 volts, the breakdown paths would have to be increased by a factor of 4 by reducing the gradient from 25 volts per mil to 6 volts per mil. Thus a .6" leakage path would have to be increased to 2.4 inches in order to function at 15,000 volts in argon. From a dielectric standpoint, nitrogen could be substituted for air with minimal effects.

In original slip ring design considerations, the electrode spacing in air was based on a value of $.25\sqrt{\text{kilovolts}}$, as given by Paul and Burrowbridge in NASA-SP-208. Consultations with personnel of the General Electric Co. Research and Development Center, Schenectady, N. Y., indicated that a less conservative electrode spacing could be used. The dielectric breakdown between electrodes in air takes place at voltage gradients over 75 volts/mil; with a safety factor of 3, the allowable gradient will be 25 volts/mil. The table below shows a comparison of electrode spacings between the different assumptions.

ELECTRODE SPACING - INCHES

Voltage	$.25\sqrt{kv}$	75 v/mil	25 v/mil
2000	.35	.03	.08
3000	.43	.04	.12
6000	.61	.08	.24
9000	.75	.12	.36
12000	.86	.16	.48
15000	.97	.2	.6

B.9 DIELECTRIC STRESS

The dielectric stress in small gaps between the gallium retaining liner and Textolite insulator disk was calculated to determine its magnitude relative to the breakdown stress.

Considering insulators in series between electrodes, the voltage across any one can be calculated from

$$V_1 = \frac{\frac{t_1}{k_1}}{\sum \frac{t}{k}} \quad V$$

where V_1 = voltage across insulation

t_1 = insulation thickness

k_1 = dielectric constant of insulation

$$\sum \frac{t}{k} = \frac{t_2}{k_2} + \frac{t_3}{k_3} + \text{-----} + \frac{t_n}{k_n}$$

V = applied voltage

For simplicity, if two insulations are considered, the voltage gradient across one of them will be

$$\frac{V_1}{t_1} = \frac{1}{k_1} \frac{1}{\frac{t_1}{k_1} + \frac{t_2}{k_2}} \quad V$$

letting $t_1 = .001"$, $k_1 = 1$ } air

$t_2 = .18"$ } Textolite

$k_2 = 5$ }

$V = 15{,}000$ volts

The voltage gradient across the air is

$$\frac{V_1}{t_1} = \frac{1}{.001 + \frac{.18}{5}} \times 15{,}000$$

$$= 408{,}000 \text{ volts/in.}$$

This is in excess of the voltage breakdown electrodes in air (75,000 volts/inch). At an applied voltage level of 2000 volts which is the voltage for high voltage rings, the comparable gradient is 55,000 volts per inch.

It is not immediately evident as to what phenomenon will take place in the gap. There could be a spark discharge between the liner and the Textolite insulation. This depends upon the electrical conductivity characteristics of the insulator. On the other hand, a corona discharge could be present. In either case, a discharge or an ionization of the air, could lead to an ultimate failure of insulation.

The voltage gradient across the air gap between the liner and the Texolite can be eliminated. This can be accomplished by putting a conducting paint on the Textolite surfaces which are in proximity with the liner. A material that is being considered for this is Eccobond solder V-91 which is a two part epoxy based conductive adhesive. It can be brushed on to the adherents and has excellent adhesion to metals and plastics. Its volume resistivity is less than .002 ohm-cm.

B.10 FLUID FLOW CHARACTERISTICS

It is of interest to examine the fluid flow characteristics of the gallium. First, the Reynolds number will be determined

$$N_{re} = \frac{DV\rho}{\mu}$$

where N_{re} = Reynolds number

D = Characteristic dimension

V = Characteristic velocity

ρ = Density of fluid

μ = Viscosity of fluid

Assuming

4" diameter gallium ring

1 revolution per day

ρ = 6.0 grams/cm^3

μ = 1.5 centipoises

$$N_{re} = .147\ D$$

where D is in centimeters

If the gallium is considered to be flowing in the cavity or if one electrode is rotating relative to the other, the characteristic dimension, D, will be twice the clearance. For the slip ring, this will be

$$D = 2 \times .063 \times 2.54$$

$$= .32 \text{ cm}$$

and $N_{re} = .047$

For a probe wire moving in the gallium and remote from walls, D = wire diameter .025", and $N_{re} = .0094$.

The flow in an annulus between concentric cylinders tends to become unstable due to centrifugal force when the inner cylinder is rotated. This phenomenon has been investigated by a number of authors. The conditions that define the appearance of circular flow patterns called Taylor vortices with inner cylinder rotation have been given as

$$N_{re} > 41.3\sqrt{\frac{R_1}{R_1 - R_2}}$$

where R_1, R_2 are the radii of the cylinders

Taking values of R_1 of 2.1 inches and R_2 of 2.0 inches

$$N_{re} > 190$$

for any vortices to appear.

The transition from laminar to turbulent flow for various geometries is as follows:

	Transition Reynolds Number
Pipes	> 2100
Sphere	> 0.1
Cylinder	> 0.1
Annulus between rotating cylinders of $R_1 = 2.1"$, $R_2 = 2.0"$	
a. Inner cylinder rotating	> 190
b. Outer cylinder rotating	$> 50,000$
Probable Reynolds Number in slip ring N_{re}	< 0.1

In summary, it appears that for slip ring configurations being considered, the flow characteristics of or through the liquid metal is so small so as to be well within the laminar region.

B.11 VENTING ANALYSIS

An analysis was made to determine the venting characteristics of the slip ring. The venting rate is of concern since it is desired that internal gas pressure drop rapidly enough so that there is no dielectric breakdown after the spacecraft is in orbit and the slip ring is energized. For the venting analysis, a pressure-time curve of the external environment seen by the slip ring during launch was assumed based on a modified Titan III C launch profile.

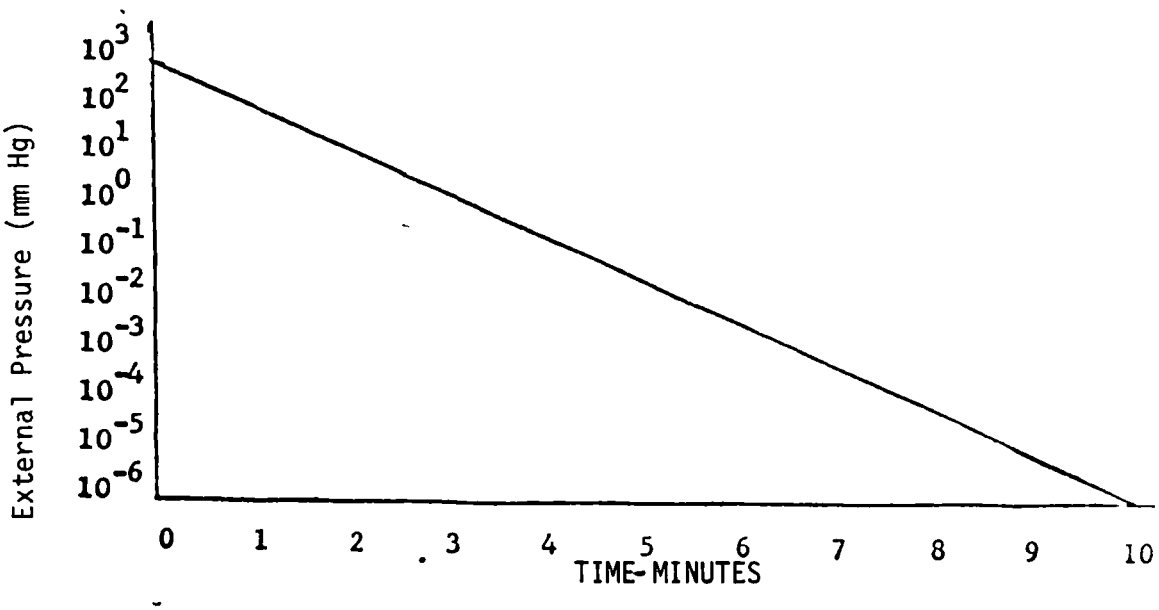

In the analysis, a step-by-step approach will be followed and it will be shown that the internal pressure will closely follow the external environment based on the diameter of the venting port. There are three regimes of gas flow depending upon the pressure and the size of the vent. These are as follows:

Continuum Flow	$aP\,\mu > 500$
Molecular Flow	$aP\,\mu < 5$
Transition Flow	$5 < a\,\mu < 500$

where P is the pressure in microns

a is the characteristic dimension, cm

For a circle, it is the radius.

In this analysis, the flow characteristics in the continuum and molecular regimes will be studied.

B.11.1 Continuum Flow Regime

First, the flow characteristics will be examined after 1 minute has elapsed at which time the external pressure dropped by an order of magnitude. The internal pressure in the slip ring is assumed to be 760 mm Hg and the external pressure is 76 mm. The pressure ratio is

$$\frac{P_2}{P_1} = .1$$

This is below the critical pressure ratio

$$\left(\frac{P_2}{P_1}\right)_c = \left(\frac{2}{k+1}\right)^{\frac{k-1}{k}} = .53, \text{for air}$$

where k = ratio of specific heat at constant pressure to that at constant volume, adiabatic exponent

= 1.4, for air

Therefore, the initial velocity of the venting gas (air) will be limited by the sonic velocity.

The air will flow out of the slip ring under either adiabatic or isothermal conditions, most likely adiabatic. The sonic velocity will be determined for both adiabatic and isothermal conditions in order to bound its limits. For adiabatic flow,

$$\frac{V^2}{2g} = \left(\frac{k}{k-1}\right)\left(\frac{P_1}{w_1}\right)\left(1 - \frac{P_2}{P_1}\right)^{\frac{k-1}{k}}$$

$$= \frac{k}{k-1} \quad RT \quad \left[1 - \left(\frac{P_2}{P_1}\right)^{\frac{k-1}{k}}\right]$$

where R = gas constant, 53.3, ft./°R, for air

T = temperature, °R

V = velocity, ft./sec.

Substituting the appropriate values in this equation, the sonic velocity, V_s, is

V_s = 965 ft./sec. at 0°F

For isothermal conditions, the sonic velocity is

$$V_s = \sqrt{kg\ RT}$$

solving,

V_s = 1055 ft./sec.

Thus, the limiting flow velocity is less assuming adiabatic conditions and this value will be assumed.

Assuming a 1 in. diameter venting port having a coefficient of .5, which is conservative, the rate of flow will be

$Q = CAV$

where Q = flow rate ft.

C = orifice coefficient

A = area of vent, $ft.^2$

$$Q_s = C\ AV_s$$

$$= .5 \quad \left(\frac{1^2 \times .785}{144}\right) \quad 965$$

$= 2.62\ ft.^3/sec.$

An upper limit of volume of air in the slip ring is approximately

$$V_a = 9\ \pi\ (1)\ (20)$$

$$= 565\ \text{in.}^3 \qquad = .327\ \text{ft.}^3$$

Although the pressure in the slip ring will drop rapidly as venting occurs, it is of interest to calculate the time required to vent assuming constant pressure. At the initial venting rate, the time required to vent the slip ring is

$$t \approx \frac{V_a}{Q}$$

$$\approx .125 \text{ seconds}$$

It is also of interest to determine the flow rate at a small pressure differential across the vent at which critical flow will not occur. If a constant pressure differential of 10 mm Hg is assumed and the internal pressure is 76 mm Hg, Bernoulli's equation for imcompressible flow can be used:

$$Q = CA \sqrt{2gh}$$

where h is the pressure differential, ft. of fluid

$$h = \left(\frac{10}{305}\right)\left(\frac{849}{.0075}\right)$$

$$= 3700 \qquad \text{ft of air}$$

$$Q = .5\ (5.44 \times 10^{-3}) \sqrt{2\ (32.2)\ 3700}$$

$$= 1.33\ \text{ft.}^3/\text{sec.}$$

$$t = .246 \text{ seconds}$$

Based on the assumed pressure-time characteristics, the pressure drops from 760 mm Hg to 76 mm Hg in one minute. Under conditions of constant pressure and critical flow, the slip ring will vent in .125 seconds; and under constant pressure differential of 10 mm Hg, it will vent in .25 seconds.

B.11.2 Molecular Flow Regime

The molecular flow regime occurs when

$$a\,P_\mu < 5$$

In this regime, the time required to reduce the pressure from P_1 to P_2 is given by

$$t = \frac{V}{s} \ell n \frac{P_1}{P_2}$$

where t = time

V = volume

s = pumping speed

$$s = Af$$

$$= 3.64\, A \sqrt{\frac{T}{M}} \text{ liters/sec.}$$

where f = pumping rate,

A = orifice area

T = temperature, °K

M = molecular weight of gas

The time, t, will be computed under the following conditions:

P_1 = the upper limit of the molecular flow regime, a $P_\mu < 5$

P_2 = the lower limit of critical pressure from a dielectric criteria, 10^{-5} torr

A = the orifice area, 1" diameter

$T = 0°C, 273°K$

$M = 28$, for air

$V =$ volume, .327 $ft.^3 = 9.3$ liters

$$P_1 < \frac{5}{.5 \times 2.54}$$

$$P_1 < 4 \text{ microns} = 4 \times 10^{-3} \text{ torr}$$

$$P_2 = 10^{-5} \text{ torr}$$

$$A = .785\ (2.54 \times 1)^2 = 1.62 \text{ cm}^2$$

Therefore, the pumping speed is

$$s = 3.64\ (1.62) \sqrt{\frac{273}{28}}$$

$$= 57.2 \text{ liters/sec}$$

The time is

$$t = \frac{9.3}{57.2} \ln \frac{4 \times 10^{-3}}{10^{-5}}$$

$$= .972 \text{ seconds}$$

Thus, it takes approximately 1 second to reduce the internal pressure in the molecular flow region from 4×10^{-3} torr to 10^{-5} torr, the point at which there is no dielectric breakdown problem.

B.12 NORMAL STRESS - WEISSENBERG EFFECT

A study was made of the normal stress or Weissenberg effect in order to determine whether this phenomenon explains the ejection of gallium contamination from the annular space between slowly rotating slip ring electrodes. The normal stress or Weissenberg effect is the tendency of certain viscoelastic fluids to flow in a direction normal to the direction of shear stress. The physical parameter which describes the Weissenberg effect is called cross viscosity and can be shown theoretically to exist in non-Newtonian fluids by applying the Bingham model to Navier-Stokes equations. A common example of the normal stress is flour dough climbing up the rod of a beater. The normal stress effect has also been observed in a wide range of materials including many polymer solutions. Another type of normal pressure effect which has been observed in non-elastic, purely plastic materials occurs when a ball or flat cylinder of material is rolled between parallel plates under gentle pressure. Under these conditions, an elongated cylinder is formed, and, depending upon the materials, as the action proceeds, the ends are sucked in. This phenomenon has been produced in polyisobutylene, a paste of asbestos fiber in liquid parafin and a paste of icing sugar in liquid parafin.

The gallium contamination which has been observed in and coming from the liquid metal slip ring is a mixture of gallium and gallium oxide. If this mixture has viscoelastic properties, then it is possible that it might be displaying the normal stress effect which causes it to move perpendicularly to the direction of shear stress in the liquid metal slip ring.

The normal stress can be measured by using either the Rheogoniometer or the Ferranti-Shirley cone-plate viscometer. The Rheogoniometer was designed by Weissenberg as a research instrument to measure, among other parameters, the normal stress. It is essentially a plate-and-cone viscometer highly instrumented so as to be able to measure the normal forces. The Ferranti-Shirley viscometer is a much less sophisticated device more suited to industrial usage. It consists of a stationary flat plate and a rotating conical disk driven by a variable speed motor through a gear train and torque spring. The torsion due to viscous drag is measured by a potentiometer on the spring.

B.13 HYDRODYNAMIC CONSIDERATIONS

The hydrodynamic motion characteristics of the liquid metal may be influenced by three forces: inertia, gravity and capillary. A number of dimensionless parameters have been defined which serve to quantitize their hydrodynamic behavior and to permit an assessment of their relative importance. These are called the Weber number, Froude number and Bond number, respectively.

The Weber number provides an estimate of the ratio of the inertial forces to the capillary forces. The Weber number is defined as

$$We = \frac{\rho V^2 L}{\sigma}$$

where We = Weber name, dimensionless

ρ = density of fluid

V = Velocity

L = characteristic dimension

σ = surface tension

Considering the Weber number:

Inertial forces dominate when We >> 1

Capillary forces dominate when We << 1

The Froude number provides an estimate of the effects of inertial forces and gravity body forces. The Froude number is

$$Fr = \frac{V^2}{g\,L}$$

where F = Froude number, dimensionless

g = acceleration

L = characteristic length

Considering the Froude number:

Inertial forces dominate when Fr >> 1

Body forces dominate when Fr << 1

The Bond number is the ratio of the Weber and Froude numbers,

$$Bo = \frac{We}{Fr}$$

$$Bo = \frac{\rho g L^2}{\sigma}$$

The Bond number compares the magnitudes of gravitational and capillary forces.

Gravitational forces dominate when $Bo >> 1$

Capillary forces dominate when $Bo << 1$

The Weber, Froude and Bond numbers will be computed for the slip ring to delineate the characteristics of the sloshing regime.

$\rho = 6.0$ grams/cm^3

$g = 980 \times 10^{-3}$ cm/sec^2

$L_1 = 4" = 10$ cm

$L_2 = \frac{.050"}{2} = .025" = .063$ cm

$\sigma = 735$ dynes/cm

The Weber number has a velocity term which will be calculated based on the operating environment vibration specification, linear acceleration of 10^{-3} g .0004 Hz to 4 Hz.

$$V = \frac{a}{w} = \frac{a}{2\pi f}$$

$f = .0004$ Hz $\quad V = \frac{980 \times 10^{-3}}{2\pi (.0004)} = 391$ cm/sec

$f = .004 \quad V = 39.1$ cm/sec

$f = .04 \quad V = 3.91$ cm/sec

$f = .4 \quad V = .391$ cm/sec

$f = 4.0 \quad V = .0391$ cm/sec

The Weber number is

$$We = \frac{\rho L_2 V^2}{\sigma}$$

$$= \frac{6\ (.063)\ V^2}{735}$$

$$= 5.15 \times 10^{-4}\ V^2 = 5.15 \times 10^{-4} \left(\frac{a}{2\ \pi\ f}\right)^2$$

f (Hz)	We
0.0004	78.5
0.004	0.785
0.04	0.785×10^{-2}
0.40	0.785×10^{-4}
4.0	0.785×10^{-6}

The Froude number is

$$Fr = \frac{V^2}{g\ L_1}$$

but $V = \frac{g}{w}$

Therefore

$$Fr = \frac{g}{w^2 L_1} = \frac{g}{(2\pi f)^2 L_1}$$

f (Hz)	Fr
0.0004	1.54×10^4
0.004	1.54×10^2
0.04	1.54
0.40	1.54×10^{-2}
4.0	1.54×10^{-4}

The Bond number is

$$Bo = \frac{L_1 L_2 g}{\sigma}$$

$$= \frac{6.0\ (10)\ (.063)\ (980 \times 10^{-3})}{735} = .005$$

Summarizing,

f	We	Fr	Bo	Dominant Force
.0004	78.5	1.54×10^{-4}	5.0×10^{-3}	Inertial
.004	78.5×10^{-2}	1.54×10^{2}	5.0×10^{-3}	Indeterminant Regime
.04	78.5×10^{-4}	1.54	5.0×10^{-3}	Capillary
.4	78.5×10^{-6}	1.54×10^{-2}	5.0×10^{-3}	Capillary
4.0	78.5×10^{-8}	1.54×10^{-4}	5.0×10^{-3}	Capillary

From this table, it appears that capillary forces will predominate above .04 Hz at accelerations of 10^{-3}g or less. At .004 Hz, the dominant force is indeterminate and at .0004 Hz and 10^{-3}g, the dominant force is definitely inertial. It should be noted that the present test plan calls for a minimum frequency of .008 Hz and a corresponding 10^{-5}g level because of equipment limitations. These conditions should put the dominant force in the capillary regime.

The analysis of the hydrodynamic behavior of the gallium in the slip ring was continued and the sloshing parameters and the resonsant frequency characteristics were studied in further detail.

Using the Bond and Weber numbers the regimes of stability and instability due to inertial and capillary forces can be delineated. For the slip ring geometry, the Bond number which is defined as:

$$Bo = \frac{\rho L^2 g}{\sigma}$$

has the value of

$$Bo = .005\ g$$

The Weber number which is defined as

$$We = \frac{\rho L V^2}{\sigma}$$

has a value of

$$We = 5.15 \times 10^{-4}\ V^2$$

for the slip ring

Considering the Bond and Weber numbers, capillary forces dominate when

$$Bo << 1$$

$$We << 1$$

This permits us to put limiting magnitudes on acceleration and velocity since

$$Bo = .005\ g << 1$$

$$We = 5.15 \times 10^{-4}\ V^2 << 1$$

Therefore,

$$g \ll \frac{1}{.005} = 200 \text{ cm/sec}^2 \quad (.2\ g)$$

$$\& \quad V \ll \frac{1}{5.15 \times 10^{-4}} = 44.0 \text{ cm/sec}$$

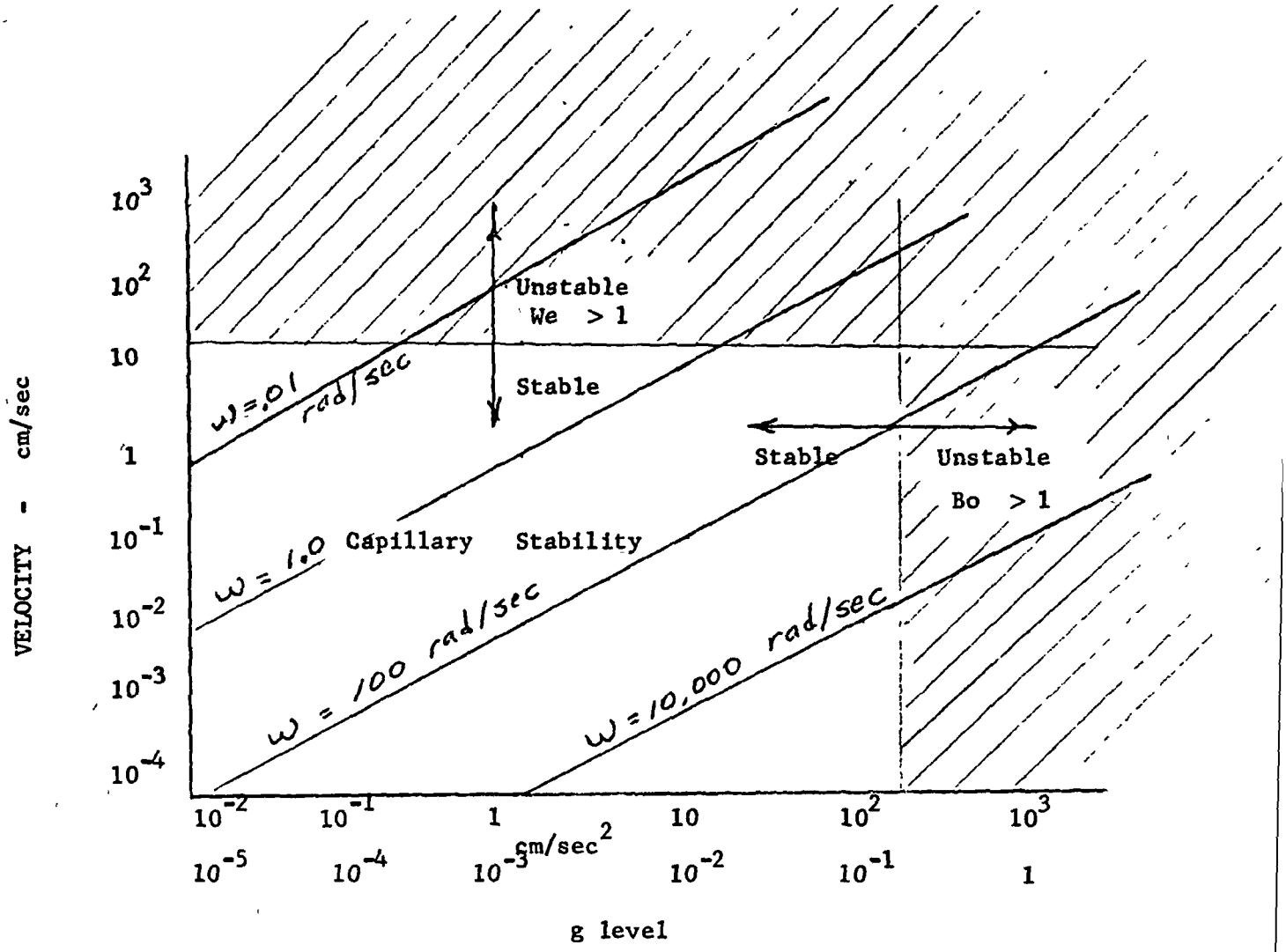

B.13-1 REGIME OF CAPILLARY STABILITY

Thus, as long as the acceleration is less than 200 cm/sec^2 (.2 g) & the velocity is less than 44.0 cm/sec, the gallium will be retained by capillary forces.

The resonant frequency of the liquid metal was determined by two techniques. First by examining the characteristics time of the system and then by a direct computation of the resonant frequency.

The characteristics time provides an order of magnitude estimate for the time required for the reorientation of a liquid following the transition from one hydrostatic regime to another. This provides an order of magnitude estimate of the resonant sloshing frequency. The characteristic time for the capillary dominated regime is

$$T = \sqrt{\frac{\rho L^3}{\sigma}}$$

For the slip ring geometry, the characteristic time will be considered three ways in order to bracket the magnitude

$$T_1 = \sqrt{\frac{\rho L_1^3}{\sigma}}$$

$$T_2 = \sqrt{\frac{L_1^2 L_2}{\sigma}}$$

&

$$T_3 = \sqrt{\frac{L_2^3}{\sigma}}$$

where L_1 = diameter of ring, 10 cm

L_2 = capillary spacing, .063 cm

using the conventional values of density and surface tension of gallium

T_1 = 2.85 seconds

T_2 = .228 seconds

T_3 = .00143 seconds

If T is considered as the time for a half-cycle, at resonance,

$$f = \frac{L}{2T}$$

and

$$f_1 = .175 \text{ Hz}$$

$$f_2 = 2.2 \text{ Hz}$$

$$f_3 = 348 \text{ Hz}$$

The lowest mode of sloshing frequency can be directly computed from

$$\Omega^2 = \tanh (1.84\ L) \left[6.26 + 1.84\ Bo \right]$$

where $\Omega^2 = \frac{\rho L^3 W^2}{\sigma}$

= low-g sloshing frequency parameter, radians/sec

ρ = density of fluid

L = characteristic length

W = sloshing frequency, radians/sec

σ = surface tension

Bo = Bond number

From previous analysis, Bo $\ll 1$ for the capillary regime. For this analysis it will be assumed that

$$Bo \approx 0$$

Two values of L will be assumed, again, to bracket the limits of resonant frequency. These values are the diameter of the slip ring, 10 cm, and capillary spacing, .063 cm.

Taking L = 10 cm and Bo = 0

$$\Omega^2 = \tanh (1.84 \times 10)\ (6.26)$$
$$= \tanh (114)$$
$$= 1$$

and taking L = .063 cm and Bo = 0

$$\Omega^2 = \tanh (.725) = .6$$

$$\Omega = .785$$

It is interesting to note that although the characteristic dimension L is varied from 10 to .063, more than 2 orders of magnitude, the sloshing parameter varies by a factor of only .785.

From

$$W^2 = \frac{\sigma}{\rho L^3} \Omega^2 ,$$

if L = 10 cm,

$$W = \sqrt{\frac{73.5\ (1)}{6(1000)}}$$
$$= .35 \text{ radians/sec}$$
$$= .056 \text{ Hz}$$

If $L = .063$ cm

$$W = \frac{735\ (.6)}{6(.063)^3}$$

$$= 544 \text{ rad/sec}$$

$$= 86.6 \text{ Hz}$$

For consistency, a third case if

$$L^3 = L_1^2 L_2$$

$$L^3 = (10)^2 (.063) = 6.3$$

and taking

$$\Omega^2 = 1$$

$$W = \frac{735(1)}{6(6.3)}$$

$$= 4.4 \text{ rad/sec}$$

$$= .70 \text{ Hz}$$

The results of the calculations of the natural frequency of sloshing are summarized as follows:

CONDITIONS	Natural Frequency of Sloshing (Hz) Characteristic Time Approach	Direct Calculation
Case 1 $L_1 = 10, L_2 = 10$	.175	.056
Case 2 $L_1 = 10, L_2 = .063$	2.2	.70
Case 3 $L_1 = .063, L_2 = .063$	348	86.6

Based on the slip ring geometry, the most probable conditions are those of Case 2 which produces a resonant frequency of 2.2 or .70 Hz, depending upon the method of calculation.

During the vibration tests with the gallium liquid, an attempt was made to determine the order of magnitude of the sloshing frequency. This was done by manually moving the slip ring back and forth and visually observing at what frequency the amplitude of liquid tended to build up. The natural frequency was found by this method to be between .5 and 2.0 Hz, most probably 1 Hz. This is in general agreement with the frequency determined by calculation.

B.14 Rate of Gallium Oxidation

Liquid metal slip ring experiments have been run in controlled atmospheres of nitrogen and argon having oxygen and water vapor contents of the order of 10 ppm or less and a continuous formation of contamination has been observed in these environments. It had been postulated that no appreciable contamination would be formed if the slip ring were operated in environments having oxygen or water vapor contents of the magnitude of parts per million. An analysis has been made which shows that this assumption is not valid.

The rate at which a surface becomes contaminated by a gaseous media can be calculated based on the kinetic theory of gases. It has been shown in the General Electric Research Laboratory Report No. 61-RL-2755C, "Ultrahigh Vacuum Techniques for the Investigation of Space Lubrication" by L. E. St. Pierre and A. J. Haltner, that the time required for a monolayer of contamination to form on $1/\varepsilon$ (63%) of a clean surface is

$$T = \frac{k}{p\lambda} \times 10^{-6}$$

where T = time, seconds

p = pressure, torr

λ = sticking coefficient, usually between 0.1 and 1.0

k = a constant

= 2.5 for oxygen

= 2.1 for water vapor

The following table shows the time constant, time to cover 63% of the surface, for various pressures, and oxygen contents.

Pressure (Torr)	Oxygen Content (ppm)	Time Constant to Oxidize 1 monolayer $\lambda = 1$ (Seconds)
760	200,000	3.3×10^{-9}
10^{-2}	2.6	2.5×10^{-4}
10^{-4}	2.6×10^{-2}	2.5×10^{-2}
10-6	2.6×10^{-4}	2.5
10-8	2.6×10^{-6}	$2.5 \times 10^{+2}$
10^{-10}	2.6×10^{-8}	$2.5 \times 10^{+4}$

From this table, it can be seen that the rate of monolayer oxide formation is quite rapid even under the best quality argon and nitrogen gases which have oxygen and water vapor contents of several parts per million. This explains the rapid formation of contamination that has been observed with slip rings assembled or operating in argon and nitrogen environments. It appears that operation only under a vacuum can prevent the continuous build-up of contamination.

APPENDIX C

VERIFICATION TEST PLAN

C.1 Introduction

The design verification test plan defines the tests, procedures and environments applicable to the components and the assembly to verify the engineering design. The test parameters measured and the environments endured are intended to provide a high level of confidence in the design and reliability of the components and assembly for the success of LMSR/SAOM flight application. Satisfactory completion of the design verification tests will demonstrate that:

a. Assembly will function properly under its expected service conditions.

b. Applicable design specifications have been met.

The system test verification program is intended to provide a high level of confidence in the design and reliability of the components and assembly for the success of flight application. Because of small sample size, statistical concepts have high limited applicability; therefore, the test program is designed to assess the conservative margin of safety by design verification testing on every major component and on the assembled unit.

C.2 Test Specimen Description

The engineering prototype liquid metal slip ring assembly will be in a flight configuration which will consist of approximately 116 slip ring assemblies, mounted on a center shaft with torque motors, bearings

and a resolver attached, attached to a support structure and enclosed by a shroud. For test and handling purposes, the LMSR assembly will be mounted in a universal test fixture assembly from the completion of final assembly until it is removed for mounting in the launch vehicle. The LMSR assembly (flight configuration) will weigh approximately forty (40) pounds and the handling and test fixture will weigh approximately 90 to 110 pounds. Thus, the LMSR and fixture assembly will weigh approximately 150 pounds.

C.3 Environmental Requirements and Test Selection

The environmental requirements for the LMSR system are summarized in Table 2. The selection of tests, sequence and rationale for selection will be presented in subsequent paragraphs of this section of the plan.

C.4 Dynamic Environments

C.4.1 Vibration

The prototype flight test specimen will be subjected to vibration first during local movement during the assembly and test cycle at the factory. This is extremely low in level because of the relative smoothness of the floors, the cushioning effect of the rubber-tired caster wheels on the handling dolly and the additional cushioning effect of the foam material used to support the test specimen on the bed of the dolly. Next the test specimen is exposed to a vibration environment during shipment between the factory and field site. However, this is reduced by some degree by the cushioning designed and built into the shipping container. The most severe of these would be during shipment by truck from the factory to the airport and from the airport to the field site. The "g" level anticipated on the cargo bed of the truck would be in the order of 2 g's in a frequency range of 2 to 150 hs. The aircraft vibration levels on the floor of the cargo deck would be in the order of 2 g's maximum over a frequency range of 12 to 1100 hz.

The next exposure would be during local moving at the field site which would be similar to conditions at the factory. The final exposure of the prototype flight test specimen would be during flight, both at launch and while in orbit. The launch vibration environment is the most severe of the vibration environments encountered during the life span of the flight test specimen. This is based on past experience with many spacecraft programs for both NASA and the Air Force. Fortunately, the prototype flight test specimen does not have to be operating during these environments, and therefore, will be frozen, The very low level

vibration level during orbit when the gallium will be in a liquid state poses no problem as shown in Section 3.3.2.1. Since there is no operating requirement during launch and the gallium is frozen, the vibration test will be primarily to verify that the LMSR prototype flight test specimen will structurally withstand the launch vibration loads and that the post vibration performance will not be degraded. A test for the orbital vibration environment need not be repeated since the loads are much lower than at launch and will not effect the test specimen structurally and a similar test was performed on an earlier prototype unit to verify that liquid gallium could withstand orbital vibration loads. Therefore the vibration test will consist of two parts. The first will be a very low level modal survey which will be used to determine the resonant frequencies of the fixture and the combination of the fixture and test specimen will be compared to those of the spacecraft and launch vehicle to insure that none of the resonant frequencies of the three are close enough to cause problems. The resonant frequencies of the fixture/test specimen combination will be used to top notch (reduce the amplitude) the control input to the shaker head at each discrete resonant frequency. The second part of the vibration test will consist of performing a launch vibration test to the requirements specified.

C.4.2 Shock

The prototype flight test specimen will be exposed to shock during the same parts of the assembly - test - launch - flight cycle as vibration. Since the test specimen will be protected by cushioning during local handling at the factory and field sites and during shipment between the factory and field sites, the most severe shock environment experienced will be during launch and flight. Structurally the critical environment is at launch (unit non-operating with gallium frozen), and operationally the critical environment is in orbit (unit operating with gallium in a liquid state). The system verification test program will include a shock test of two parts; launch shock environment and orbital shock environment as specified in Table C1.

C.4.3 Acceleration

The prototype flight test speciment will be exposed to acceleration to a limited degree prior to flight, such as during shipment. Typical shipment acceleration environments would be during acceleration or deceleration of the carrier vehicle (truck or aircraft) and probably would be of relatively low level. The highest acceleration forces the LMSR flight unit will experience would be during launch when the gallium is frozen. Thus the launch acceleration environment will be selected for the system verification test and would verify that the LMSR prototype flight test specimen will structurally withstand launch acceleration loads and that post acceleration performance will not be degraded. Acceleration during orbit would be of very low level. Typical sources of orbital accelerations are orbit adjust engines and attitude control systems. Testing to the orbital acceleration

TABLE C.1

SUMMARY OF ENVIRONMENTAL REQUIREMENTS

ENVIRONMENT	ASSEMBLY TO LAUNCH		LAUNCH	ORBIT
	FROZEN GALLIUM	LIQUID GALLIUM	FROZEN GALLIUM	LIQUID GALLIUM
Vibration	Com'l. ship. envir.	0.1g random on 1.0g static accel., all axes, 20 to 2000 Hz	sine 2 oct./min. 5-10 Hz, .9 in D.A. 20-50 Hz, 4g 50-200 Hz, 3g random 20-250 Hz, .001-.16g^2/Hz 250-2000 Hz, .16g^2/Hz	10^{-3} g (0-P sq. wave), 0-4 Hz
Shock	Com'l. ship. envir.	10g sine, 8 ms, all axes	30g sine, 8 ms, all axes	10g sine, 8 ms all axes
Acceleration	Com'l. ship. envir.		15g's, all axes	10^{-3}g
Pressure	Ambient 3.436 in. Hg.	ambient 10^{-5} to 10^{-9} torr		10^{-5} to 10^{-9} torr
Temperature	-20 to +70°C	-30 to +80°C	Later	Later
Thermal Shock	10°C/minute			
Humidity	95% at 30°C for 1 month			
Salt Spray	Seaside Atmos.			
Corrosive Atmos.	Propellant Fumes (N_2O_4 worst)			
Shelf Life	18 months			
Magnetic				100 gauss
RF				0.01 watts/m^2 800 MHz to 15 GHz

requirements were successfully performed on the LMSR/SAOM assembly with the gallium in a liquid state. Therefore, orbital acceleration tests will not be performed as part of the system verification test program.

C.4.4 Climatic Environments

C.4.4.1 Pressure and Temperature

The variations of pressure and temperature experienced by the LMSR assembly during the assembly - test - launch flight cycle will range from standard temperature and pressure conditions while at the factory, potential low pressure and temperature during shipment by aircraft to the field site, moderate changes in temperature and pressure at the field site and the extremes of low pressure and high and low (operating versus non-operating) temperature in orbit. Performance testing during system verification testing at the factory will verify operational capability at standard temperature and pressure. Capability of the LMSR assembly to perform at extremes of low pressure and high temperature will be verified by the thermal vacuum test part of the system verification test program. Since the LMSR assembly will be in a non-operating condition as the gallium will be frozen during shipment from factory to field site, system verification testing of the temperature and pressure extremes during shipment will not be required.

C.4.4.2 Thermal Shock

The LMSR assembly will possibly experience thermal shock at only a few points in the assembly - test - launch - flight cycle. This would be during transfer between a warm building such as the factory and

a truck in winter or while on an aircraft with sudden large changes in altitude. The mechanisms of failure generally associated with this test are caused by differential contraction (or expansion) or by formation and freezing of condensation on the test specimen. Since the LMSR assembly is in a non-operating condition with the gallium forzen and enveloped in a dry nitrogen atmosphere which would prevent the formation of condensation, a thermal shock test will not be conducted as part of the LSMR system verification test program.

C.4.4.3 Humidity and Salt Spray

The LMSR assembly would normally be exposed to humidity and salt spray only while on pad at the field site. However, since the LMSR assembly will be atmospherically shielded by dry nitrogen gas under a positive pressure during the complete field cycle, salt spray and humidity tests will not be included as part of the LMSR system verification plan.

C.4.4.4 Corrosive Atmosphere

The hazard of a corrosive atmosphere would be experienced by the LMSR assembly only when on pad. The greatest chance of this occurring would be during the loading of propellants. The most corrosive of the propellants associated with the booster for the spacecraft on which the LMSR assembly would be mounted is Nitrogen Tetraoxide (N_2O_4). Past experience associated with the loading of N_2O_4 on a large number of space vehicles indicates that the greatest danger will be to equipment directly under or around the propellant loading lines. If the propellant loading lines spring a leak, liquid N_2O_4 could cause considerable damage to electrical cabling, etc., while metallic structure, etc. would suffer little damage, if promptly

flushed. A corrosive atmosphere (N_2O_4) test will not be included as part of the LMSR system verification test program for two reasons. First, the LMSR assembly will be atmospherically shielded by dry nitrogen during this part of the pad cycle. Second, the location of the LMSR assembly on the space vehicle will be fairly remote from the area of propellant loading operations and a potential hazard could exist only if there was a malfunction of the propellant loading equipment.

C.4.4.5 Magnetic Field

The LMSR assembly would be exposed to a magnetic field only during orbit, which would be the earth's magnetic field. Since the design of the LMSR prototype unit does not contain anything susceptible to degradation by magnetic forces, a magnetic field test will not be included as part of the LMSR system verification test program.

C.4.4.6 RF

Principal exposure of the LMSR assembly to RF energy potentially would be in orbit when and if the LMSR would be in the field of a transmitting spacecraft antenna. Typical potential problem areas would be activation (as a malfunction) of explosive components or sensitive electronic circuits. Since the design of the LMSR prototype unit does not include anything susceptible to malfunction by RF energy, a RF test will not be included as part of the LMSR system verification test program.

C.5 Test Sequence

Fig. C2 presents the test verification program flow plan for the LMSR components and assembly and the sequence of environmental testing. Six areas of testing shall be performed: component, performance, thermal-vacuum, shock, vibration and acceleration. Performance tests shall be performed during the ambient and environmental test phases.

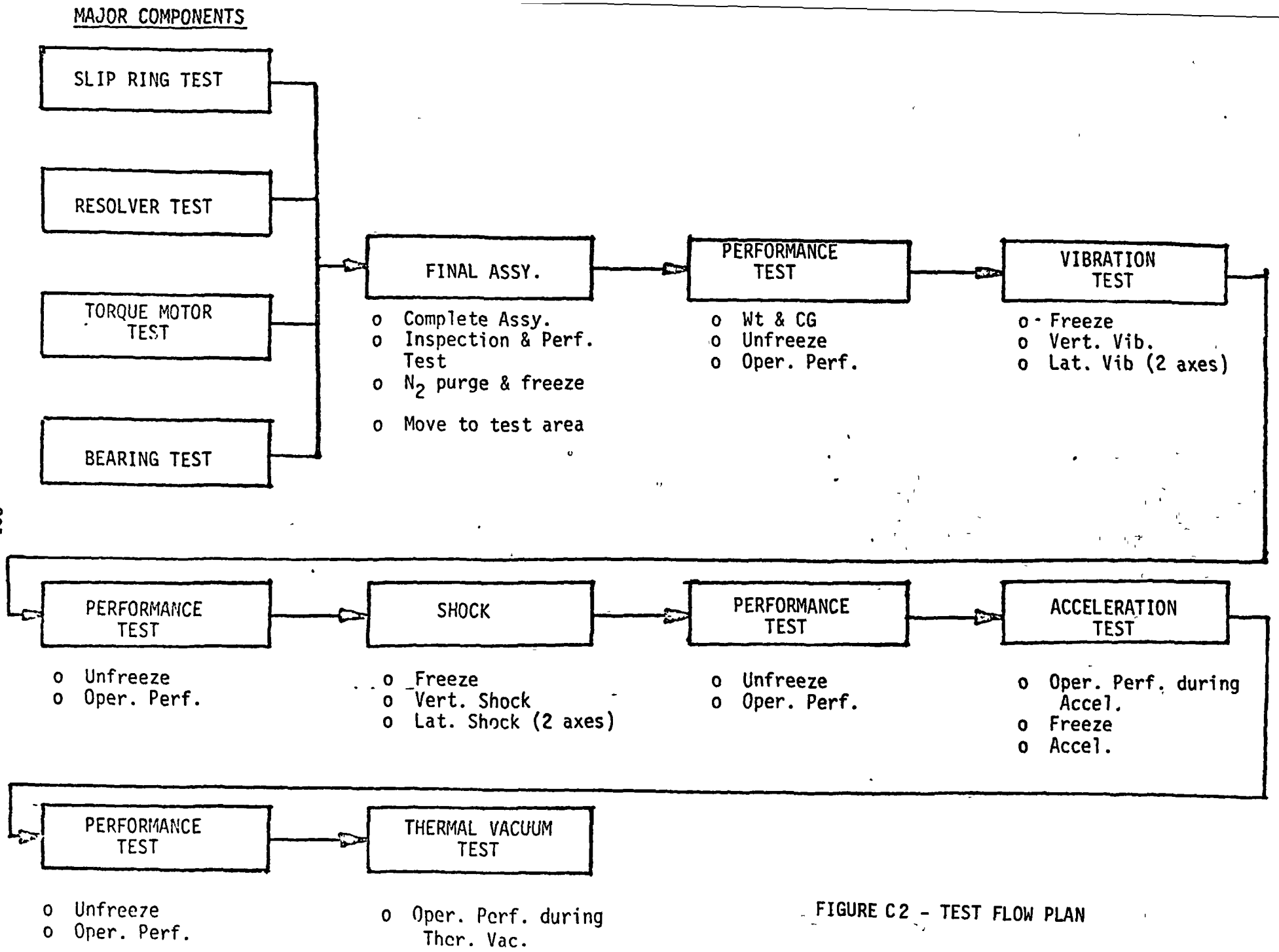

FIGURE C2 - TEST FLOW PLAN

C.6 Test Definition

C.6.1 Component Tests

Component tests will be performed on the slip rings, resolver, torque motors and bearings. The purpose of these tests is to provide preliminary information to insure that the manufacturer has met the design specifications of the hardware. Since these components are frameless, a limited amount of testing can be performed in the received condition. A detailed test schedule shall be performed in the ambient test phase to verify the operational performance characteristics. The component tests will be limited to an examination and a measurement of electrical parameters, where appropriate. The chart below lists the measurements to be performed on each component.

COMPONENT	WEIGHT	DIMENSIONS	ELECTRICAL RESISTANCE	CONTINUITY	MICROSCOPIC EXAMINATION
Slip Rings	X	X		X	X
Resolver	X		X	X	
Torque Motors	X		X	X	
Bearings	X				X

C.6.2 Performance Test

Performance tests, consisting of functional and integrity tests, will be performed during the LMSR design verification test program. The functional tests will verify proper and acceptable operation of the components before and after exposure to the specified environments. Integrity tests will be basically inspections to verify the mechanical and electrical integrity of the assembly. Performance tests shall be performed at key times during each testing phase (see Figure 43).

C.6.2.1 Functional Tests

A series of standard electrical measurements will be performed on the slip rings, torquers and resolver to assess the performance characteristics. The ambient tests will serve to check out the assembly to insure proper installation of resolver, bearings and torquer. In addition, these tests will provide the necessary baseline data to evaluate the effects of environmental testing. Complete functional tests in ambient shall be performed at the start and conclusion of the testing phase. Selected functional tests shall be required during or at the conclusion of each specified environmental exposure which is pertinent to the components ability to withstand environmental stress.

C.6.2.2 Integrity Tests

The integrity tests will be designed to verify the mechanical and electrical integrity of the LMSR assembly. These tests will be limited in scope during the actual testing phases since they will consist mainly of inspection without disassembly and other general means to assess overall performance. The outer shield containing the probes and end shields would be removed to expose the slip rings, probes and torquers for inspection at key times after the assembly has been operated or subjected to environmental exposure.

The slip rings are the most critical component of the LMSR ssembly, therefore an inspection would be required to insure that gallium spillage or creep has not occurred. Adjacent surfaces to the rings, including the outer shield, probe and Textolite discs should be carefully inspected. The presence, location and degree of formation of gallium oxide should be noted. In addition, gallium attack, particularly on the aluminum or

magnesium surfaces should be investigated. The overall appearance of the gallium in the ring, observing any voids or discontinuity in surface and the flaking or clumping of the oxide, should be noted. Every effort, short of complete disassembly, shall be made to evaluate the satisfactory performance and use of gallium. The Textolite discs should be carefully observed to detect evidence of dielectric breakdown and mechanical failure. Dielectric breakdown can be detected by carbon tracks radiating from the ring. The discs should be flexed by hand to observe or detect any cracks or failures which occurred during shock or vibration environments.

The torque motors and resolver should be examined to detect possible electrical failure i.e., shorting or insulation breakdown. The torquer commutator shall be inspected to observe possible corrosion or contact brush wear.

A detailed inspection of the bearings will be limited due to a lack of visual access. However, the inner race and balls of the single bearings could be observed to detect possible contamination from the assembly or originating within the bearing. The shaft should be rotated by hand to detect possible rubbing parts or excessive or cyclic torque variations in the bearings caused by brinnelling or eccentric or improper preloading.

C.7 Measurements

C.7.1 Measurement and Test Equipment

All measurements shall be made with instruments which are appropriate for the category involved and for the environmental conditions concerned. All inspection, measuring, and test equipment shall be calibrated at scheduled intervals against certified standards which have known valid relationships to national standards. Records shall be maintained, indicating the data of last calibration and due date. The due date or other identification attesting the due date of the next calibration shall be displayed on each item of inspection, measuring, and test equipment. Test equipment shall be checked for calibration due date, to assure that calibration does not run out during test, whenever pratical.

C.7.2 Test Tolerances

The maximum allowable tolerances for test conditions shall be as follows:

a.	Temperature	±2.5°F
b.	Relative Humidity	+0, -5% RH
c.	Vibration Amplitude	
	Sinusoidal	±10%
	Random	
	Overall rms level	±10%
	Power Spectral Density	±3 dB
d.	Vibration Frequency	±2% or ± 1/2 cps (whichever is greater)

e.	Weight	± 1/4%
f.	Pressure	± 10% to 10^{-5} torr
g.	Acceleration	±10%
h.	Shock	±15% g

C.7.3 Data Log and Report

A chronological log shall be kept throughout design verification tests and shall contain all test program data, identification, procedure descriptions, and a record of all pertinent events during the test program. After each test program, the responsible test engineer shall prepare a report. The data collected shall be recorded on a log sheet for each test environment. Strip chart, thermo-couple and other recordings taken during measurement or operational cycle shall be attached to this log and referenced by test number. Data point graphs of the test data shall also be presented.

C.7.4 Test Failure

C.7.4.1 Criteria for Failure

Degradation or change in performance of any assembly which exceeds limits established by its specification and applicable test procedure during any test period shall be considered a failure. Testing shall be discontinued until the malfunction (including design defects) is evaluated. If the corrective action consists of simple repair, such as replacement with identical parts, the complete test procedure under which failure occurred (such as vibration, shock, etc.) shall be repeated in its entirety without equipment failure before proceeding to the next test. If corrective action,

such as redesign, is required, the test procedure under which failure occurred shall be repeated as indicated above for repair action. In addition, if such redesign affects the results of previously completed tests, such tests shall be repeated.

C.7.4.2 Failure Reporting

Upon occurrence of a failure(s), a telephone report shall be made to the LMSR Project Manager or his designated representative followed by a confirmation in writing. A discrepancy analysis shall be made and a verbal report of corrective action taken shall be made immediately to the LMSR Project Manager or his designated representative followed by a confirmation in writing.

REFERENCES

Fluid Mechanics & Hydraulics, R. Giles, Schaum Publishing Co., New York, 1962.

Applied Hydrodynamics, Second Edition, H. R. Vallantine, Plenum Press, New York, 1967.

The Dynamic Behavior of Liquid in Moving Containers, NASA SP-106, H. N. Abramson, Editor. National Aeronautics & Space Administration.

Vacuum Technology & Space Simulation, D. J. Santeler, D. H. Holkebor, D. W. Jones, F. Pagano. NASA SP 105, National Aeronautics & Space Administration.

Rheology, V. G. W. Harrison, Academic Press, New York, 1954.

Rheology, Volume II, F. R. Eirich, Academic Press, New York, 1958.

Principles of Electricity & Electromagnetics, 2nd Edition, G. P. Harnwell, McGraw-Hill, 1949, P. 75.

Fundamentals of Electricity & Magnetism, 3rd Edition, L. B. Loeb, John Wiley, New York.

Principles of Electricity, 2nd Edition, Page & Adams, Van Nostrand, New York, 1931.

Applied Hydro and Aeromechanics, L. Brandt and O. G. Tietjens, Dover Publications, New York, 1957.

Essentials of Fluid Mechanics, L. Prandtl. Hafner Publishing Co., New York.

Viscosity & Flow Measurement, Van Wazer, Lyons, Kim and Colwell, Interscience Publishers, New York, 1963.

The Physics of Electricity & Magnetism, W. Scott, John Wiley, New York, 1950.

Electrical Discharges in Gases, F. M. Penning, Macmillan Co., New York, 1957.

Static Fields in Electricity & Magnetism, D. H. Trevena, Buttersworth, London, 1961.

Molybendum Compounds, D. H. Killeffer, and A. Linz, Interscience Publishers, New York, 1952.

REFERENCES (Cont'd)

Experimental Liquid Metal Slip Ring Project, NASA CR-72780
R. B. Clark, Hughes Aircraft Co.

An Experimental Liquid Metal Slip Ring to Transfer Power Between Rotating Satellite Parts, NASA CR-72790, S. M. Weinberger, General Electric Co.

Ultrahigh Vacuum Technique for the Investigation of Space Lubrication, L. E. St. Pierre & A. J. Haltner, General Electric Research Report No. 61-RL-2755C.

DISTRIBUTION LIST

National Aeronautics & Space Administration
Headquarters
Washington, D. C. 20546

Attention:	ED/L. Jaffee	1 copy
	ECC/A.M.G. Andrus	10 copies
	EC/R.B. Marsten	1 copy
	RP/W. H. Woodward	1 copy

NASA-Lewis Research Center
21000 Brookpark Road
Cleveland, Ohio 44135

Attention:	J. H. Childs (M.S. 3-3)	1 copy
	H. W. Plohr (M.S. 54-1)	1 copy
	W. H. Robbins (M.S. 501-1)	1 copy
	H. O. Slone (M.S. 501-6)	2 copies
	Technology Utilization Officer (M.S. 3-19)	1 copy
	Library (M.S. 60-3)	2 copies
	Report Control Office (M.S. 5-5)	1 copy
	N. T. Musial (M.S. 500-311)	1 copy
	R. R. Lovell (M.S. 54-3)	50 copies
	Contract Section B (M.S. 500-313)	1 copy
	A. F. Forestieri (M.S. 302-1)	1 copy

NASA-George C. Marshall Space Flight Center
Huntsville, Alabama 35812

Attention:	Library	1 copy

NASA-Goddard Space Flight Center
Greenbelt, Maryland 20771

Attention:	Library	1 copy

NASA-Ames Research Center
Moffett Field, California 94035

Attention:	Library	1 copy

NASA-Langley Research Center
Langley Station
Hampton, Virginia 23365

Attention:	Library (M.S. 185)	1 copy

NASA-Manned Spacecraft Center
Houston, Texas 77001

Attention:	Library	1 copy
	F. E. Eastman (EB8)	3 copies
	C. Robinson (EP52)	1 copy

Jet Propulsion Laboratory
4800 Oak Grove Drive
Pasadena, California 91103

Attention:	Library	1 copy
	W. Hasbach	1 copy

NASA Scientific and Technical Information Facility
Box 7500
Bethesda, Maryland 20740

Attention:	NASA Representative	3 copies

General Dynamics, Convair Division
P.O. Box 1128
San Diego, California 92112

Attention:	F. J. Dore/Advanced Programs Laboratory	1 copy

Air Force - Aero Propulsion Laboratory
Wright-Patterson Air Force Base
Ohio, 45433

Attention:	L. D. Massie (APIP-2)	1 copy

Philco-Ford Corporation
Western Development Laboratories Division
3939 Fabian Way
Palo Alto, California 94303

Attention:	R. G. Wales	1 copy
	D. L. Elder	1 copy

TRW Incorporated
TRW Systems
One Space Park
Redondo Beach, California 90270

Attention:	H. Low	1 copy
	W. Wellens	1 copy

Federal Communications Commission
521 12th Street
Washington, D. C. 20554

Attention: M. Fine — 1 copy

Ball Brothers Research Corporation
Box 1062
Industrial Park
Boulder, Colorado 80302

Attention: R. M. Ringeon — 1 copy
C. L. Anderson — 1 copy
V. Frubel — 1 copy

Lockheed Missiles and Space Company, Incorporated
P. O. Box 504
Sunnyvale, California 94088

Attention: J. W. Plummer — 1 copy
E. E. Crowther — 1 copy

Communications Research Centre
Shirley Bay, P. O. Box 490
Station "A"
Ottawa, Ontario Canada
KIN8T5

Attention: C. A. Franklin — 1 copy
W. F. Payne — 1 copy

U. S. Information Agency
25 M Street, S. W.
Washington, D. C. 20547

Attention: IBS/EF/G. Jacobs — 1 copy

Naval Electronic Systems Command
PME 116
Washington, D. C. 20350

Attention: Lt. Commander L. Wardel — 1 copy

McDonnell Douglas Corporation
5301 Bolsa Avenue
Huntington Beach, California 92647

Attention: J. Chester (A-3-BBDO-830) — 2 copies

Poly Scientific Division
Litton Industries
1213 N. Main Street
Blacksburg, Virginia 24060

Attention: E. Glossbrenner — 2 copies

Spar Aerospace Products
925 Caladonia Road
Toronto, Ontario 315
Canada

Attention: S. Ahmed — 1 copy
T. Ussher — 2 copies

COMSAT Laboratories
Box 115
Clarksburg, Maryland 20734

Attention: W. L. Pritchard — 2 copies

Hughes Aircraft Company
Technology Division
Box 92919 Airport Station
Los Angeles, California 90009

Attention: R. B. Clark — 1 copy

General Electric Company
Space Systems
Valley Forge Space Center
P. O. Box 8555
Philadelphia, Pennsylvania 19101

Attention: S. Weinberger — 3 copies